

Mikołaj Frasoński

**Binding partners of the neurexophilin-neurexin
complex identified in Nxph1-GFP^{tg/-} and Nxph3-
GFP^{tg/-} mice**

2021

Biologie

**Binding partners of the neurexophilin-neurexin
complex identified in Nxph1-GFP^{tg/-} and Nxph3-
GFP^{tg/-} mice**

Inaugural-Dissertation

zur Erlangung des Doktorgrades

der Naturwissenschaften im Fachbereich Biologie

der Mathematisch-Naturwissenschaftlichen Fakultät

der Westfälischen Wilhelms-Universität Münster

vorgelegt von

Mikołaj Frasoński

Aus Danzig, Polen

- 2022 -

Dekan

Prof. Dr. Jürgen Gadau

Erster Gutachter:

Prof. Dr. Markus Missler

Zweiter Gutachter:

Prof. Dr. Bruno Moerschbacher

Tag der mündlichen Prüfungen

17.06.2022

Tag der Promotion

18.10.2022

Content

■ Introduction	9
1.1 <i>Synapses</i>	9
1.2 <i>Cell adhesion molecules</i>	9
1.2.1 Synaptic cell adhesion molecules: Neurexins.....	10
1.2.2 The function of neurexins	11
1.2.3 The structure of neurexins and their binding partners	12
1.3 <i>Neurexophilins</i>	15
1.3.1 Expression of neurexophilins.....	15
1.3.2 The structure and properties of neurexophilins	16
1.3.3 Function of neurexophilins	21
1.4 <i>The aim of the study</i>	22
■ Materials and Methods	23
2.1 <i>Materials</i>	23
2.1.1 Animals	23
2.1.2 Antibodies	24
2.1.3 Apparatus	25
2.1.4 Cell cultures	26
2.1.5 Chemicals.....	27
2.1.6 Media and Supplements	28
2.1.7 Solutions and media for cell culture	29
2.1.8 Molecular biology kits	31
2.1.9 Oligonucleotides	31
2.1.10 Plasmids	33
2.1.11 Software	34
2.2 <i>Methods</i>	35
2.2.1 Molecular biology methods	35
2.2.2 Biochemical procedures	44
■ Results	51

3.1	<i>The differences between neurexophilins</i>	51
3.1.1	Nxph1	51
3.1.2	Nxph2	52
3.1.3	Nxph3	53
3.1.4	Nxph4	54
3.2	<i>All neurexophilin isoforms bind to the same epitope of Neurexin1α</i>	55
3.3	<i>Searching for novel binding partners of the neurexophilin/neurexin complex</i>	59
3.4	<i>GluN1 binds to neurexins in adult brains</i>	64
3.5	<i>NMDAR, GABA_BR, LRRTM2, Nlgn1, mGluR3 and mGluR5 interact with Nxph3-GFP/αNrxn complex during different stages of development</i>	69
3.6	<i>Recombinant GluN1-GFP binds to neurexins</i>	74
■	Discussion	79
4.1	<i>All neurexophilins bind to the same epitope of Nrxn1α</i>	79
4.2	<i>NMDAR is a novel binding partner of neurexins</i>	80
4.3	<i>NMDAR interacts with α-neurexin/neurexophilin complex in mature brains</i>	82
4.4	<i>Other age-dependent interactions</i>	82
4.5	<i>Limitations and recommendations</i>	86
4.6	<i>Conclusion and outlook</i>	88
■	References	91
■	Summary	122
■	Abbreviations	123
■	List of figures	125
■	List of tables	125
■	Lebenslauf	127
■	Acknowledgment	128

Introduction

1.1 Synapses

Nerve cells communicate with each other and with other cells through specialized intercellular junctions called synapses. The transfer of information via synapses from a presynaptic to a postsynaptic nerve cell is fast and highly efficient. Communication between neurons is mediated by two classes of synapses: electrical and chemical synapses (Pereda, 2014; Connors and Long, 2004). In electrical synapses, the cytoplasm of adjacent cells is connected directly by clusters of intercellular channels called gap junctions (Pereda, 2014). Gap junctions allow the transfer of ions and small metabolites between two neurons (Bennett and Zukin, 2004). Electrical synapses promote the coordinated activity of networks of extensively coupled neurons (Connors and Long, 2004) and promote mechanisms of lateral excitation in sensory systems (Pereda, 2014).

In contrast, chemical synapses are formed by presynaptic and postsynaptic terminals separated by the synaptic cleft. Neurotransmitters released from presynaptic terminals diffuse through the synaptic cleft to activate specific receptors located in the postsynaptic cells, which generates a postsynaptic response. There are two main types of chemical synapses: inhibitory and excitatory synapses, which differ in the protein composition of synaptic densities (Rollenhagen and Lübke, 2006; Barberis, 2020). In principal neurons, excitatory synapses occur mainly on dendritic spines (Bourne and Harris, 2008). Meanwhile, inhibitory synapses can be found on the shafts of dendrites, initial axon segments, or on cell bodies (Sheng and Kim, 2011).

1.2 Cell adhesion molecules

Cell adhesion molecules (CAMs) are a functional category of membrane-anchored glycoproteins located on the surface of cells. Most CAMs are transmembrane proteins or are attached to the cell membrane via glycosylphosphatidylinositol (GPI) anchor. A typical example of CAMs contains multiple cell adhesion domains in the extracellular region and a short cytoplasmic tail. That tail often possesses a PDZ binding motif at the carboxy-terminus, a binding target of the synaptic scaffolding proteins. The extracellular domains of CAMs form adhesion bonds by binding to molecules on adjacent cells, which can occur homophilically by binding to the same molecules or

Introduction

heterophyically, where binding occurs between distinct proteins (Missler, Südhof and Biederer, 2012). CAMs are also expressed in neurons, and there is a separate group of CAMs present at synapses. Synaptic cell adhesion molecules (SCAMs) connect neuronal pre- and postsynaptic sites and mediate essential trans-synaptic signaling operations (Südhof, 2021). SCAMs mediate the mechanical stabilization of neurons (Sytnyk *et al.*, 2002) and promote the formation of synapses (Dityatev, 2004). Moreover, SCAMs recruit neurotransmitter receptors and synaptic scaffolding proteins, which together take part in neurotransmission and maturation of neurotransmitter release mechanisms (Shetty *et al.*, 2013). It has also been demonstrated that SCAMs mediate stabilization of synaptic ultrastructure in mature neurons (Mendez *et al.*, 2010; Puchkov *et al.*, 2011; Benson and Huntley, 2012), remodeling and plasticity (Schachner, 1997; Gerrow, 2006; Sytnyk *et al.*, 2006) and regulate neurotransmitter release (Sytnyk *et al.*, 2006; Andreyeva *et al.*, 2010). SCAMs are represented by members of many cell adhesion molecules families, including cadherins, integrins, immunoglobulin superfamily (IgSF) CAMs, neuroligins, and neurexins (Südhof, 2021).

1.2.1 Synaptic cell adhesion molecules: Neurexins

Neurexins are a family of synaptic cell adhesion proteins essential for Ca^{2+} -dependent transmission, synapses formation, and differentiation. Initially, neurexins were identified as receptors for α -latrotoxin, a spider toxin that triggers a massive release of synaptic vesicles (Ushkaryov and Südhof, 1993; Ushkaryov *et al.*, 1994). Neurexins are mainly expressed in brain neurons (Ushkaryov *et al.*, 1992), but it was also reported that *Nrxn1* mRNA is abundantly produced in astrocytes (Zhang *et al.*, 2013a). In mammals, neurexins are encoded by three different genes (*nrxn* 1-3) expressed in both excitatory and inhibitory synapses of the central and peripheral nervous system. Moreover, *nrxn1* and *nrxn3* genes are the longest in the mammalian genome occupying nearly 0,1% of the entire human genome (Rowen *et al.*, 2002; Tabuchi and Südhof, 2002). The size of *nrxn* genes suggests that their expression is limited to postmitotic cells like neurons since their transcription in fast-dividing cells would take too long to be completed (Rowen *et al.*, 2002; Reissner, Runkel and Missler, 2013). Although *Nrxns* are mainly expressed in the brain, it has also been reported that mRNAs of distinct neurexins isoforms are differentially distributed in the central nervous system (CNS) (Ullrich and Südhof, 1995). Each neurexin gene

Introduction

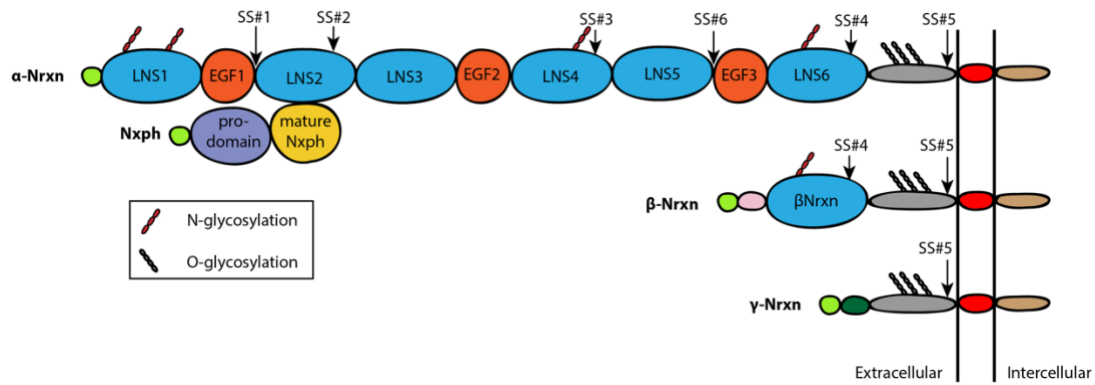


Figure 1.1. Domain organisation of neurexins and neurexophilins. Schematic representation of the domain structure of α -neurexins (α -Nrxn), β -neurexins (β -Nrxn), and γ -neurexins (γ -Nrxn) with approximate positions of alternative splice sites indicated by arrows. Neurexophilins bind to the LNS2 domain of α -neurexins and contain a signal peptide (green), pro-domain that goes through a proteolytic cut (violet), and the mature domain of Nxph (yellow). α -neurexins are characterised by an LNS (blue)-EGF (orange)-LNS (blue) cassette that is repeated three times. β -Nrxn starts from its exon that encodes signal peptide (green), unique 37 residues long histidine-rich β -neurexin sequence (pink), and LNS domain identical to α LNS6 (blue). γ -neurexin is also synthesised from its promoter in the *nrxn1* gene and contains, a signal peptide, a γ -specific sequence (dark green) and the stalk region (gray). Transmembrane sequence (red) and the intracellular domain (brown) do not differ between neurexins. Sites of N-glycosylation and O-glycosylation are marked. EGF, epidermal growth factor-like domain; LNS, laminin-neurexin-sex hormone-binding globulin (modified from Wilson *et al.*, 2019 and Reissner *et al.*, 2013).

produces two main isoforms synthesized from independent promoters: a longer α -neurexin and a shorter β -neurexin (Figure 1.1). A single α -neurexin locus was also found in invertebrate genomes like in *Drosophila melanogaster*, *Apis mellifera*, and *Caenorhabditis elegans*; β -neurexin was reported only in *C. elegans* (Haklai-Topper *et al.*, 2011). It was also shown that the murine *nrxn1* gene possesses a third promoter that produces short Nrxn1 γ (Figure 1.1). The extracellular sequence of γ -neurexin contains only the extracellular juxtamembrane sequence of Nrxn1 α and Nrxn1 β (Sterky *et al.*, 2017).

1.2.2 The function of neurexins

Neurexins were identified as essential SCAMs required for proper synaptic transmission. A constitutive α -neurexins knockout (KO) studies revealed that even a single Nrxn1 KO showed a reduced survival rate of mice (Missler *et al.*, 2003). The deletion of all three α -neurexins in mice is lethal, caused by an impairment of Ca^{2+}

Introduction

influx during an action potential (Missler *et al.*, 2003). Moreover, constitutive knockout studies of all β -neurexins showed a significant synaptic phenotype without reducing a survival rate of animals (Anderson *et al.*, 2015). β -neurexins deletions also demonstrated suppressing presynaptic release probability in cultured hippocampal neurons (Anderson *et al.*, 2015). Surprisingly, KO of β -neurexin revealed that β -neurexins perform an independent function from α -neurexins by regulating postsynaptic endocannabinoid synthesis (Anderson *et al.*, 2015). Another report showed that neurexins perform different tasks in distinct classes of neurons. Conditional deletion of all α - and β -neurexins from parvalbumin-positive interneurons in the prefrontal cortex caused a 30% decrease in the number of synapses and 50% decay of the synaptic strength without any impairments in action-potential-driven Ca^{2+} influx (Chen *et al.*, 2017).

On the other hand, deletion of neurexins in somatostatin-positive interneurons did not change the number of synapses but caused a 50% loss in Ca^{2+} influx driven by action potential (Chen *et al.*, 2017). Although pan-neurexin KO produced different results in distinct classes of neurons, there are not many reports about the function of individual neurexin variants. Conditional deletion of *Nrxn3* in the hippocampal CA1 region showed two interesting phenotypes: a 40% decrease in AMPAR-mediated excitatory responses caused a loss of postsynaptic AMPA receptor numbers; and a block of postsynaptic NMDAR-mediated long-term potentiation (LTP) (Aoto *et al.*, 2015). In contrast, the same conditional KO of the *Nrxn3* gene introduced in the olfactory bulb caused a 60% decrease in GABAR-mediated inhibitory response, which was rescued by the GPI-anchored *Nxph3 β* (Aoto *et al.*, 2015). Taken together, it seems that *Nrxn3* performs distinct molecular functions in different brain localizations, and *Nrxn1* and *Nrxn2* might also have specific roles in various classes of synapses.

1.2.3 The structure of neurexins and their binding partners

Neurexins are N-glycosylated, but heavily O-glycosylated at the stalk region (Fig. 1.1) (Ushkaryovso *et al.*, 1994). It has recently been shown that neurexins are heparan sulfate proteoglycans (HS), and this glycosylation mediates the binding of neurexins to their synaptic partners (Zhang *et al.*, 2018). Moreover, mice lacking HS showed structural and functional impairments in synapses and reduced survival rates (Zhang *et al.*, 2018). Neurexins belong to the presynaptic type I membrane proteins, which possess an extensive extracellular N-terminal sequence and a short cytoplasmic C-

Introduction

terminal tail. The extracellular domains of α -Nrxns and β -Nrxns differ in length; however, their transmembrane and C-terminal regions are the same (Reissner, Runkel and Missler, 2013). Extracellular sequences of α -Neurexins possess six Laminin-Neurexin-Sex hormone domains (LNS) interspersed by three epidermal growth factor-like domains (EGF) (Fig.1.1). The crystal structure of a Nrxn1 α fragment from LNS2 to LNS6 domains showed an L-shaped form. The longer arm comprises the LNS2-LNS3-EGF2-LNS4-LNS5 domains, while EGF3-LNS6 domains form the shorter component (Chen *et al.*, 2011; Miller *et al.*, 2011). In contrast, β -neurexins contain only a single LNS domain, which is identical to LNS6 of α -neurexins and 37 residues long N-terminal sequence characteristic for β -neurexins (Ushkaryov *et al.*, 1992; Ushkaryov & Südhof, 1993; Ushkaryov *et al.*, 1994; Reissner *et al.*, 2013). One of the characteristic motifs of neurexin LNS domains is a β -sheet sandwich composed by strands β 3, β 8, β 9 and β 10, β 4, β 5, β 6 and β 7 and a neighboring two-stranded sheet of β 2 and β 11 (Reissner *et al.*, 2013). Every neurexin LNS domain has a Ca^{2+} coordination site at its rim, which is rigid and does not go through conformational change upon calcium-binding. Moreover, Ca^{2+} binds to the negatively charged pocket of α LNS6/ β LNS and neutralizes it, allowing neuroligin and other proteins (Table 1) to make mainly hydrophobic contacts with neurexins (Reissner *et al.*, 2008).

Table 1. Interaction partners of neurexins.

Protein	Binding site	Requirement for		Reference
		Splice insert	Ca^{2+} binding	
<i>Binding partners specific α-Nrxn</i>				
Neurexophilin	α LNS2	-	-	(Missler, Hammer and Südhof, 1998)
<i>Shared by α-Nrxn and β-Nrxn</i>				
Neuroligin	α LNS6, β Nrxn	(-/+SS#4	+	(Ichtchenko <i>et al.</i> , 1995)
Dystroglycan	α LNS2, α LNS6, β Nrxn	-SS#2, -SS#4	+	(Sugita <i>et al.</i> , 2001)
GABA(A)R	α LNS6, β Nrxn	-SS#4	-	(Zhang <i>et al.</i> , 2010)
LRRTM	α LNS6, β Nrxn	-SS#4	+	(de Wit <i>et al.</i> , 2009)
Cerebellin	α LNS6, β Nrxn	+SS#4	-	(Joo <i>et al.</i> , 2011)
CL1	α LNS6, β Nrxn	+SS#4	-	(Boucard, Ko and Südhof, 2012)
C1qL	stalk region Nrxn3	+SS#5	-	(Matsuda <i>et al.</i> , 2016)
SorCS1	α LNS6, β Nrxn	-	-	(Savas <i>et al.</i> , 2015)
amyloid- β	extracellular domain	-	-	(Brito-Moreira <i>et al.</i> , 2017)
IgSF21	extracellular domain	-	-	(Tanabe <i>et al.</i> , 2017)
CaV2 α 2 δ 3 subunit	α LNS1, α LNS5	-	-	(Tong <i>et al.</i> , 2017)

Introduction

Calsyntenin	α LNS6, β Nrxn	-	-	(Lu <i>et al.</i> , 2014)
Synaptotagmin	cytoplasmic domain	-	+	(O'Connor <i>et al.</i> , 1993)
Znf804a	cytoplasmic domain	-	-	(Owen, Williams and O'Donovan, 2009)
CASK	PDZ motif	-	-	(Hata, Butz and Südhof, 1996)
Mint	PDZ motif	-	-	(Biederer and Südhof, 2000)
AF-6	PDZ motif	-	-	(Zhou <i>et al.</i> , 2005)
CA10/CA11	stalk region	-	-	(Sterky <i>et al.</i> , 2017)

Summary of α -neurexins and β -neurexins (Nrxn) interacting proteins. Note that neuroligins preferentially bind to neurexins with the out insert in splice site 4 (-SS#4) and the presence of +SS#4 modifies that binding. LNS, laminin-neurexin-sex-hormone-binding globulin changed from (Reissner, Runkel and Missler, 2013).

Up to now, only a few LNS domains were identified as the ones involved in binding to extracellular partners of neurexins, including: (1) the α LNS2 domain specific for α -neurexins that binds to neurexophilins and dystroglycan (Missler, Hammer and Südhof, 1998; Sugita *et al.*, 2001; Reissner *et al.*, 2014), (2) the α LNS6/ β LNS that binds to neuroligins, LRRTMs, GABAAR, cerebellins, latrophilins and CL1 (Ichtchenko *et al.*, 1995; de Wit *et al.*, 2009; Ko *et al.*, 2009; Siddiqui *et al.*, 2010; Uemura *et al.*, 2010; Zhang *et al.*, 2010; Boucard, Ko and Südhof, 2012); (3) the juxtamembranous sequences on the stalk region of both α - and β -neurexins that bind to CA10 and CA11 and C1qls (Matsuda *et al.*, 2016; Sterky *et al.*, 2017). It has also been reported that isolated LNS1 and LNS5 domains co-immunoprecipitated with α 2 δ 3 domain of voltage activated calcium channel (Cav2) (Tong *et al.*, 2017). Interestingly, although neuroligins and LRRTMs do not have similar structures, they both compete for the same Ca²⁺-binding epitope on α LNS6/ β LNS (Araç *et al.*, 2007; Fabrichny *et al.*, 2007; Chen *et al.*, 2008; Siddiqui *et al.*, 2010). Dystroglycan binds Ca²⁺-dependently to both α LNS2 and α LNS6, although these two domains do not have similar surfaces (Reissner *et al.*, 2014). Intracellularly, C-terminus of neurexins contains a potential endoplasmic retention signal, a cytoskeleton integrating protein 4.1 and a PDZ-domain-binding motif that allows binding of MAGUK proteins like CASK and MINTs and is required for trafficking of neurexins (Hata, Butz and Südhof, 1996; Biederer and Südhof, 2000, 2001; Fairless *et al.*, 2008). Besides MAGUKs, other proteins bind to the cytoplasmic domain of neurexins, including synaptotagmin and Znf804a (O'Connor *et al.*, 1993; Owen, Williams and O'Donovan, 2009). As mentioned above, there are six conserved alternative splice sites in α -neurexins coding sequences (SS#1-SS#6) and two in β -neurexins (SS#4 and

SS#5), and their permutations allow thousands of possible variants of neurexins isoforms (Reissner, Runkel and Missler, 2013). Alternative splicing plays a crucial role in all neurexin genes because binding to postsynaptic interacting proteins is splice site-dependent (Table 1). Positions of splice sites as well as sequences of splice inserts are evolutionary conserved, which also points to the importance of alternative splicing in neurexin genes (Ullrich and Südhof, 1995; Rowen *et al.*, 2002; Rissone *et al.*, 2007; Zeng *et al.*, 2007; Biswas *et al.*, 2008).

1.3 Neurexophilins

Neurexophilins are the family of low molecular weight cysteine-rich glycoproteins exhibiting a domain structure like that of neuropeptides (Murthy, Mains and Eipper, 1986; Missler and Südhof, 1998). Nxph1 is the best described member of the neurexophilin family. Initially, it was discovered as a 29-kDa protein co-purified with neurexin 1 α from a mouse brain by immobilized α -latrotoxin (Petrenko *et al.*, 1996). However, Nrnx1 α binds to α -latrotoxin separately without Nxph1 and does not require Nxph1 for binding (Davletov *et al.*, 1995). Nxph1 forms a tight complex with neurexin 1 α , which could be dissociated only in near desaturating conditions in guanidinium thiocyanate presence (Petrenko *et al.*, 1996).

1.3.1 Expression of neurexophilins

In contrast to neurexins that are expressed in the whole brain (Ullrich and Südhof, 1995), expression of neurexophilins is restricted only to neuronal subpopulations (Petrenko *et al.*, 1996; Beglopoulos *et al.*, 2005). This suggests that complexes of α -Neurexins with neurexophilins are not ubiquitous (Beglopoulos *et al.*, 2005). Molecular cloning of cDNAs from mammalian brains revealed that there are at least four genes related to neurexophilins (*nxph1*, *nxph2*, *nxph3*, *nxph4*), where rodents express only neurexophilins 1, 3, and 4 on detectable level (Missler and Südhof, 1998). Nxph1 was reported to be expressed in inhibitory GABAergic interneurons (Petrenko *et al.*, 1996). Moreover, mRNA of Nxph1 was detected within periglomerular cells in the olfactory bulb during the early postnatal period and not in the embryonic olfactory bulb, which suggests that Nxph1 might be involved in late glomerular formation and maturation (Clarris, Mckeown and Key, 2002). Nxph3 is mostly expressed in excitatory neurons of layer 6b of the cerebral cortex, mainly in excitatory neurons, granule cells in the vestibulocerebellum, and Cajal-Retzius cells

Introduction

during development (Beglopoulos *et al.*, 2005). Nxph4 is expressed in subsets of neurons interconnected in components of several functionally defined brain circuits, *among other things*, sensory circumventricular organs: subfornical organ, which controls fluid balance (Fry and Ferguson, 2007) and area postrema essential for energy homeostasis (Cottrell and Ferguson, 2004) (Tan *et al.*, 2016). The Knock-in approach of Nxph4 coexpression with LacZ showed that Nxph4 is also expressed in nuclei cerebellar Golgi cells (Meng *et al.*, 2019).

1.3.2 The structure and properties of neurexophilins

Sequence analysis revealed that neurexophilins are composed of four domains: a N-terminal signal peptide (I), a N-terminal non-conserved region (II), a highly conserved central N-glycosylated domain containing no cysteine residues (III), a short linker region (IV), and a C-terminal cysteine-rich domain (V) (Fig. 1.2). There are three disulfide bonds near loop regions, which link cysteine pairs C194-C231, C210-C21 and C239-C256 (Reissner *et al.*, 2014, Wilson *et al.*, 2019).

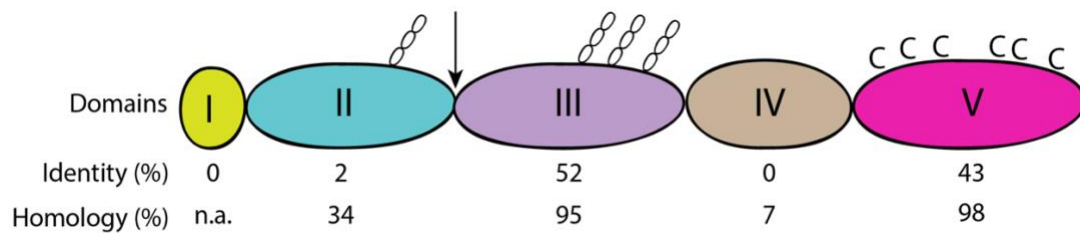


Figure 1.2. Domain structure of neurexophilins. Neurexophilins are composed of five domains (roman numbers). Unfiled ellipses represent conserved N-glycosylation and letter C represent conserved cysteines, which are present on domain V. The arrow indicates a proteolytic cleavage site between domains II and III. The sequence identities and homology between four neurexophilins are shown below the skim (modified from Missler and Südhof, 1998b).

The signal peptide presence and the fact that no other hydrophobic regions present in neurexophilins initially suggested that they are secreted glycoproteins (Missler and Südhof, 1998). Neurexophilins are translated as pro-forms and processed to mature proteins by proteolytic cleavage in the secretory pathway, shown by a time-dependent proteolytic digest from neuron-like cells (PC12) infected with full-length Nxph1 (Missler and Südhof, 1998). Sequence analysis revealed that the cut occurs directly after putative proteolytic cleavage motif KXKK (Missler and Südhof, 1998), conserved and present in all four neurexophilins (Fig. 1.3, Lys-118).

Introduction

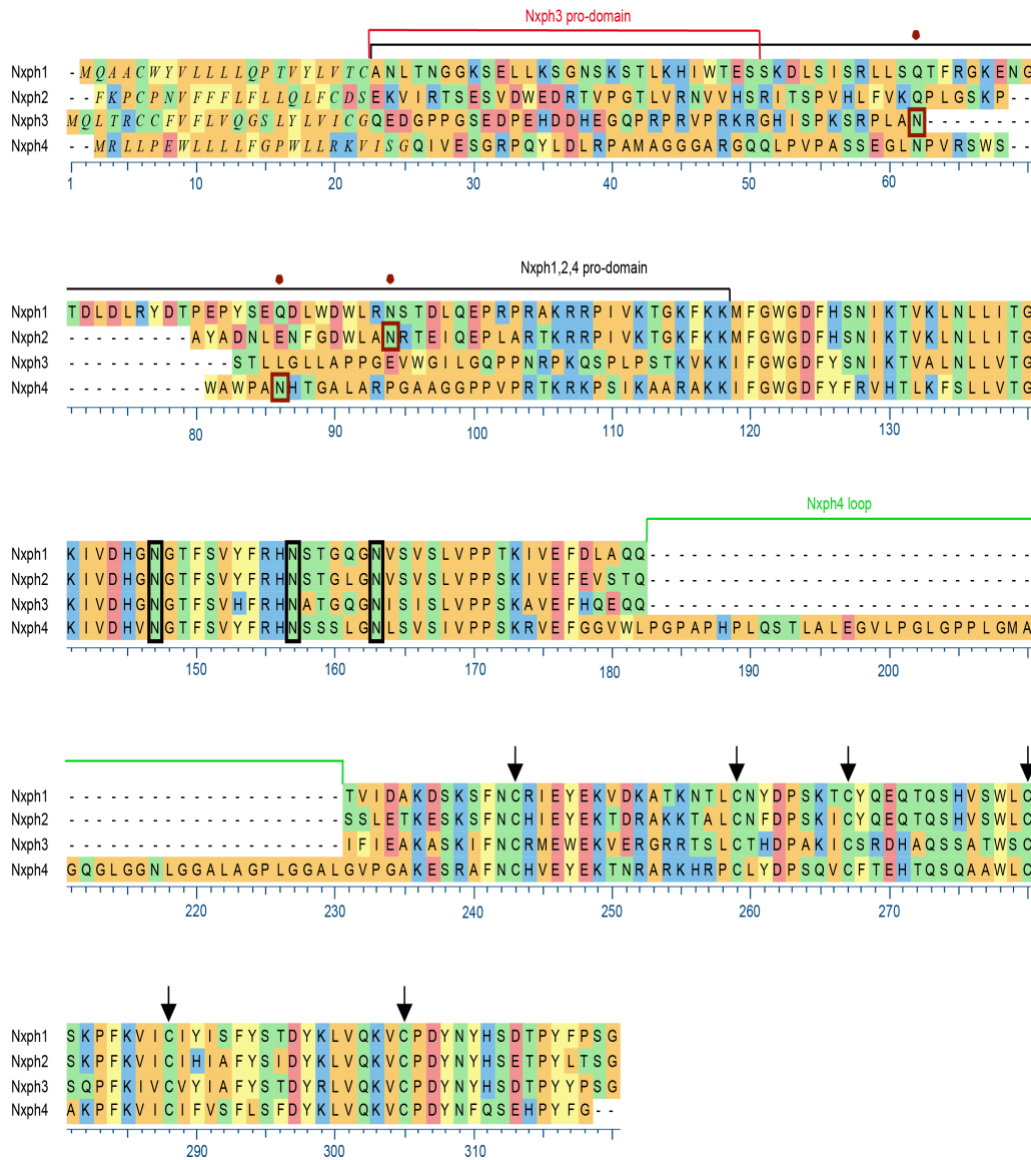


Figure 1.3. Primary structure of rat neurexophilins. The amino acid sequences of the four neurexophilins (Nxph1-Nxph4) are aligned for maximum homology, with hyphens indicating gaps. Sequences are identified on the left and numbered below. Residues that are identical in all sequences are marked in the same color. The putative signal sequences are shown at the beginning. The putative signal sequences are shown in *italics*. Pro-domain of Nxph1, Nxph2, and Nxph4 is marked by the black line, which starts after the signal peptide and ends on the conserved KXKK/RXKK proteolytic cutting site. The Pro-domain of Nxph3 is marked by the red line, which begins after the signal peptide and ends on the PRKR proteolytic cutting site suggested in this work (Chapter 3.1.3), which is not conserved in the other three neurexophilins. Black boxes mark three conserved N-glycosylation sites in all mature neurexophilins, and red dots mark N-glycosylation sites of Nxph2 (N94), Nxph3 (N62), and Nxph4 (N86) in their pro-domains. Arrows indicate six cysteines present in all neurexophilins. The green line marks the loop that is characteristic only to Nxph4. Figure modified from (Petrenko *et al.*, 1996). Sequences were obtained from www.uniprot.org.

Introduction

Pull down with Fc-tagged Nrnx1 α from neurons showed that Nrnx1 α preferentially binds to the processed form of Nxph1 (Missler and Südhof, 1998). Nxph1/ α Nrnx complex formation is required for neurexophilins to reach the neuronal presynaptic site, shown in neuronal cell culture studies (Neupert *et al.*, 2015). Since neurexophilins colocalize with α -neurexins, it is suggested that the function of neurexophilins depends on their complex formation with neurexins.

Determination of the neurexophilin binding site in α -neurexins showed that only the LNS2 domain of α -neurexins bind to neurexophilins (Missler, Hammer and Südhof, 1998) and the binding occurs calcium independently (Sugita *et al.*, 2001, Reissner *et al.*, 2014). Both Nrnx1 α LNS2 domain and Nxph1 are mainly composed of β -sandwiches formed by β -strands (Wilson *et al.*, 2019). The β -sandwich of Nxph1 is formed by two anti-parallel β -sheets built of six β -strands (β_1 - β_3 , β_4 , β_7 - β_8) and two anti-parallel to each other β -strands that are exposed to the solvent (Wilson *et al.*, 2019) (Fig. 1.4). The binding epitope of Nrnx1 α to Nxph1 has been narrowed to a region on the β_{10} sheet of Nrnx1 α LNS2 domain (Reissner *et al.*, 2014). Later, the crystal structure of Nrnx1 α LNS2-Nxph1 complex showed that both β_{10} and β_7 strands of Nrnx1 α take part in binding to Nxph1 (Wilson *et al.*, 2019). It was shown that complex formation requires hydrophobicity on Ile-401 residue (Fig. 1.5), but not on nearby side chains of Leu-402 or threonines 403-405.

Further analysis of Nxph1-Nrnx1 α interaction revealed that it occurs in a side chain-independent β - β sheets manner, where even a single T404P mutation impaired complex formation (Reissner *et al.*, 2014). This result also explains why the binding between Nxph1 and α -Neurexins occurs calcium- and splice site-independently (Missler, Hammer and Südhof, 1998). Alternative splicing on LNS2 domains of Nrnx1 showed to modulate the structure of Nxph1-LNS2 complex. Nrnx1 α LNS2 domain occurs in two main populations: LNS2^{SS2-} with no insert and LNS2^{SS2A+} that contains eight residues long insert (Fig. 1.4). Interestingly, LNS^{SS2A+} domains show a six-times higher affinity to Nxph1 than insert-free LNS2 domains (Wilson *et al.*, 2019). This result is opposite to Nrnx1-Nlgn1 interactions where it was revealed that the Nrnx1 β that contain a 30-residues long insert in SS4 binds to Nlgn1 with a lower affinity than its insert-free isoform (Boucard *et al.*, 2005, Elegheert *et al.*, 2017). The binding epitope of neurexophilins to LNS2 domain of α -neurexins has only been proved for Nxph1 so far but based on sequences of other neurexophilins it is very well possible that they all could act similarly. The only neurexophilin that stands out from

Introduction

other members of neurexophilin family is Nxph4. Although Nxph4 has a similar domain structure as Nxph1, it possesses a ~50 glycine- and proline-rich residues loop sequence that connects $\beta 4$ and $\beta 5$ (Fig. 1.3), which is not present in the other three neurexophilins (Missler & Sudhof, 1998). The difference in sequence length could lead to some distinct binding properties and functions of Nxph4, however, it has not been investigated so far.

It also has been reported that neurexophilins have a competitor for the binding epitope on LNS2 domain of α -neurexins. Nxph1 occupies the same binding epitope as α -dystroglycan (DAG1) and binds to α -neurexins with a higher affinity (Reissner *et al.*, 2014). Nxph1 binds to α -Neurexins splice site 4 (SS#4) independently, but α DAG binds to Nrnx1 α /Nxph1 complex only in absence of an insert in SS#4. This phenomenon suggests an antagonistic relationship and a competition between these two binding partners of neurexins (Reissner *et al.*, 2014).

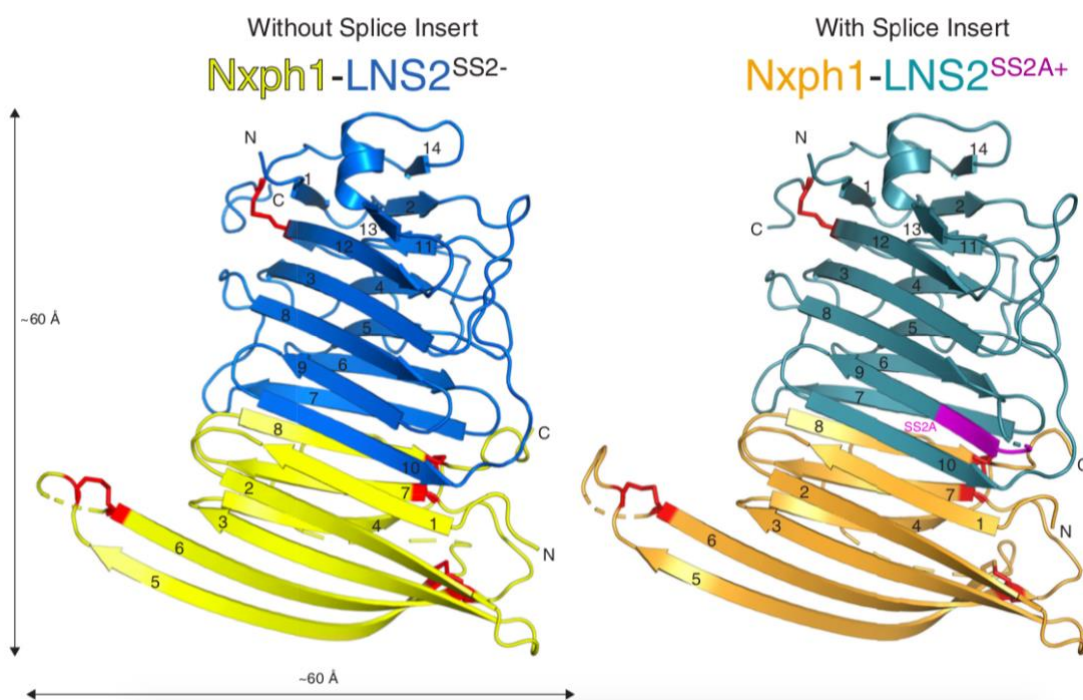


Figure 1.4 Crystal structures of Nxph1-LNS2^{SS2-} and Nxph1-LNS2^{SS2A+} complexes. The figure shows an overall architecture of Nxph1-LNS2 complexes with numbered β -strands and indicated C- and N- terminals. SS2A insert is marked in magenta. Disulfide bonds are presented as red sticks and dashed lines show disordered regions. Adapted from Wilson *et al.*, 2019.

Introduction



Figure 1.5 Primary and secondary structures of the splice insert-free neuroligin-1 LNS2 domain in complex with neuroligin-1. The crystal structure revealed that Nxph1-LNS2 interaction occurs between β_7 and β_{10} of LNS2 and β_1 and β_8 of Nxph1. Residues labeled in red (Val-358, Ile-401, Leu-402, Thr-404) were mutated and tested in a co-immunoprecipitation assay with neuroligin 1. Ile-401 was identified as a residue involved in binding to neuroligin 1 (Reissner *et al.*, 2014). Residues of Nxph1 labeled in green (Tyr-249, Leu-251) form a deep hydrophobic binding pocket of Nxph1. Residues of LNS2 labeled in cyan (Thr-405, Tyr-407) were also indicated as the ones which also take part in binding to Nxph1 (Wilson *et al.*, 2019). 6PNP structure was downloaded from the protein data bank. Modified from (Wilson *et al.*, 2019).

1.3.3 Function of neurexophilins

Although the structure of neurexophilins has been under investigation for many years, it is still not known what the exact function of these α -neurexin specific ligands are. *Nxph1* knockout in mice is not lethal and revealed no obvious phenotype related to the loss of one of the neurexophilins (Missler, Hammer and Südhof, 1998). Later it was shown that *Nxph1* plays a role in short-term synaptic plasticity. Genetic deletion of *Nxph1* impaired GABA_B receptor (GABA_BR)-dependent short-term depression of inhibitory synapses in the nucleus reticularis thalami (NRT), the region where *Nxph1* is highly expressed. However, the ectopic expression of *Nxph1* in excitatory terminals of the neocortex, which generally do not contain this molecule, showed an inverted phenotype and reduced short-term facilitation (Born *et al.*, 2014). There are not so many reports about other neurexophilins. In case of *Nxph3*, *Nxph3* knockout mice showed no structural phenotype; however, it displayed impairments in sensorimotor gating and motion coordination tasks but not in other behavioral tests (Beglopoulos *et al.*, 2005). *Nxph4* knockout mice showed anxiety, defects in motor coordination, and reduced weight (Meng *et al.*, 2019). Deletion of *nxph4* caused reduced Golgi-granule cell inhibitory synapse number and impaired neurotransmission onto granule cells, which possibly contributed to the observed motor deficits in mice (Meng *et al.*, 2019). Neurexin1 α was confirmed to interact with *Nxph4* *in vivo* when both proteins coimmunoprecipitated together from synaptosomes obtained from *Nxph4* KI mice brains (Meng *et al.*, 2019). Moreover, it was also shown that *Nxph4* interacts with postsynaptic receptor GABA_ARs in the cerebellum (Meng *et al.*, 2019). In case of *Nxph2*, it was shown that patients with the chromosomal deletion in 2q22.1, a region where there are loci of inter alia: *Nxph2*, histamine N-methyltransferase (HNMT), low density lipoprotein receptor-related protein 1B (LRP1B) and Rho GTPase activating protein 15 (ARHGAP15), have severe intellectual disability, omphalocele, hypospadias, and high blood pressure (Mulatinho *et al.*, 2012).

1.4 The aim of the study

In this PhD project, I focused on neurexophilins, specific ligands of α -neurexins. The crystal structure of Nxph1 in complex with the LNS2 domain of Nrnx1 α has been revealed recently (Wilson *et al.*, 2019), which makes Nxph1 the most investigated member of the neurexophilin family so far. However, It is still unclear if other neurexophilins use the same interface to interact with neurexins and what is the function of these neurexin-specific ligands.

At first, I asked if the other three neurexophilin family members (Nxph2, Nxph3, Nxph4) interact with the same binding epitope on the LNS2 domain of Nrnx1 α . I performed in vitro protein-protein interaction studies where I co-expressed various neurexophilins with neurexin1 α in a heterologous system to map if they share the same interface as Nxph1-Nrnx1 α . In the second part of my project, I wanted to gain more knowledge about the function of neurexophilins by a search for novel binding partners of Nxph1 and Nxph3. To do so, I performed brain pull-down experiments from transgenic mice ectopically overexpressing Nxph1-GFP and Nxph3-GFP to screen through synaptic receptors that could potentially interact with neurexophilins or neurexophilins in complex with neurexins.

Materials and Methods

2.1 Materials

2.1.1 Animals

Mice of *Nxph1* transgenic (*Nxph1*-GFP^{tg/-}) and *Nxph3* transgenic (*Nxph3*-GFP^{tg/-}) were used in pull-down assays in search for novel binding partners of neurexins. Animals were held at the animal facility of the Universitätsklinikum Münster and in the Institute of Anatomy and Molecular Neurobiology under local institutional and governmental regulations for animal welfare. Both *Nxph1*-GFP^{tg/-} and *Nxph3*-GFP^{tg/-} were generated in our lab by Kerstin Piechotta from WT C57BL/6N mouse strain obtained from JANVIER LABS, France.

Nxph1-GFP^{tg/-} transgenic mice were designed to ectopically overexpressing GFP-tagged *Nxph1* under the control of *Thy1.2* promoter (Born *et al.*, 2014). The transgenic vector used for the preparation of mice was constructed using plasmid pCMVD2, which encodes full-length *Nxph1* (Missler & Sudhof, 1998b). EGFP was inserted (junctional amino acid sequence: *Nxph1* . . . PYFPSGPGPGMVSKGEE ...EGFP... GMDELYKPGstop . . . *Nxph1* 3'-UTR) and transferred to pEX21 to generate pThy*Nxph1*C'EGFP. *Nxph1*-GFP^{tg/-} mice were produced by pronucleus injection, and PCR genotyped founder mice and progeny. Heterozygous *Nxph1*-GFP^{tg/-} mice were used to perform pull-down experiments.

Nxph3-GFP^{tg/-} transgenic mice line used in this study was designed similarly as *Nxph1*-GFP^{tg/-}, but overexpressed GFP-tagged *Nxph3* under *Thy1.2* promoter. In brief, 800 bp PCR fragment of *Nxph3* ORF from full-length *Nxph3* cDNA (Missler & Sudhof, 1998b) was cloned into *EcoRI*/*Bam*HI sites of pCMV5. The *Kpn*I site was introduced in front of the *Nxph3* stop codon through QuikChangeTM protocol (2.2.1.2), and a PCR fragment of EGFP was cloned into this *Kpn*I site to form the pCMV5-*Nxph3*C'EGFP construct. Next, a 1.5 kb of *EcoRI*-*Bam*HI fragment coding for *Nxph3*-GFP was cut from pCMV5- *Nxph3*C'EGFP and blunt-end cloned into the unique *Xho*I site of the mouse *Thy1.2* expression vector pEX*Thy1* resulting in the transgenic vector pThy*Nxph3*C'EGFP. Finally, *Nxph3* transgenic mice were generated by pronuclear injection of linear pThy*Nxph3*C'EGFP. Heterozygous *Nxph1*-GFP^{tg/-} mice were used to perform pull-down experiments.

Materials and Methods

2.1.2 Antibodies

Primary antibody	Species	Dilution WB	Producer
anti-Actin (A5060)	rabbit	1:1000	Sigma
anti-CASK (PAB2776)	rabbit	1:250	Abnova
anti- α -Dystroglycan (05-593)	mouse	1:500	Millipore
anti-GABA-A receptor α 1 (224203)	rabbit	1:500, unboiled	Synaptic Systems
anti-GABA-B receptor R1 (sc-14006)	rabbit	1:500, unboiled	Santa Cruz
anti-GFP (ab290)	rabbit	1:3000	Abcam
anti-GluN1 (114011)	mouse	1:250; 8M Urea	Synaptic Systems
Anti-GluN2A (AB1555P)	rabbit	1:250	Millipore
Anti-GluN2B (AB65783)	rabbit	1:250	Abcam
anti-GluR1 (AB1504)	rabbit	1:500	Chemical
anti-GluR2/3 (AB1506)	rabbit	1:500	Chemical
anti-GluR5 (07-258)	rabbit	1:500	Upstate
anti-mGluR3 (AB166608)	rabbit	1:1000	Abcam
anti-mGluR5 (AB5675)	rabbit	1:1000	Millipore
anti-LRRTM2 (AB106627)	rabbit	1:500	Abcam
anti-Myc (11667149001)	mouse	1:500	Roche

Materials and Methods

anti-Neurexin 123 (175003)	rabbit	1:500	Synaptic Systems
anti-Neurologin 1 (129111)	mouse	1:5000	Synaptic Systems
anti-Neurologin 2 (129203)	rabbit	1:500	Synaptic Systems
anti-Neurologin 3 (129103)	rabbit	1:1000	Synaptic Systems
anti-Neurexophilin (Loop99)	1 rabbit	1:1000	Eurogen etec
anti-Neurexophilin (F508)	1+3 rabbit	1:500	UTSW
anti-PSD95 (75-028)	mouse	1:1000	Neuro Mab
anti-Synapsin (E028)	rabbit	1:10000	UTSW
anti-SSTR5 (PA3-112)	rabbit	1:2000	Thermo Fisher
anti-turbo GFP (AB513)	rabbit	1:1000	Evrogen
Secondary antibody			
Mouse-IgG (H+L) (170-6516)	goat	1:15000	BioRad
Rabbit-IgG (H+L)	goat	1:15000	BioRad

2.1.3 Apparatus

Apparatus	Model	Company name
Acrylamidgel chamber	Mini-Protean	Bio-Rad, München
Agarose gel chamber		GE Healthcare, Freiburg
Analytic balance	LA 120S	Sartorius, Göttingen

Materials and Methods

Autoclave		Integra Bioscience, Fernwald
Bacterial shaker	Innova 40	Eppendorf, Wesslingen- Berzdorf
Benchtop Shaker		IKA, Wilmington, USA
Bath chamber	Custom made	UKM Werkstätten
Digital scale		Sartorius, Göttingen
Filter-Set	Chroma ET Filter-Set	Chroma, Olching
Gel documentary system	2D ECL	INTAS, Göttingen
Heating block		Eppendorf, Wesslingen- Berzdorf
Incubator		Sanyo, Gunama, Japan

2.1.4 Cell cultures

Human embryonic kidney (HEK293) cells (Life Technologies, Darmstadt) were used to transfect membrane-associated proteins and secreted Fc-tagged proteins.

Consumables

Consumables	Model	Company name
Plates, for Cell culture	Ø 100 mm	Corning, Wiesbaden
SDS-Page gel-loading tips	Round tip, 0.5 mm OD	Corning, Wiesbaden
Spectrophotometry cuvettes	UVette, disposable, 220 - 1.600 nm	Eppendorf, Wesslingen- Berzdorf

Materials and Methods

2.1.5 Chemicals

Chemicals	Company name
Acetic acid (AcOH)	Roth, Karlsruhe
Adenosin-5'-triphosphat disodium salt (Na ₂ -ATP)	Roth, Karlsruhe
Acrylamid-Bisacrylamid	Roth, Karlsruhe
Agarose	Biozym, Hessisch Oldendorf
Alcalic Phosphatase	NEB, Frankfurt a. M.
Ammonium acetate	Sigma, Taufkirchen
Ammoniumpersulfat (APS)	Roth, Karlsruhe
β-mercaptoethanol	Roth, Karlsruhe
Calcium chloride (CaCl ₂)	Roth, Karlsruhe
Disodium phosphate (Na ₂ HPO ₄)	Roth, Karlsruhe
DNase	Sigma, Taufkirchen
DNA- standard	Life Technologies, Darmstadt
dNTP's	Life Technologies, Darmstadt
Dithiothreiol (DTT)	Roth, Karlsruhe
Ethylenediaminetetraacetic acid (EDTA)	Roth, Karlsruhe
ECL Western Blot reagent (ECL)	GE Healthcare, Freiburg
Ethanol (70%, 96%) (EtOH)	UKM Apotheke
Ethidium bromide	Roth, Karlsruhe
GFP-Trap Magnetic Agarose	Chromotek
Glucose, D-(+)	Sigma, Taufkirchen
Glycerol	Roth, Karlsruhe
Glycine	Roth, Karlsruhe
HEPES	Life Technologies, Darmstadt
InstantBlue	Merck, Darmstadt
iProof Taq, High Fidelity DNA Polymerase	Bio-rad, München

Materials and Methods

Isopropyl alcohol	Roth, Karlsruhe
Lysozyme	Roth, Karlsruhe
Magnesium chloride (MgCl ₂)	Roth, Karlsruhe
Methanol (MeOH)	AppliChem, Darmstadt
Milk Powder	Bio-rad, München
Monosodium phosphate (NaH ₂ PO ₄)	Roth, Karlsruhe
Paraffin	Roth, Karlsruhe
Phosphate buffered saline (PBS)	BioChem, Karlsruhe
Potassium chloride (KCl)	Roth, Karlsruhe
Potassium hydroxide (KOH)	AppliChem, Darmstadt
Precision Plus Protein™ All Blue Prestained Protein Standards	Bio-rad, München
Protease Inhibitor Cocktail Set III	Merck, Darmstadt
Protein-A Sepharose beads (SephA beads)	GE Healthcare, Freiburg
Sucrose	Roth, Karlsruhe
Sodium acetate	Roth, Karlsruhe
Sodium bicarbonate (NaHCO ₃)	Roth, Karlsruhe
Sodium chloride (NaCl)	Roth, Karlsruhe
Sodium dodecylsulphate (SDS)	Roth, Karlsruhe
Sodium hydroxide (NaOH)	Roth, Karlsruhe
Tetramethylethyldiamin (TEMED)	Sigma, Taufkirchen
Tris-HCl	Roth, Karlsruhe
Triton X-100	Roth, Karlsruhe
Tryptanblue	Life Technologies, Darmstadt

2.1.6 Media and Supplements

Media and Supplements	Company name
Ampicillin	Sigma, Taufkirchen

Materials and Methods

Bovine serum albumin (BSA)	GE Healthcare, Freiburg
Dulbecco's Modified Eagle's Medium (DMEM)	Sigma, Taufkirchen
Fetal calf serum (FCS)	Life Technologies, Darmstadt
Normal goat serum (NGS)	Life Technologies, Darmstadt
NZY+-Medium	Roth, Karlsruhe
Penicillin/Streptomycin	Life Technologies, Darmstadt

2.1.7 Solutions and media for cell culture

HEK293 cell culture medium

490 ml DMEM, 5 ml penicillin/streptomycin

HEK293 cell culture medium 2% FCS

490 ml DMEM, 5 ml penicillin/streptomycin, 2 ml FCS

HEK293 cell culture medium 10% FCS

490 ml DMEM, 5 ml penicillin/streptomycin, 50 ml FCS

Calcium buffer for HEK93 transfection

250 mM CaCl₂ * 2H₂O (sterile filtrated)

Freezing medium

90% FCS, 10% DMSO

Phosphate buffer for HEK293 transfection (2X HEPES)

274 mM NaCl, 40 mM HEPES, 12 mM D(+)-Glucose, 10 mM KCl, 1,4 mM Na₂HPO₄ (pH 7.05, sterile filtered)

Solutions and media used in biochemical assays

Blocking solution

5% milk powder, 5% NGS in PBS

Materials and Methods

Homogenisation buffer

50mM Tris-HCl pH 7.5, 5 mM CaCl₂, 80 μM NaCl, 50 μl Proteinase inhibitor cocktail

Loading buffer (10x)

57% glycerol, 100 mM Tris (pH 8.0), 10 mM EDTA, 0,001% bromophenol blue

Lower Tris (for separation polyacrylamide gel)

1,5 M Tris (pH 8.8), 0.4% SDS

Lysis buffer for cells

NaCl 80mM, 50 mM Tris/HCl (pH 7.5), 5 mM CaCl₂, 1% Triton X-100, 1:100 Protease inhibitors cocktail (added just before use)

Ponceau S

0,2% Ponceau-S, 5% acetic acid

2x sample buffer +

20% glycerol, 4.6% SDS, 0.125 M Tris (pH 6,8), 5% β-mercaptoethanol, bromophenol blue

2x sample buffer with 8M urea

20% glycerol, 4.6% SDS, 0.125 M Tris (pH 6,8), 5% β-mercaptoethanol, 8M urea, bromophenol blue

SDS-PAGE 10x running buffer (for 1L)

30,3 g Tris, 144 g glycine, 10 g SDS

5x Soriano Buffer (blue, ready to load; 10 ml)

1M (NH₄)₂SO₄, 1M Tris (pH 8.0), 1M MgCl₂, 1M β-mercaptoethanol, 0,005 M EDTA, 4,528 ml dH₂O, 0,640 ml Tween 20, Bromophenol blue

STET buffer

Materials and Methods

8% sucrose, 0.5% Triton X-100, 10 mM Tris (pH 8.0), 50 mM EDTA (pH 8.0)

TE-buffer

10 mM Tris, 1 mM EDTA (pH 8.0)

TEA-buffer (50 x)

2 mM Tris, 50 mM EDTA, 4% acetic acid (pH 8.5)

Transfer Buffer for Western Blot (1L)

3g Tris, 14,4 g glycine, 20% methanol

Upper Tris (for stacking polyacrylamide gel)

0,5 M Tris (pH 8.0), 0,4% SDS

2.1.8 Molecular biology kits

Kit name	Application	Company name
QUIAEX II Gel Extraction Kit	DNA extraction	QIAGEN, Düsseldorf
NucleoSpin Plasmid	Mini-Prep	Macherey Nagel, Düren
NucleoBond PC500	Maxi Prep	Macherey Nagel, Düren
iProof™ High Fidelity	PCR	Bio-Rad, München
QuikChange® Lightning Site-directed Mutagenesis Kit	Site- Mutagenesis	Agilent Technologies, Waldbronn

2.1.9 Oligonucleotides

Oligonucleotides used for amplification of a gene of interest and site-directed mutagenesis. All oligonucleotides were produced by Sigma, Taufkirchen.

ID	Mutation	Sequence	RE	Direction
<i>Neurexin</i>				
MM08-67	Nrxn1 β -Fc	GGACATGGTCATCATTGTGGCTGT	<i>KasI</i>	Forward

Materials and Methods

			GGCTGGCGCCGTGA		
MM08-68	Nrxn1 β -Fc		CAGAGTCAGGCCGCTCACGGCGCC AGCCACACAGAGTCAG	<i>KasI</i>	Reverse
MM05-188	Nrxn1 β D137A-Fc		TGAAAGGACTCCGCTTGTGAAAGG ACTCCGCTTGTGAAAG	<i>BamHI</i>	Forward
MM05-189	Nrxn1 β D137A-Fc		AGGCCGCTCACGGCGCCAGCCACA CAGAGTCAGGTGAAAG	<i>BamHI</i>	Reverse
MM05-111	Nrxn1 α -Fc		CAGGCCGCTCCAGGCCGCTCCAGG CCGCTCCAGGCCGCTC	<i>EcoI</i>	Forward
MM05-112	Nrxn1 α -Fc		ATGGTCATCATGGTCATCATGGTC ATCATGGTCATCATGGTCATC	<i>EcoI</i>	Reverse
MM05-103	Nrxn1 α LNS2-Fc		GGACTCCGCTTGTGGACTCCGCTT GTGGACTCCGCTTGT	<i>NdeI</i>	Forward
MM05-104	Nrxn1 α LNS2-Fc		CCGCTTGTGGACTCCCGCTTGTGG ACTCCCGCTTGTGGACTC	<i>NdeI</i>	Reverse
MM08-08	Nrxn1 α LNS2 I401D-Fc		TTGTGAAAGTTGTGAAAGTTGTGA AAGTTGTGAAAG	<i>SalI</i>	Forward
MM08-09	Nrxn1 α LNS2 I401D-Fc		CATCATGGTCATCATGGTCATCCA TCATGGTCATCATGGTCATC	<i>SalI</i>	Reverse
MM08-04	Nrxn1 α LNS2 V358D-Fc		CATCATGGTTCATCATGGTTCATC ATGGTTCATCATGGT	<i>SpeI</i>	Forward
MM08-05	Nrxn1 α LNS2 V358D-Fc		AAAGGACTCCGCTTGTGAAAGAA AGGACTCCGCTTGTGAAAG	<i>SpeI</i>	Reverse
MM08-124	Nrxn1 α LNS2 L402D-Fc		CTTGTGAAAGCTTGTGAAAGCTTG TGAAAGCTTGTGAAAG	<i>ClaI</i>	Forward
MM08-125	Nrxn1 α LNS2 L402D-Fc		TGTGAAAGCTTGTGTGTGAAAGCT TGTGTGTGAAAGCTTGTG	<i>ClaI</i>	Reverse
MM08-144	Nrxn1 α LNS2 T404P-Fc		AGGACTCCGCTTGTGAAAGAAAG GACTCCGCTTGTGAAAG	<i>BamHI</i>	Forward
MM08-145	Nrxn1 α LNS2 T404P-Fc		AGGACTCCGCTTGTGAAAGAAGG ACTCCGCTTGTGAAAGA	<i>BamHI</i>	Reverse
MM08-100	Nrxn1 α ECD		ACTCCGCTTGTGAAAGAAACTCC GCTTGTGAAAGAAA	<i>EcoI</i>	Forward
MM08-101	Nrxn1 α ECD		TGTGAAAGCTTGTGATGTGAAAGC TTGTGATGTGAAAG	<i>EcoI</i>	Reverse
<i>Neurexophilin</i>					
MM08-150	Nxph1 mat		ACTCCGCTTGTGAACTCCGCTTGT GAACTCCGCTTGTGA	<i>BamHI</i>	Forward
MM08-151	Nxph1 mat		TGAAAGCTTGTGATGTGTGAAAGC TTGTGATGTG	<i>BamHI</i>	Reverse

Materials and Methods

MM09-160	Nxph3 mat	CTTGTGAAAGCTTGTGAAAGCCTT GTGAAAGCTTGTGAAAGC	Spe1	Forward
MM09-161	Nxph3 mat	CTTGTGAAAGCCTTGTGAAAGCCT TGTGAAAGC	Spe1	Reverse
MM09-140	Nxph1-GFP	CTTGTGAAAGCCTTGTGAAACTTG TGAAAGCCTTGTGAAA	Age1	Forward
MM09-141	Nxph1-GFP	TGAAAGCCTTGTGAAATGAAAGCC TTGTGAAATGAAAGCC	Age1	Reverse
MM09-17	Nxph3-GFP	GAAAGCTTGTGAAAGCCGAAAGC TTGTGAAAGCC	HindIII	Forward
MM09-18	Nxph3-GFP	AGCCTTGTGAAAGCCTTAGCCTTG TGAAAGCCTT	HindIII	Reverse
MM09-70	Nxph2-tGFP	CCGCTTGTGAACTCCGCTTGTGAA CTCCGCTTGTGA	Spe1	Forward
MM09-71	Nxph2-tGFP	AGCTTGTGATGTGTGAGCTTGTGA TGTGTGAGCTTGTGATGTGTG	Spe1	Reverse
MM09-67	Nxph4-Myc	TCCGCTTGTGAACTCCTCCGCTTGT GAACTCCTCCGCTTGTGAACTCC	Cla1	Forward
MM09-68	Nxph4-Myc	TCCGCTTGTGAACTCCTCCGCTTGT GAACTCCTCCGCTTGTGAACTCC	Cla1	Reverse

2.1.10 Plasmids

Plasmid	Description	Reference
pCI-EGFP-NR1	GluN1-GFP	Barria <i>et al.</i> , 2002
pCMV D2	Nxph1	Petrenko <i>et al.</i> , 1998
pCMV-LNS2-Ig	Nrxn1 α LNS2-Fc	C. Reissner, Münster
pCMV LNS2-I401D-Ig	Nrxn1 α LNS2 I401D-Fc	M. Klose, Magdenburg
pCMVIg-LNS2-L402D	Nrxn1 α LNS2 L402D-Fc	M. Klose, Magdenburg
pCMVIg-LNS2-V358D	Nrxn1 α LNS2 V358D-Fc	M. Klose, Magdenburg

Materials and Methods

pCMV-LNS2-T404P	Nrxn1 α LNS2 T404P-Fc	M. Klose, Magdenburg
pCMV Nrx1a-1-Ig	Nrxn1 α ECD-Fc	Ushkaryov <i>et al.</i> , 1994
pCMV Nrx1a Δ N17-Ig	Fc control protein	Reissner <i>et al.</i> 2008
pCMV5 Nrxn1a-1sol- Δ SS4	Nrxn1 α ECD	M. Klose, Magdenburg
pCMV Nrx1b-1-Ig	Nrxn1 β -Fc	C. Reissner, Münster
pCMV Nrx1b/D137R-Ig	Nrxn1 β D137A-Fc	C. Reissner, Münster
pCMV Nxph1-C'EGFP	Nxph1-GFP	Kerstin Pichotta, Münster
pCMV Nxph2-tGFP	Nxph2-turboGFP	Origene
pCMV Nxph3 #1	Nxph3	C. Reissner, Münster
pCMV Nxph3-C'EGFP	Nxph3-GFP	E. Eismann, Münster
pCMV Nxph3mat-Ig	mature Nxph3-Fc	E. Eismann, Münster
pCMV Nxph4 myc (#1)	Nxph4-Myc	V. Beglopoulos, Göttingen

2.1.11 Software

Program name	Application	Company name
ImageJ 64	WB Image analysis	NIH, Bethesda, USA
DNASTAR	Molecular cloning design	DNAStar, USA
Adobe Photoshop	creation of WB figures	Adobe Inc., USA
Adobe Illustrator	creation of WB figures	Adobe Inc., USA

2.2 Methods

2.2.1 Molecular biology methods

In this section, I describe all molecular biology methods that I had to create plasmids encoding genes of interests. These plasmids were then used to transfect cell lines, produce proteins, and test their interactions *in vitro*. Molecular cloning, which is a term used to describe the construction of plasmids includes following methods: the amplification of DNA sequences that encode proteins or fragments of proteins by polymerase chain reaction (PCR), restriction digestion of multiplied DNA fragments and DNA vectors by specific endonucleases and ligation of both components together to obtain functional plasmids. After constructed plasmids were verified by restriction digest and DNA sequencing, they were transfected in cell lines to produce soluble or membrane proteins that could be used in my PhD project

2.2.1.1 Polymerase chain reaction for cloning

Polymerase chain reaction (PCR) is a method that allows amplifying specific sequences of DNA *in vitro*. To its proper working, it requires not only the DNA template from which the segment must be multiplied but also specific primers designed to bind to two ends of this sequence, DNA polymerase, deoxyribonucleotides and buffer that contains Mg^{2+} cations required for the proper function of DNA polymerase. The annealing temperature was calculated based on % of GC of matching region in primers (melting temperature minus 3°C). PCR products were tested on an agarose gel, purified by QIAEXII gel extraction kit, digested with restriction enzymes and cloned into the vector.

Optimal primers flanking region of interest were designed with DNASTAR software. The procedure was performed according to the protocol of the manufacturer (iProof™) as follows:

Volume	Substance
14,5µl	H ₂ O
1µl	10x PCR buffer
1µl	dNTPs
1µl	Forward primer

Materials and Methods

1µl	Reverse Primer
1µl	DNA template
0,5µl	DNA polymerase

and the following program was applied:

Cycle step	Temperature	Time	Number of cycles
Initial denaturation	98°C	30 s	1
Denaturation	98°C	5-10 s	
Annealing	45-72°C	10-30 s	25-35
Elongation	72°C	15-30 s / kb	
Final elongation	72°C	5-10 min	1
Store	4°C	end	

2.2.1.2 In vitro site-directed mutagenesis using QuikChange Kit

To introduce point mutations on plasmids carrying recombinant genes of interests, I used QuikChange Kit. This site-specific mutagenesis of double-stranded plasmids is based on the PCR method and requires two synthetic oligonucleotide primers containing the desired point mutation. Extension of the oligonucleotide primers generates a mutated plasmid containing staggered nicks. Following temperature cycling, the product is treated with *DpnI* for 5 min at 37°C, leaving newly synthesised non-methylated DNA untouched. The *DpnI* endonuclease is specific for methylated DNA and is used to digest the parental DNA template and to select for mutation-containing synthesised DNA. DNA isolated from almost all *E. coli* strains is dam methylated and therefore susceptible to *DpnI* digestion. The nicked vector DNA containing the desired mutations was transformed into chemical-competent cells (2.2.1.3) supplied by manufacturer or stored at -20°C until were needed.

The reaction mixture for mutagenesis PCR:

Materials and Methods

Volume	Substance
5 µl	10x reaction buffer
1 µl	dNTP mix
1 µl	Forward primer
1 µl	Reverse primer
1,5 µl	Quik solution reagent
39,5 µl	dH ₂ O
1 µl	QuikChange Lighting enzyme

Thermal cycling

Cycle step	Temperature	Time	Number of cycles
Initial denaturation	95°C	2 min	1
Denaturation	95°C	20 sec	18
Annealing	60°C	10 s	
Elongation	68°C	30 sec/kb	
Final elongation	68°C	5 min	1
Store	4°C	end	

2.2.1.3 Heat pulse transformation and culturing on plates

E.coli XL10-Gold ultracompetent cells were transformed with mutated plasmid DNA by the heat pulse method. 45µl aliquot of cells was taken from -20°C, gently thawed on ice and transferred to pre-chilled 14 mL round-bottom Snap tube. 2µl of β-mercaptoethanol was added to cells and incubated on ice for 2 min. 2µl of *DpnI*-treated PCR products were added, gently mixed and incubated for 30 min on ice. Snap tubes were placed in a pre-warmed water bath (42°C) for the 30s. Next, tubes were incubated on ice for 2 min, 0,5mL of preheated (42°C) NZY⁺-medium was added and incubated for 1h at 37°C under shaking at 250 rpm. Each transformation reaction was plated on LB-agar plates containing appropriate antibiotics (1:1000). Transformation plates were incubated at 37°C for less than 16h.

2.2.1.4 Express Mini (Holmes and Quigley, 1981)

This standard procedure of quick isolation of plasmids from *E.coli* cells was first described by Holmes and Quigley (Holmes and Quigley, 1981). In this method, cell membranes are being enzymatically destroyed, which allows purifying enough DNA that can further be used to perform restriction analysis of, e.g., mutated constructs obtained by QuikChange™.

5 ml LB medium with an appropriate antibiotic (1:1000) were inoculated with single colonies from LB agar plates and grown overnight at 37°C under shaking at 250 rpm. Next day, 1,5ml of culture aliquot was spun down at 12.000xg for 1 min and resuspended with 300 µl STET-buffer. The remainder (3,5 ml) of the overnight culture was spun down, and pellets were stored at -20°C until usage for Mini-Prep of successfully identified clones. Freshly prepared 25 µl of lysozyme (10 mg/ml) was added to the STET mixture and incubated precisely for 45 s at 99°C. This was followed by centrifugation for 10 min at 12.000xg at RT and pellets were removed by toothpicks. Soluble DNA in supernatant was precipitated by 50 µl sodium acetate and 500 µl 100% ethanol through centrifugation for 15 min at 12.000xg rpm at RT. The supernatant was discarded, and remaining DNA pellets were washed briefly by rinsing with 500 µl ice-cold (-20°C) 70% ethanol. Pellets were dried for 15 min at 37°C and resuspended (10 min, 50°C) in 30µl 10mM Tris-HCl buffer pH 8.5 and directly proceed with endonuclease restriction digestion.

2.2.1.5 Restriction enzyme digestion of DNA

Restriction enzyme digestion of DNA is a method used for molecular cloning of DNA and to identify positive clones after site-directed mutagenesis. This happens with the help of bacterial endonucleases that cut double-stranded DNA at specific palindromic recognition sites. Digest occurred overnight in 20-50 µl reaction volume at 37°C or other temperature, suggested by the manufacturer. NEB recommended buffers used. Approximately 300 ng of DNA was needed, and reaction last for minimum 1h.

Reaction mixture:

Volume 20	Volume 50	Substance
2 µl	5 µl	10x reaction buffer
2 µl	5 µl	DNA plasmid

Materials and Methods

0,4 µl	1 µl	Restriction enzyme (1 U/µl)
15,6 µl	39 µl	dH2O

2.2.1.6 Agarose gel electrophoresis

DNA fragments can be easily separated by agarose gel electrophoresis according to their size, where the smaller the fragment is, the faster it migrates (Meyers *et al.*, 1976). Gel concentration varies from 0,8 % to 1,2 %. Bigger fragments migrate better in higher gel concentrations, and smaller fragments separate better in low concentrated gels. 0,56 g or 2,4 g of agarose were dissolved accordingly in 70 ml or 300 ml of 1x TAE buffer in a microwave. After the solution was cooled down, ethidium bromide was added to the final concentration of 1µg/µl (1:10000). Agarose solution was poured to the chamber, and the comb was placed in it. After cooling at RT, the gel was placed in the electrophoresis chamber and covered with 1x TAE buffer. Samples were mixed 6 to 1 with loading buffer and were loaded on a gel next to a DNA molecular weight standard. Samples migrated at 80V for a small gel and at 120V for a big gel for around 30-60 min. After electrophoresis bands were made visible by UV transilluminator and photographed. The size of DNA bands was estimated by a DNA molecular weight marker that migrated together with samples on a gel.

2.2.1.7 Purification of DNA by QIAEX[®] II Gel Extraction Kit

QIAEX[®] II Gel Extraction Kit (QIAGEN) was used to isolate DNA fragments from agarose gels. It is commonly used as a purification step after DNA restriction digest or PCR reactions. In this method DNA bands of the correct size can be easily extracted after electrophoresis, bound to the affinity resin to purify them from agarose and eluted to obtain pure DNA fragments. DNA bands were cut out from agarose gel and put into a 1,5 ml microcentrifuge tubes. 750 µl QX1-buffer (pH-indicator) and 12 µl of QIAEX[®] DNA-binding beads suspension was added to tubes and incubated at 50°C for 10 min under shaking (1200 rpm) on a heating block. Beads were precipitated (11.000xg for 30s), washed once with QX1-buffer and twice with PE-buffer. Resulting pellets were air-dried for about 15 min before DNA was eluted by

Materials and Methods

incubation in 20 µl dH₂O at 50°C for 5 min after final centrifugation (11.000xg for 30s) supernatants contain purified DNA fragments.

2.2.1.8 Dephosphorylation of 5' DNA ends

To prevent vector re-ligation during cloning procedures in which vector has been cut with only one enzyme or a blunt-ended, 5' phosphate groups were removed by treatment with 1 µl alkaline phosphatase at 37°C for 30 min.

2.2.1.9 Ligation

The amplified PCR fragment was cloned into the vector with T4 DNA-ligase at 16°C overnight. The ligation mixture contained the vector and the PCR fragment of interest in a molar ratio of 1:5.

The following reaction mixture was used:

Volume	Substance
12 µl	dH ₂ O
1 µl	Vector DNA (~2100 bp, 40ng/µl)
1 µl	Insert DNA (~700 bp, 40ng/µl)
1 µl	Ligation buffer 10x
1 µl	T4 DNA Ligase (400 U/µl)

2.2.1.10 Electrotransformation of bacteria with plasmid DNA

Electrotransformation is a technique in which an electrical field is applied to cells to increase the permeability of the cell membrane, allowing DNA to be introduced into the cell (Neumann *et al.*, 1982). It is used in molecular biology to transform *E.coli* cells with plasmid DNA, which happens once cells are exposed to high voltage (2,5 kV). 160 ng of plasmid DNA (ligation mixture diluted 1:4 with TE for mini-prep or 1:300 for maxi-prep) was mixed with 40 µl of electro-competent bacterial cells, which were kept on ice for 45s in advance. The mixture was transferred to an ice-cold electroporation cuvette (0.2 cm, BioRad) and pulsed at 2,5 kV in a pulser (E.coli Pulser, BioRad). Electroporated bacteria were then mixed with 1 ml of LB medium and incubated at 37°C for 1h under shaking (250 rpm) in snap tubes. For mini-prep DNA preparation, bacteria were then plated on LB agar plates containing appropriate

Materials and Methods

antibiotic (1:1000) and grown overnight at 37°C. For maxi-prep DNA preparation, 4 ml of LB medium was added to each tube along with proper antibiotic and incubated for further 4h. 1 ml of culture was then added to 500 ml of LB medium containing antibiotics (kanamycin or ampicillin; 1:1000) and incubated overnight at 37°C.

2.2.1.11 Plasmid DNA mini-preparation (NucleoSpin® Plasmid)

Minipreparation of plasmid DNA is rapid, small-scale isolation of plasmid DNA from bacteria. Mini-preps are used in the process of molecular cloning to analyse bacterial clones transformed with plasmids. Purification of plasmid DNA from bacterial cells required for DNA sequencing (GATC, Konstanz) was performed by using NucleoSpin® Plasmid kit (Macherey-Nagel). An *E.coli* cell pellet from 3,5 ml overnight culture was resuspended in 250 µl buffer A1 by pipetting. After the addition of buffer A2, the tube was gently inverted 6-8 times, and the solution was incubated for a maximum of 5 min at RT. Neutralisation was done by addition of 300 µl of buffer A3 and inverting 6-8 times again to avoid isolation of genomic DNA. The mixture was spun down for 5 min at 11.000 xg at RT and obtained supernatant was placed on DNA-binding matrix Spin-columns. DNA was bound to the matrix by centrifugation for 1 min at 11.000 xg rpm, and flow-through was discarded. Silica membrane was washed by preheated (50°C) 500 µl AW buffer and 600 µl buffer A4 followed by centrifugation for 1 min at 11.000 xg. After removal of flow-through, silica membrane columns were dried by an additional centrifugation for 2 min at 11.000 xg rpm. DNA was eluted after incubation with 50 µl buffer AE for 1 min at RT, followed by centrifugation at 11.000 xg for 1 min.

2.2.1.12 Plasmid DNA maxi-preparation (NucleoBond® PC500)

Maxi-preparation is a technique of plasmid DNA isolation, which allows obtaining high concentrated plasmid DNA for long time storage. Here, I used NucleoBond® PC 500 kit (Macherey-Nagel). 500 ml of bacterial cell culture (*E.coli* XL-Blue MRF) was spun down for at 6.000xg 4°C for 15 min. Pellet was carefully resuspended in 12 ml RES buffer (containing RNase A). After addition of 12 ml of LYS buffer (provided by manufacturer) cell suspension was gently mixed by inverting and afterwards incubated for 5 min at RT. Next, 12 ml of NEU buffer (provided by manufacturer) was added to stop cell lysis, and the mixture was loaded on pre-equilibrated NucleoBond® column by 25ml of EQV buffer (provided by manufacturer).

Materials and Methods

NucleoBond® columns contain filter and matrix, which bind plasmid DNA. Flow-through was discarded, and 15 ml of EQV buffer was added on a filter. Next, the filter was discarded, and the column matrix was washed by 25 ml of WASH buffer. Flow-through was discarded, and 15 ml of ELUTION buffer (provided by manufacturer) was added, and the through-through was collected in 50 ml falcon tube. This was followed by addition of 10,5 ml of isopropanol and briefly vortexing to precipitate DNA. Tubes were then centrifuged at 15.000 rpm at 4°C for 30 min. After discarding the supernatant 4ml of 70% ethanol was added to DNA pellet, which was followed by centrifugation at 15.000 rpm at RT for 5 min. DNA-pellet was dried at RT for 15-30 min and then dissolved in 500 µl of TE buffer on a Thermo block preheated to 37°C.

2.2.1.13 Concentration analysis of plasmid DNA

Determination of double-stranded plasmid DNA was done using UV spectrophotometer (Eppendorf). DNA was diluted 1:60 in water and absorbance in 260 nm was measured as well as the ratio of 260 nm / 280 nm. The DNA concentration for mini-preparation is typically around 100-300 ng/ml, while for maxi-preparation is around 1-5 µg/µl. Optimal 260 nm / 280 nm ratio was 1.8.

2.2.1.14 DNA-sequencing and sequence analysis

GATC Biotech AG, Konstanz performed DNA sequencing. Plasmid DNA was diluted to 100 ng/µl in 10mM Tris (pH 8.0). Sequencing data were analysed using SeqMan software (DNASStar).

2.2.1.15 Preparation of mouse genomic DNA for PCR

Genotyping of mice was performed to verify if mice specimens are transgenic. Verification occurred by the PCR from genomic DNA that was isolated from the tissue. Earpieces were added to 0,5 ml SNET buffer with 0,25 mg/ml proteinase K and incubated at 55°C overnight. 200 µl of tissue lysate was transferred into an Eppendorf tube, mixed with the same amount of phenol-chloroform-isoamyl alcohol and centrifuged at 18.000 xg for 10 min. The supernatant was transferred to a new tube, and 150 µl of isopropanol was added. The tube was incubated on ice for 5 min, followed by centrifugation at 16.000 xg for 10 min. The supernatant was removed carefully, and the pellet was dried at RT. The pellet was resuspended in 200 µl of TE buffer, and genomic DNA was used in further steps of genotyping.

Materials and Methods

2.2.1.16 PCR for genotyping of *Nxph1-GFP^{tg/-}* and *Nxph3-GFP^{tg/-}*

PCR was used for regular genotyping of transgenic mice. Genomic DNA was first extracted from the tissue as described (the above one). PCR reaction, in this case, requires amplification of GFP fragments of DNA in 5xSoriano buffer that contains bromophenol blue. After PCR samples are ready to be loaded on a gel.

The following reaction mixture was used:

Volume	Substance
12 µl	dH2O
1 µl	dNTPs
2,5 µl	DMSO
0,2 µl	BSA (10 mg/µl)
1 µl	Primer forward 10 µM
1 µl	Primer reverse 10 µM
5 µl	5x Soriano buffer
0,1 µl	Invitrogen Taq
4 µl	DNA

following PCR program was used for *Nxph1-GFP^{tg/-}*:

Cycle step	Temperature	Time	Number of cycles
Initial denaturation	93°C	10 min	1
Denaturation	93°C	30 sec	40
Annealing	55°C	45 s	40
Elongation	65°C	2 min	40
Final elongation	65°C	10 min	1
Store	4°C	end	

Materials and Methods

following PCR program was used for Nxph3-GFP^{tg/-}:

Cycle step	Temperature	Time	Number of cycles
Initial denaturation	93°C	10 min	1
Denaturation	93°C	30 sec	40
Annealing	63°C	45 s	40
Elongation	65°C	2 min	40
Final elongation	65°C	10 min	1
Store	4°C	end	

Genotyping of Nxph1-GFP^{tg/-} was performed using the following primers to amplify a transgenic allele with a product length around 600 bp: MM06-68 (5'-GCTGAGGTATTCATCATGTGCTCCG) versus MM06-69 (5'-CAAGTAGACGGTGGGCTGCAGG).

Genotyping of Nxph3-GFP^{tg/-} was performed using the following primers to amplify a transgenic allele with a product length around 600 bp: MM06-68 (5'-GCTGAGGTATTCATCATGTGCTCCG) versus MM06-70 (5'-GGCTGATGGAGATGTTACCCTGGC).

2.2.2 Biochemical procedures

To investigate protein-protein interactions, I used three types of experiments. First, I co-expressed Fc-tagged LNS2 variants with neurexophilins in HEK293 cells to test if all members of neurexophilin family share the same binding epitope to Nrnx1 α . In this case, co-expressed proteins were secreted to the medium and purified from other medium components by protein A agarose beads (Reissner *et al.*, 2014). Second, brain pull-down assays where I tested which proteins bind to neurexin/neurexophilin complex. In this case, brain tissue must be first lysed to release synaptic proteins from cell compartments and membranes. This allows testing if free brain proteins can precipitate with the GFP-trap or Fc-tagged fusion proteins. Third, the recombinant protein pull down assay from HEK293 cells lysates. In this case, GluN1-GFP was

Materials and Methods

expressed in HEK293 cells and later purified by pull-down with Fc-tagged proteins. Results of all types of experiments were revealed by western blot.

2.2.2.1 Cryonic storage and re-cultivation of HEK293 cells

To express recombinant proteins, I used a mammalian HEK293 cell line. HEK (Human Embryonic Kidney) cells were derived from embryonic kidney tissue and are modified by shared adenoviral Ad5 DNA (Thomas and Smart, 2005). HEK293 are preserved by cryonic storage in liquid nitrogen to ensure a continuous cell supply. Cells were detached from culture dishes with 0,25% trypsin-EDTA, centrifuged at 300 g at RT for 5 min and resuspended in freezing medium. „Slow down freezing” was done for 2-3 days at -80°C until tubes were stored in liquid nitrogen.

Thawing of cells was carried out using a water bath preheated to 37°C. Afterwards, cells were collected in pre-warmed 10% FCS DMEM medium, centrifuged at 300 xg at RT for 5 min, resuspended in fresh 10% FCS DMEM culture medium and incubated at 37°C with 5% CO₂ in culture dishes.

2.2.2.2 Expression of proteins in HEK293 cells

The calcium phosphate method allows modifying HEK293 cells to express recombinant proteins genetically. The procedure is based on a slow mixing of HEPES-buffered saline containing sodium phosphate with a CaCl₂ solution containing plasmid DNA. The DNA–calcium phosphate co-precipitates adhere to the cell surface and are taken up by the cell, presumably by endocytosis (Kingston *et al.*, 2001). All the recombinant proteins cloned on designed plasmids are expressed from the CMV promoter, which allows sufficient gene expression in HEK293 cells. One day before transfection cells were split with trypsin-EDTA, plated on 10 cm dishes and maintained at 37°C, 5% CO₂ in Dulbecco’s modified Eagle’s medium (DMEM) supplemented with 10% fetal calf serum (FCS) and 5% penicillin-streptomycin.

Transfection procedure: 28 µl of plasmid (8-16 µg/µl) in TE (10mM Tris, pH 8, 1mM EDTA) was mixed with 672 µl of 250 mM CaCl₂ and 700 µl of 2x HEPES buffer (50 mM HEPES, 280 mM NaCl, 1.5 mM Na₂HPO₄, pH 7.05). The mixture was incubated for 20 min at room temperature and dropped on 10 cm Petri dishes with cells. Fresh FCS-free medium was provided after 16 h of incubation and cells maintained for another 48 h at 37°C till harvesting.

2.2.2.3 Preparation of HEK293 homogenates

Cells transfected with plasmids encoding membrane proteins of interests were harvested 72h after transfection. Sets of 5 dishes were scrapped and transferred together with medium to 50 ml tubes and centrifuged at 300 xg RT for 5 min. The supernatant was discarded, cells were resuspended in 1ml of the Lysis Buffer. Lysates were incubated at 4°C for 30 min under rotation, which was followed by centrifugation for 10 min at 15000 xg to get rid of cells debris. The supernatant was collected and used for pull-down experiments. A small aliquot of the lysate was taken and mixed with 2xSB+ sample buffer in 1:1 ratio, boiled at 99°C for 5 min and stored at -80°C to test it on polyacrylamide gels.

2.2.2.4 Membrane protein extraction from rodent brain

To perform pull-down experiments from mice brains, a protocol for extraction of proteins from tissues was used. Mice were killed by cervical dislocation, and forebrains were quickly dissected out from the skull without brainstems. Each forebrain was placed in a single cold round-bottom tube and homogenised in 2 ml ice-cold homogenisation buffer. Brains were homogenised by Polytron homogeniser at 22000 xg for 30s. Next, the lysis buffer was added in a ratio of 1:1 and homogenate were left under rotation at 4°C for 2h. Brain lysates were centrifuged at 220000 xg at 4°C for 30 min (MLA-55, Beckmann). The supernatant was recovered and immediately used for pull-down experiments. A small aliquot of the brain lysate was taken and mixed in 1:1 ratio with 2x Sample Buffer to test it on polyacrylamide gels. Pulldown samples had to be prepared by three different procedures depending on which proteins of interest I wanted to immunodetect. First, incubated with 2xSB at RT under rotation for 20 min to detect GABA_AR α 1 and GABA_BR R1. Second, boiled at 99°C for 5 min in 2xSB supplemented with 8 M Urea to detect NMDAR GluN1, GluN2A and GluN2B subunits. Third, boiled with 2xSB at 99°C for 5 min to detect all other proteins, e.g., Neurexins and Neuroligins.

2.2.2.5 Pull-down experiments with the GFP-Trap

GFP-Trap is an affinity resin used for immunoprecipitation of GFP-fusion proteins. It consists of an anti-GFP nanobody coupled to magnetic agarose beads. Once nanobodies are bound to GFP-fusion proteins, the complexes can be easily separated in the magnetic field. I used GFP-trap in brain pull-downs with transgenic mice lines

Materials and Methods

overexpressing GFP-tagged N_xph1 and N_xph3. 20 µl of the GFP-Trap was added to the volume of the brain lysates representing a single brain and rotated at 4°C overnight. Experiments also included a negative control consisted of magnetic agarose beads without anti-GFP nanobody. I added 20 µl of control to the volume of a lysate that represents a single brain. On the next day, resins were collected by placing tubes on a magnetic rack that allows separation of magnetic beads from brain lysates. Resins were washed three times in H-buffer containing 0.1% Triton X at 4°C for 5 min. Samples were eluted in three different ways based on which proteins wanted to be immunodetected by western blot assay: elution in 80 µl of 2x sample buffer and rotation at RT for 20 min to detect GABA_AR α1 and GABA_BR R1, elution in 80 µl 2x sample buffer supplemented with 8 M urea followed by boiling at 99°C for 10 min to detect NMDAR GluN1, GluN2A and GluN2B subunits or elution in 80 µl 2x sample buffer followed by boiling at 99°C for 10 min to detect all other proteins. Supernatants were collected by separation of magnetic beads from supernatant on magnetic racks and directly proceeded with SDS-PAGE or were frozen at -80°C.

2.2.2.6 Pull-down experiments with Fc-tagged proteins

Fc-tagged extracellular domains of proteins produced in HEK293 cells allow investigating protein interactions in vitro. Once fusion proteins are being secreted to the medium, they can be bound to protein A beads (25µl per medium collected from 5 plates) and used for pull-down experiments. Binding of protein A to Fc-tagged proteins occurs under rotation at 4°C overnight, followed by washing three times for 5 min in 50mM Tris-HCl pH 7.5. To estimate the amount of protein bounded to beads that can be used in a pull-down experiment, 1/10 of beads must be boiled for 5 min at 99°C, loaded on SDS-PAGE and stained by coomassie as described. Proper even amounts of beads must be added to the brain or cell lysate and left on rotation at 4°C overnight. On the next day, beads must be washed three times for 5 min in H-buffer+0.1% Triton X. Next, beads are boiled at 99°C for 5 min in 2xSB+ in three different ways as described above (2.2.2.5). Samples can be tested directly by Western Blot or froze at -80°C.

2.2.2.7 Polyacrylamide gel electrophoresis (SDS-PAGE)

SDS-PAGE is an electrophoresis technique that allows separation of proteins by their molecular weight in response to an electric field. First, protein samples are being

Materials and Methods

denatured in a sample buffer containing SDS and β -mercaptoethanol at 99°C or RT. SDS provides negative charge to proteins, which then migrate in a gel irrespective of their isoelectric point. β -mercaptoethanol reduces disulphide bonds which allows separation of multisubunit into monomers. To allow the best separation, gel concentration varies from 7,5% to 15% depending on the size of the protein. To separate high molecular weight proteins, lower gel concentration was used, while higher concentration is better to separate low molecular weight proteins.

Protein electrophoresis equipment (BIORAD) was used to prepare gels. The glass walls from the gel casting apparatus were cleaned with water and soap. The separation gel was poured first, covered with a thin layer of distilled water and left to polymerise (20-40 min). Next, the water layer was removed, the stacking gel was poured on the top of the separation gel, and then comb with ten pockets was inserted. After polymerisation (10-15 min), the comb was removed, the gel cassette was placed into the electrophoresis chamber and covered with 1x Running Buffer. Before running the gel, protein samples must be first denatured as described in sections 2.2.2.4, 2.2.2.5 and 2.2.2.6. 20 μ l of lysate and 40 μ l of sample mix was loaded on the gel. The electrophoresis was running at 100V till the head reached the separation gel, and then at 200 V for another 30-40 minutes. After the electrophoresis gel was directly used for immunoblotting or coomassie staining.

ingredient	Separation gel				Stacking gel
	7,5%	10%	12%	15%	3,75%
dH ₂ O	2.5ml	2.5ml	1.75ml	1.5ml	1,25ml
Tris Buffer*	1.25ml	1.5ml	1.25ml	1.5ml	0,5ml
AMBA	1.25ml	2ml	2ml	3ml	0,25ml
10% APS	15 μ l	17 μ l	15 μ l	17 μ l	12 μ l
Temed	7 μ l	8 μ l	7 μ l	8 μ l	5 μ l

* Tris buffer, for separation gel pH 8,8 (lower tris) and pH 6,8 for stacking gel (upper tris).

2.2.2.8 Western blotting

Western blotting is a technique that allows detection of proteins using specific antibodies. Protein samples separated by SDS-PAGE have to be first transferred electrophoretically to a nitrocellulose membrane to allow immunodetection.

2.2.2.8.1 Protein transfer from a gel to a nitrocellulose membrane

Once SDS-PAGE is finished the separation gel must be assembled in a transfer cassette together with other components in the following order: sponge, blotting paper, separation gel, nitrocellulose membrane, blotting paper, sponge. This „sandwich” must be placed in a chamber filled with ice-cold transfer buffer. Protein transfer occurs at 100 V for 1,5 h or 14 V at 4°C overnight. After the transfer cassette must be disassembled to remove the membrane. Quick Ponsou S staining was performed (5-10min) to check the efficiency of protein transfer rapidly. The background was destained with water, and the membrane was photographed for documentation.

2.2.2.8.2 Immunodetection

The first step of every immunodetection process is a 1 h incubation of the membrane in the Blocking Solution to reduce non-specific binding to the proteins. Next, the membrane has to be incubated with the primary antibody designed to bind a specific epitope of the protein of interest. Incubation, last overnight at 4°C in blocking solution on a shaking platform and antibody concentration, used varies depending on the manufacturer instructions. On the next day, the membrane has to be washed three times for 5 min in PBS-TWEEN followed by incubation with the secondary antibody in 1:15000 dilution at RT. After that, the membrane has to be rewashed three times for 15 minutes at RT with PBS-TWEEN on a shaking platform. The immunodetection occurs because heavy chains of secondary antibodies are labelled with horseradish peroxidase (HRP), which allows detection by chemiluminescence (ECL). In this process, HRP reduces hydrogen peroxide and resulting active oxygen oxidases luminol which releases light that can be detected. The ECL reaction was done according to the manufacturer protocol (Biorad) in which reagents 1 and 2 had to be mixed in a ratio of 1:1 and the mixture had to be placed on a membrane followed by incubation for 5 min at RT. The membrane must be placed in a dark chamber where

Materials and Methods

the camera detects emitted light after 10 s, 1 min and 10 min of developing. Pictures are saved in a Western Blot documentation system (Biorad).

2.2.2.9 Coomassie staining

To test amounts of bound Fc-tagged proteins to protein, A beads Coomassie staining of SDS-PAGE gel was performed. Beads must be boiled in sample buffer at 99°C for 5 min and tested by SDS-PAGE followed by coomassie staining by InstantBlue on a shaking platform at RT for 15 min. Once proteins are visible gel must be briefly washed in water, photographed, and analysed by ImageJ software.

Results

3.1 The differences between neurexophilins

In my research, I focused on neurexophilins and their physical interactions with neurexins and other synaptic proteins. I performed experiments with recombinant neurexophilins, expressed in heterologous gene expression systems (Nxph1, Nxph2, Nxph3, Nxph4) and transgenic mice overexpressing GFP-tagged variants of Nxph1 and Nxph3. Although all four Nxph protein sequences have similar lengths, I observed remarkable differences in molecular weight between calculated and observed sizes of neurexophilins during the initial phase of my study. To make identification of the differently sized bands on immunoblots safe, I started by analyzing and summarizing the size differences.

3.1.1 Nxph1

The calculated molecular weight of the mature rat Nxph1 is ~17 kD [D=1g/mol], but the observed molecular weight of recombinant non-tagged rat mature Nxph1 expressed in HEK293 cells is ~25 kD (Fig 3.1, lane 1). The possible explanation for such a difference in size might be glycosylation. There are three conserved N-glycosylation sites at amino acid positions N146, N156, and N162 present in all four neurexophilins (Fig. 1.3). Analysis of the glycosylation pattern by mass spectrometry showed that two N-glycosylation sites of Nxph1 are occupied by complex type glycans and one by high mannose-type oligosaccharides (Reissner *et al.*, 2014). These three N-linked glycans add ~8 kD difference to the calculated molecular weight ~17 kD, resulting in an observed molecular weight of Nxph1 ~25 kD (Table 1).

For the Nxph1-GFP expressed in HEK293 cells, the observed molecular weight is ~52 kD, which fits the observed molecular weight of non-tagged Nxph1 extended by the size of the ~27 kD GFP tag (Fig 3.1, lane 2). In my work, I also performed brain pull-down experiments on transgenic mice overexpressing Nxph1-GFP (Nxph1-GFP^{tg/-}). Nxph1-GFP was precipitated as a single ~52 kD band from the brain lysate (Fig. 3.1, lane 3), which corresponds to a calculated molecular weight of the mature Nxph1-GFP (Table 1).

Results

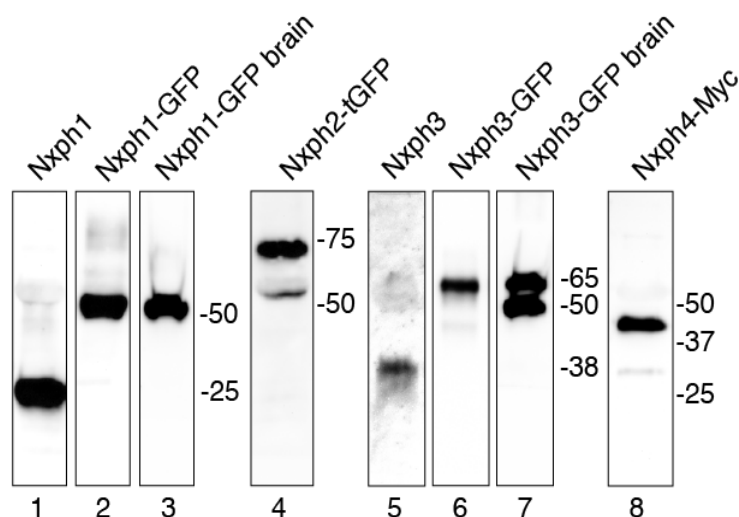


Figure 3.1. Immunoblot alignment of Nxph1, Nxph2, Nxph3 and Nxph4 variants used in this project. Rat non-tagged Nxph1 and Nxph1-GFP expressed in HEK293 cells are visible at the molecular weight of ~25 kD in lane 1 (anti-Nxph1, Eurogenetec, 1:1000, Rabbit) and ~52 kD band in lane two respectively (anti-GFP, Abcam, 1:3000, Rabbit). Nxph1-GFP overexpressed in mice brains is visible in lane three as a 52 kD band (anti-GFP, Abcam, 1:3000, Rabbit). Rat Nxph2-tGFP expressed in HEK293 cells is present as two bands of ~52 kD and ~70 kD in lane 4 (anti-tGFP, Evrogen, 1:1000, Rabbit). Rat non-tagged Nxph3 and Nxph3-GFP expressed in HEK293 cells are visible at the molecular weight of ~38 kD in lane 1 (anti-Nxph3, F508, 1:500, Rabbit) and ~65 kD in lane 6 (anti-GFP, Abcam, 1:3000, Rabbit). Nxph3-GFP overexpressed in mice brains shows two bands of ~52 kD and ~65 kD in lane 7 (anti-GFP, Abcam, 1:3000, Rabbit). Rat Nxph4-Myc expressed in HEK293 cells is present as two bands of ~30 kD and ~40 kD in lane 8 (anti-Myc, Roche, 1:500, Rabbit).

3.1.2 Nxph2

Nxph2 was expressed in HEK293 cells as a rat tGFP tagged variant. Nxph2-tGFP is present as two bands on western blot: the prominent ~70 kD and the less intense 52 kD band (Fig. 3.1, lane 4). The mature Nxph2 has precisely the same sequence length as mature Nxph1 and Nxph3 and is also proteolytically digested after KXKK motif (Fig. 1.3). Nxph2 used in this experiment is C-terminally turbo-GFP tagged, which has the same molecular weight as a GFP tag (~27 kD). It was cloned from copepod *Pontellina plumata* gives stronger green signal than the classical GFP (Shagin *et al.*, 2004). The calculated molecular weight of the mature Nxph2-tGFP is 44 kD (Table 1), which, combined with 3 N-glycans, fits the observed molecular weight of 52 kD. However, Nxph2-tGFP is also observed as a higher, more intense band of ~70 kD

Results

(Fig. 3.1, lane 4). Full-length pro-Nxph2 that is not exposed to proteolytic processing is longer and has an additional N-glycosylation site at position N92 (Fig. 1.3). The calculated molecular weight of pro-Nxph2-tGFP is 54 kD, and it has four N-glycosylation sites. Therefore, observed value fits more to the calculated weight of the pro-Nxph2-tGFP that was not processed through proteolytic digest after KFKK motif. This might be caused by the turbo-GFP tag that hinders the processing of pro-Nxph2-tGFP to its mature form.

3.1.3 Nxph3

Surprisingly, although mature Nxph3 and Nxph1 have precisely the same sequence length (Fig. 1.3), the observed molecular weight of non-tagged Nxph3 expressed in HEK293 cells is ~38 kD (Fig 3.1, lane 5). The difference of ~13 kD in size between Nxph1 and Nxph3 cannot represent different glycosylation type of Nxph3 since both mature forms of Nxph1 and Nxph3 share the same three N-glycosylation sites (Fig. 1.3). The explanation for the molecular weight difference between mature forms of Nxph1 and Nxph3 might be another proteolytic cleavage site in Nxph3. Proteomic data shows that Nxph3 has a second cutting site, which occurs closer to its N-terminal part after RKG motif (Fig. 1.3, Arg-50), making the mature Nxph3 sequence longer than Nxph1 (Missler and Südhof, 1998). Different processing of Nxph3 changes the length of the mature protein and adds a fourth N-glycosylation site at position N62 (Fig. 1.3). The calculated molecular weight of the mature Nxph3 is ~22 kD, which makes it already ~5 kD higher (Table 1). Four glycosylation sites give an additional ~16 kD, which fits the observed molecular weight of ~38 kD (Fig 3.1, lane 5; Table 1). Another possible explanation of the higher molecular weight of Nxph3 might be the lack of proteolytical processing when cells are expressed in HEK293 cells. The calculated molecular weight of the pro-Nxph3 is 27 kD, but together with the same four already mentioned N-glycosylations gives 37 kD, which is closer to the observed molecular size of 38 kD.

The observed molecular weight of the recombinant Nxph3-GFP is ~65 kD, which fits the observed molecular weight from non-tagged recombinant Nxph3 (~38 kD) extended by the size of the GFP tag (Fig 3.1, lane 6). In my experiments, I also performed pull-downs from transgenic Nxph3-GFP^{tg/-} mice brains. Results from transgenic mice overexpressing Nxph3-GFP show two ~52 kD and ~65 kD bands

Results

precipitated from brain lysates (Fig. 3.1, lane 7). Since the upper band fit the size of the recombinant Nxph3-GFP expressed in HEK293 cells, the lower band might be a less glycosylated form of Nxph3-GFP, which fits the calculated mature Nxph3-GFP without glycosylation ~52 kD. Another explanation for the lower band is that it is on the same molecular weight as Nxph1-GFP, suggesting that some population of pro-Nxph3-GFP is proteolytically processed not only from RKG motif but also from KXKK proteolytic cleavage site (Table 1). The alternative idea is that C-terminal GFP-tag might hinder proteolytic cleavage of Nxph3-GFP after RKG sequence, giving two populations of Nxph3-GFP with different molecular weights.

3.1.4 Nxph4

Rat Nxph4-Myc was only tested in the recombinant experiment while co-expressed in HEK293 cells. Nxph4-Myc is present as two bands: the intense higher ~40 kD and the lower ~30 kD (Fig. 3.1, lane 8). Nxph4 is unique compared to the other three neurexophilins because it has an additional 50 glycine- and proline-rich residues long loop that connects Nxph1 analogues of β 4 and β 5 sheets (Wilson *et al.*, 2019). Mature Nxph4 is also processed after KXKK motif and possesses 3 N-glycosylation sites as Nxph1 (Fig. 3.1). Myc-tag is a ten amino acid residues tag of the size of 1,2 kD. The calculated molecular weight of the mature Nxph4-Myc is 23 kD, which with N-glycans of ~8 kD (Reissner *et al.*, 2014) fits the observed lower band of Nxph4-Myc. Pro-form of Nxph4 has an additional N-glycan at position N86, which in total gives four N-glycosylation sites on pro-Nxph4. The calculated molecular weight of pro-Nxph4-Myc is 30 kD (Table 1), which, together with four N-glycosylations, fits the observed molecular weight of Nxph4-Myc as previously reported (Meng *et al.*, 2019). The result where pro-Nxph4-Myc is more abundant than its mature form suggests that 50 residues long loop somehow disturbs proteolytic digest of Nxph4 since Myc tag is a small polypeptide that should not statically disrupt this process.

In summary, recombinant neurexophilins expressed in heterologous cells and brain show unexpected molecular weights on immunoblots. Interestingly, although mature Nxph1 and Nxph3 have the same sequence length, they differ in size, which can be explained by a different proteolytic cutting site in Nxph3. In Nxph2-tGFP and Nxph4-Myc, both proteins were present more abundantly in their proforms, suggesting that proteolytic cleavage in HEK293 cells could be somehow disturbed. Based on

Results

sequence analysis and specificity of neurexophilins signals, I assume that obtained neurexophilins variants are correct, folded, and functional. Post-translational processing of neurexophilins was not further analyzed in this thesis.

Table 2. Observed and calculated molecular weight of neurexophilins.

		mature form			Pro-form				
	Proteolytic cleavage site	calculated size w/t N-glycosylation [kD]	nr. of N-glycosylation sites	Calculated size with N-glycosylation	Calculated size w/t N-glycosylation [kD]	nr. of N-glycosylation sites	Calculated size with N-glycosylation	observed size [kD]	The possible Nxph form
Nxph1	KFKK (Lys-118)	17	3	24,5	28	6	43	25	mature form
Nxph1-GFP	KFKK (Lys-118)	44	3	51,5	55	6	70	52	mature form
Nxph3	RKR (Arg 50)	22	4	32	27	4	37	38	proform
Nxph3-GFP	RKR (Arg 50)	49	4	59	54	4	64	65	proform
	KFKK (Lys-118)	44	3	51,5				52	mature form (KFKK)
Nxph2-tGFP	KFKK (Lys-118)	44	3	51,5	54	4	64	70	proform
								52	mature form
Nxph4-Myc	KFKK (Lys-118)	23	3	30,5	30	4	40	40	proform
								30	mature form

The table shows all non-tagged and tagged rat Nxph1-Nxph4 variants used in this project. Nxph3 can be processed at two proteolytic cleavage sites (after Arg-50 and after Lys-118) giving two populations of mature proteins with different length and number of N-glycosylation sites. Nxph2-tGFP and Nxph4-Myc were observed as two bands, where the upper one was more abundant and fits to the calculated molecular weight of proforms with glycosylation. In my calculations, I set the approximate size of a single N-glycosylation to 2,5 kD (Reissner *et al.*, 2014).

3.2 All neurexophilin isoforms bind to the same epitope of Neurexin1 α

Since Nxph1 and Nxph3 differ in protein size, I asked whether Nxph3, Nxph2 and Nxph4 bind to the same epitope of Nrxn1 α . Beside of Nrxn1 α /Nxph1 complex, interactions of other neurexophilins (Nxph 2-4) with neurexins were not investigated

Results

extensively so far. Here, I used Fc-tagged LNS2 WT and different variants of LNS2, which carry point mutations around previously determined Nrnx1 α binding epitope to Nxph1: 1 α V358D, 1 α I401D, 1 α L402D, 1 α T404P (Wilson *et al.*, 2019; Reissner *et al.*, 2014). Due to the lack of specific antibodies for the detection of some native neurexophilins, I used their tagged variants: Nxph1-GFP, Nxph2-tGFP, Nxph3-GFP, Nxph4-Myc (Fig. 3.2A). To brace against potential artefacts from epitope-tagging, I

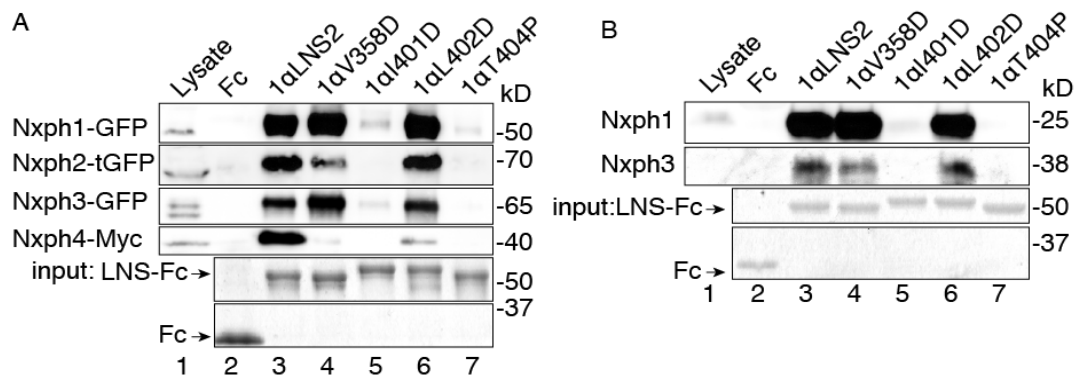


Figure 3.2. Mapping Nrnx1 α binding epitope to neurexophilins. (A) Binding assay after co-expression of tagged neurexophilins with WT (lane 3) or mutated (lanes 4-7) LNS2-Fc in HEK293 cells. Secreted fusion proteins were bound to protein A sepharose beads and tested by Western Blot. Neurexophilins were immunodetected by anti-GFP (Abcam 1:3000, Rabbit), anti-tGFP (Origen, 1:1000, Rabbit) and anti-Myc (Roche 1:500, Mouse) antibodies. Double band in Nxph3-GFP lysate (lane 1) corresponds to two different glycosylated versions of this protein. Input shows equal amounts of fusion protein used in the experiment. (B) same as in (A) but with non-tagged Nxph1 and Nxph3. Neurexophilins were immunodetected with anti-Nxph1 (Eurogenetec, 1:1000, Rabbit) and anti-Nxph3 (F508, 1:500, Rabbit). Input shows amounts of Fc and LNS2-Fc variants used in the experiment.

have also decided to test non-tagged variants of Nxph1 and 3 (Fig. 3.2B).

I started with the validation if GFP-tagged Nxph1 has the same binding properties as non-tagged Nxph1 (Reissner *et al.*, 2014). Nxph1-GFP is visible as a single ~50 kD band in the lysate (Fig. 3.2a, 1st panel, lane 1), and binds to 1 α LNS2-Fc with a prominent 52 kD band (Fig. 3.2a, 1st panel, lane 3), which corresponds to the calculated molecular weight of Nxph1 extended by the GFP tag (Table 1). 1 α V358D-Fc and 1 α L402D-Fc successfully pulled down Nxph1-GFP (Fig. 3.2a, 1st panel, lanes 4 and 6), while 1 α I401D-Fc and 1 α T404P-Fc did not precipitate Nxph1-GFP (Fig. 3.2a, 1st panel, lane 5) as it was shown for non-tagged Nxph1 (Reissner *et al.*, 2014).

Results

Since I proved that GFP-tag does not change the binding profile of Nxph1 to LNS2, I tested the other neurexophilin isoforms as tagged variants. The second panel of figure 3.2, shows the mapping of the binding epitope of Nrnx1 α LNS2 domain to Nxph2-tGFP. Immunoblotting of anti-tGFP antibody showed a prominent band ~70 kD in the cell lysate (Fig. 3.2a, 2nd panel, lane 1), which was strongly enriched by 1 α LNS2-Fc (lane 3). Nxph2-tGFP was pulled down by 1 α V358D-Fc (Fig. 3.2a, 2nd panel, lane 4) and 1 α L402D-Fc (Fig. 3.2a, 2nd panel, lane 6) but neither by 1 α I401D-Fc (Fig. 3.2a, 2nd panel, lane 5), 1 α T404P-Fc (Fig. 3.2a, 2nd panel, lane 7) nor by a control (Fig. 3.2a, 2nd panel, lane 2). Although the observed molecular weight of Nxph2-tGFP is higher than expected (Table 1), it binds to the same epitope of LNS2 domain.

Although Nxph1 and Nxph3 protein sequences have the same length, they show different molecular weight on immunoblots. Therefore, I asked whether Nxph3 interacts to the same binding epitope of Nrnx1 α LNS2 as Nxph1. Nxph3-GFP is present in the lysate as a double band of ~67 kD (Fig. 3.2a, 3rd panel, lane 1), which got enriched in pull-down samples as a single intense band by 1 α LNS2-Fc (Fig. 3.2a, 3rd panel, lane 3), 1 α V358D-Fc (Fig. 3.2a, 3rd panel, lane 4) and 1 α L402D-Fc (Fig. 3.2a, 3rd panel, lane 6). Neither 1 α I401D-Fc (Fig. 3.2a, 3rd panel, lane 5) nor 1 α T404P-Fc (Fig. 3.2a, 3rd panel, lane 7) successfully pulled Nxph3-GFP. These results show that Nxph3-GFP binds to the same binding epitope of Nrnx1 α LNS2 domain as Nxph1-GFP and Nxph2-tGFP.

Nxph4-Myc does not behave exactly in the same way as other members of its family when co-transfected with LNS2-Fc variants. Although it was profusely pulled down by 1 α LNS2-Fc (Fig. 3.2a, 4th panel, lane 3), Nxph4-Myc was precipitated with forty times lower amount (ImageJ quantification) by 1 α V358D-Fc (Fig. 3.2a, 4th panel, lane 4) and ten times lower by 1 α L402D-Fc (Fig. 3.2a, 4th panel, lane 6) in comparison to 1 α LNS2-Fc. In line with previous experiments, 1 α I401D-Fc and 1 α T404P-Fc completely impaired binding to Nxph4-Myc, therefore I assume that binding epitope of Nrnx1 α LNS2 is the same to all four neurexophilins.

Nxph4 possess a very long loop between β 4 and β 5 strands, which might impair its binding properties to LNS2 (Wilson *et al.*, 2019). Because of its unique feature Nxph4 binding affinity to Nrnx1 α LNS2 domain might differ in comparison to Nxph1. To test the impact of the long loop in Nxph4 on its binding affinity, I co-transfected 1 α LNS2-Fc with Nxph1-GFP (Fig. 3.3, upper panel) and Nxph4-Myc (Fig

Results

3.3, lower panel) using different conditions with variable NaCl concentration (80 mM to 500 mM). 1 α LNS2-Fc pulled down Nxph1-GFP in a profuse way in all six salt concentration conditions (Fig. 3.3, upper panel, lanes 1-4), which was not a surprise based on the previous reports that Nrnx1 α /Nxph1 complex could only be destroyed under highly denaturing conditions (Petrenko *et al.*, 1996). However, in case of Nxph4-Myc, the binding was reduced ten times (ImageJ analysis) in 500 mM NaCl (lane 1) compared to 80 mM NaCl (Fig. 3.3, lane 4). This result suggests that additional 50 residues long loop in Nxph4 sterically disturbs the formation of a strong Nxph4-LNS2 complex.

Since there are two antibodies available to detect non-tagged Nxph1 and Nxph3 I also tested these variants (Fig. 3.2B). The anti-Nxph1 antibody is specific for Nxph1, while the second available neurexophilin antibody detects Nxph1 and Nxph3. Nxph1 and Nxph3 were hardly detectable in lysates (Figure 3.2b, both panels, lanes 1), but both were precipitated by 1 α LNS2-Fc (Fig. 3.2b, lane 3). Co-transfection of non-tagged neurexophilins 1 and 3 with LNS-Fc and different variants carrying point mutations, showed the same results as for GFP-tagged Nxph1 and Nxph3 (Fig. 3.2a). Non-tagged Nxph1 and Nxph3 were pulled down by LNS2 V358D-Fc (Fig. 3.2b, both panels, lane 4) and LNS2 L402D-Fc (Fig. 3.2b, both panels, lane 6), but neither by LNS2 I401D-Fc (Fig. 3.2b, both panels, lane 5) nor LNS2 T404P-Fc (Fig. 3.2b, both panels, lane 7).

In line with GFP-tagged variants of Nxph1 and Nxph3, their non-tagged versions showed that both neurexophilins interact with the same binding epitope on LNS2

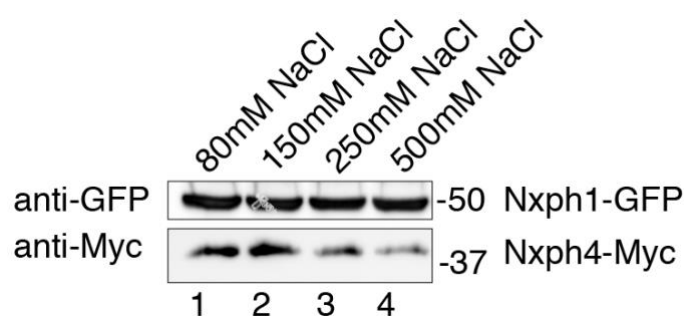


Figure 3.3. Binding of Nxph4-Myc to Nrnx1 α LNS2 is weak at high salt concentration. Nxph1-GFP (upper panel) and Nxph4-Myc (lower panel) were coexpressed with Nrnx1 α LNS2-Fc. Secreted fusion proteins were bound to protein A sepharose beads and washed in rising NaCl concentration (80 mM- 500 mM). Binding of Nxph1-GFP remains strong even in 500 mM NaCl, while binding of Nxph4-Myc decreases gradually with increasing NaCl concentration. Tested antibodies were indicated in Fig. 3.2.

Results

domain of Nrnx1 α . Another difference between Nxph1 and Nxph3 is that these two proteins are expressed in a different type of synapses. Nxph1 mRNA hybridization assay showed that it is expressed only in inhibitory interneurons (Petrenko *et al.*, 1996), while Nxph3 was shown by β -galactosidase staining of Nxph3 knock-in mice brains to be present in excitatory synapses (Beglopoulos *et al.*, 2005). Taken together, it could be possible that Nxph1/ α Nrnx complex might have different binding partners than Nxph3/ α Nrnx complex, which I wanted to investigate further in next experiments.

3.3 Searching for novel binding partners of the neurexophilin/neurexin complex

After I determined that all four neurexophilins interact with the same binding epitope on Nrnx1 α , I wanted to investigate the function of these α -neurexin specific ligands. Here I performed brain pulldowns from transgenic Nxph3-GFP^{tg/-} mice which ectopically overexpresses Nxph3-GFP under Thy1.2 promoter. By using this mouse line, I wanted to check if overexpression of Nxph3-GFP changed binding properties of known partners of neurexins in the brain and hopefully help to find new protein interactors of neurexophilin/ α -neurexin complex. The idea behind the generation of these animals was to overexpress Nxph3-GFP in the neocortical layer 5, a region where Nxph3 is usually not present (Beglopoulos *et al.*, 2005). Previous reports showed that although genotyping of Nxph3-GFP^{tg/-} confirmed the presence of Nxph3-GFP in transgenic mouse genome, the green GFP signals were not detected under fluorescent microscope neither in brain slices nor in cell-cultured neurons prepared from these transgenic brains (Blanche, 2015). Moreover, although indulgent neurexophilins are present in interneurons (Petrenko *et al.*, 1996, Beglopoulos *et al.*, 2005), pictures from electron microscopy showed that Nxph3-GFP molecules are primarily present in excitatory neurons (Blanche, 2015). These interesting features encouraged me to investigate if Nxph3-GFP^{tg/-} mouse model could provide more answers to the function of Nxph3. Here I performed pulldowns with Fc-tagged β - and α -neurexins or Nxph3 in complex with Nrnx1 α (Fig. 3.4) to validate if known and hopefully any new binding partners of neurexins could be precipitated from these mice brains. I screened for several pre- and postsynaptic receptors, which required various purification procedures to establish the protocol that would allow me to detect all proteins of interests (see Discussion).

Results

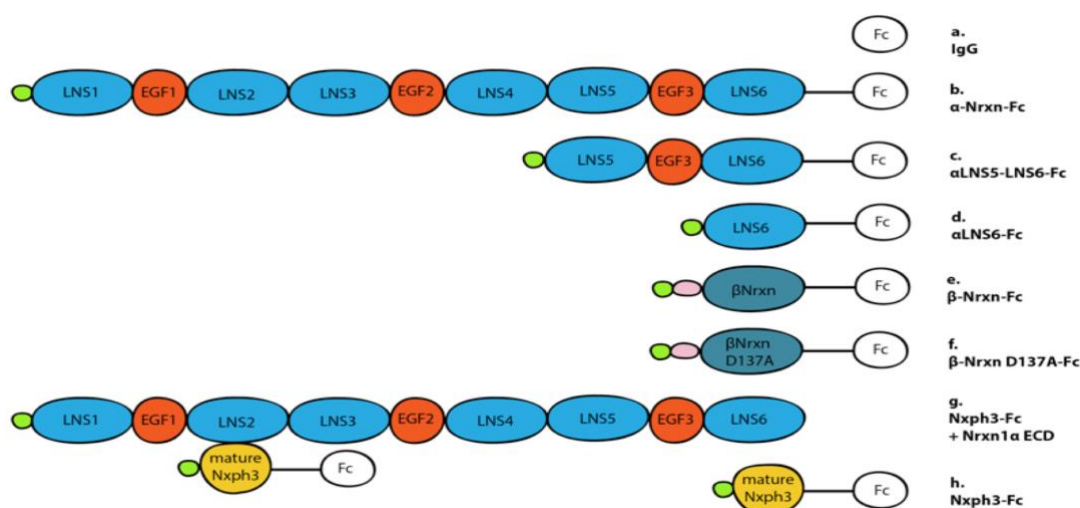
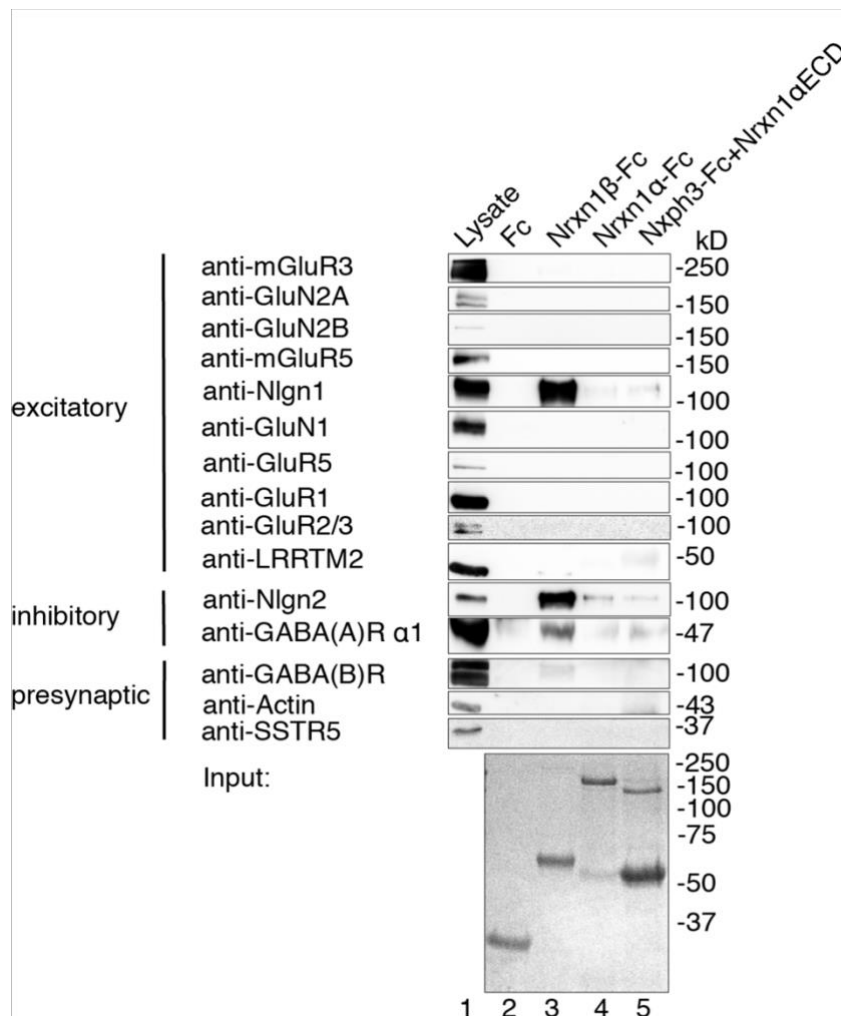


Figure 3.4. Diagram of recombinant proteins used for binding assays. Fusion proteins of the Fc domain of human IgG with indicated fragments from extracellular sequences of neurexins and mature Nxph3. β -Nrxn D137A-Fc carries a point mutation in the calcium coordination site (Reissner et al., 2008). Nxph3-Fc do not contain pro-domain characteristic for neurexophilins as described in Fig. 3.2. Symbols and colors of domains are the same as in Fig. 1.1. Modified from Missler *et al.*, 1998.

First, I purified Fc-tagged extracellular domains of Nrxn1 α , Nrxn1 β , Nxph3 cotransfected with the non-tagged extracellular domain of Nrxn1 α and a control Fc tag from HEK293 cells (Fig. 3.4, a, b, f, h). After fusion proteins were secreted into the medium, they got bound to protein A sepharose beads and incubated with the brain lysate. Brain lysate from adult animals was prepared as described in Materials and Methods. I incubated each Fc-tagged fusion protein with the same volume of the brain lysate, which represents half of a forebrain (Fig. 3.5). Amounts of fusion proteins used in the pull-down are shown on coomassie staining picture (Fig. 3.5, input), and were adjusted in a way that all neurexins gave similar quantity. The reason for this approach was to get as much Nxph3-Fc/Nrxn1 α ECD complex (Fig. 3.5, input lane 5, 50 and 150 kD bands), since purification of coexpressed Nxph3-Fc and Nrxn1 α ECD gives two populations of these molecules: free Nxph3-Fc and Nxph3-Fc in complex with Nrxn1 α ECD. Note that although the amount of Nrxn1 β -Fc presented on input picture (Fig. 3.5, input, lane 3) looks equal to Nrxn1 α -Fc (Fig. 3.5, input, lane 4) and Nrxn1 α ECD (Fig. 3.5, input, lane 5, upper band) it occurs in higher molarity than its longer analogues because it is a smaller isoform of Nrxn1 α that contains only a single LNS6/ β LNS domain. With a single experiment, I could test maximally three antibodies on the immunoblot; therefore, to obtain my results, I had to perform this pull-down four times.

Results

In this experiment, I tested synaptic proteins from excitatory synapses, inhibitory synapses and presynaptic side (Fig. 3.5). I started with the best-characterized neurexin binding partners: Neuroligins 1 and 2 (Ichtchenko *et al.*, 1995; Ichtchenko, Nguyen and Südhof, 1996). Nlgn1 was pulled down by Nrnx1 β -Fc (Fig. 3.5, lane 3), Nrnx1 α -Fc (Fig. 3.5, lane 4) and Nxph3-Fc + Nrnx1 α ECD (lane 5), however enrichment of Nlgn1 was observed only with Nrnx1 β -Fc. Nlgn2 was detected in the lysate as a 100 kD band and pulled down by all three Fc tagged fusion proteins (Fig. 3.5, lanes 3-5), but the enrichment of Nlgn2 is visible again only in the fraction precipitated by Nrnx1 β -Fc (Fig. 3.5, lane 3). Leucine-rich repeat transmembrane protein 2 (LRRTM2) was identified as a neurexin partner by the affinity chromatography (de Wit *et al.*, 2009). LRRTM2 was immunodetected in the brain lysate as a ~50 kD band (Fig. 3.5, lane 1), but is also precipitated only with Nrnx1 β -Fc (Fig. 3.5, lane 3).



Results

GABA_AR was also reported to physically interact with neurexins in a brain pull-down (Zhang *et al.*, 2010). GABA_AR was pulled by all recombinant neurexins (Fig. 3.5, lanes 3-5) and the most intense signal was obtained with Nrnx1 β -Fc. These results show that it was possible to pull down known postsynaptic partners of neurexins (Nlgn1, Nlgn2, LRRTM2, GABA_AR) from transgenic animals overexpressing Nxph3-GFP.

After I validated that it was possible to pull down already known partners of neurexins from Nxph3-GFP^{tg/-} brains, I tried to investigate if the neurexin/neurexophilin3 complex could also precipitate any other known receptor. GABA_BR is a presynaptic metabotropic γ -butyric acid receptor present in both excitatory and inhibitory synapses (Jones *et al.*, 1998). R1 subunit of GABA_BR is visible as a double band in lysates at a molecular weight around 100 kD, which

Figure 3.5. Screening for potential new binding partners of neurexins in transgenic Nxph3-GFP^{tg/-} mice brains. Transgenic Nxph3-GFP^{tg/-} brain lysates show strong protein signals of selected excitatory, inhibitory, and presynaptic proteins (lane 1). Lysates were incubated with Nrnx1 β -Fc (lane 3), Nrnx1 α -Fc (lane 4) and Nxph3-Fc+Nrnx1 α ECD (lane 5) immobilized on protein A sepharose beads for pull-down experiments. Nrnx1 β -Fc, Nrnx1 α -Fc and Nxph3-Fc+Nrnx1 α ECD pulled down Nlgn1 (lanes 3-5, 5th excitatory panel), Nlgn2 (lanes 3-5, 1st inhibitory panel; anti-Nlgn2 Synaptic systems 1:500, Rb), GABA(A)R (lanes 3-5, 2nd inhibitory panel), GABA(B)R (lanes 3-5, 1st presynaptic panel) and LRRTM2 but with very weak signal (lanes 3-5, 10th excitatory panel; anti-LRRTM2 Abcam 1:500, Rb). mGluR5 (lanes 3-5, 1st excitatory panel; anti-mGluR5 Millipore 1:1000, Rb), mGluR3 (lanes 3-5, 4th excitatory panel, anti-mGluR3 Abcam 1:1000, Rb), NMDAR subunits: GluN2A (lanes 3-5, 2nd excitatory panel; anti-GluN2A Millipore 1:250, Rb), GluN2B (lanes 3-5, 3rd excitatory panel; anti-GluN2B Abcam 1:250, Rb), GluN1 (lanes 3-5, 6th excitatory panel), AMPAR subunits: GluR1 (lanes 3-5, 8th excitatory panel; anti-GluR1 (lanes 3-5, 8th excitatory panel; Chemicon 1:1000, Rb) and GluR2/3 (lanes 3-5, 9th excitatory panel), GluR5 (lanes 3-5, 7th excitatory panel; anti-GluR5 (Upstate, 1:500, Rb), actin (lanes 3-5, 2nd presynaptic panel anti-Actin Sigma 1:1000, Rb) and SSTR5 (lanes 3-5, 3rd presynaptic panel; anti-SSTR5 Thermo Fisher 1:2000, Rb) were not successfully pulled by Fc-tagged neurexins. Input shows equal amounts of fusion proteins used in the experiment, however since Nrnx1 β is a smaller isoform of Nrnx1 α that contains only single LNS domain Nrnx1 β -Fc is present in higher molarity than Nrnx1 α -Fc and Nxph3-Fc+Nrnx1 α ECD and therefore pulled down more proteins from brain lysate. None of the listed proteins was pulled down by control which consists of Fc-tag alone (lane 2). Protein panels were combined into groups of excitatory, inhibitory and presynaptic proteins and arranged by molecular weight (kD).

Results

corresponds to two isoforms of a receptor, higher R1a with two sushi domains and lower R1b without sushi domains (Blein *et al.*, 2004). Interestingly, GABA_BR gave a signal in the pulldown (lane 3), which although is very weak it points on the specificity since the control remained empty (lane 2). NMDA receptors (N-methyl-D-aspartate [NMDA] receptors) are glutamate-gated cation-passing channels that play a significant role in neurotransmission in excitatory (glutamatergic) synapses. NMDAR consists of GluN1 subunits, GluN2 subunits of four types (GluN2A, GluN2B, GluN2C, GluN2D) and/or GluN3 (GluN3A, GluN3B), which are encoded by distinct genes in the mammalian genome (Sanz-Clemente *et al.*, 2013). GluN1, GluN2A and GluN2B subunits of NMDA receptor were detected as ~120 kD (GluN1) and ~150 kD bands (GluN2/B) in brain lysate (Fig. 3.5, lane 1), but unfortunately were not pulled down by Fc-tagged proteins (Fig. 3.5, lanes 3-5). I also checked if other glutamate receptors could be precipitated from transgenic brains. However, neither of them was pulled by Fc-tagged proteins, including AMPA receptor subunits GluR1 and GluR2/3, detected only in the lysate as two ~100 kD bands (lane 1); kainite receptor GluR5, visible as a ~110 kD band in the lysate (Fig. 3.5, lane 1); metabotropic glutamate receptors mGluR3 and mGluR5, detected as ~250 kD and ~150 kD bands in the lysate (Fig. 3.5, lane 1). As the last try, I also tested somatostatin receptor 5 (SSTR5), which was detected in the pull-down samples from *Nxph3-GFP^{tg}* brains tested by proteomics (data not shown), which could suggest that it might be a binding partner of α Nrxn/*Nxph3* complex. SSTR5 was not immunoprecipitated (Fig. 3.5, lanes 3-5) but were detected in the lysate as ~37 kD band. Actin was also not pulled down (Fig. 3.5, lanes 3-5) and was detected only in the lysate as a 43 kD band (Fig. 3.5, lane 1), which indicates no contamination and no unspecific binding to agarose beads. None of the listed synaptic receptors was pulled down by a control Fc protein (Fig. 3.5, lane 2).

These results shows that overexpression of *Nxph3-GFP* did not alter binding properties of known partners of neurexins, since it was possible to pull known Nlgn1, Nlgn2, LRRTM2 and GABA_AR. Binding to these proteins occurs through LNS6/ β LNS domain of neurexins, therefore it is not a surprise that Nrxn1 β -Fc precipitated the highest number of postsynaptic receptors. Nrxn1 β contains only a single LNS6/ β LNS domain responsible for binding to i.e., Nlgn1, Nlgn2, LRRTM2, GABA_AR (Tanaka *et al.*, 2011, de Wit *et al.*, 2009, Zhang *et al.*, 2010). Nrxn1 β -Fc

Results

(Fig. 3.5, input, lane 3) is a smaller molecule than Nr_{xn1} α -Fc and Nr_{xn1} α ECD (Fig. 3.5, input, lanes 4 and 5). Therefore, it occurs in higher molarity than its longer isoforms and therefore it precipitated more synaptic receptors. Surprisingly, GABA_BR was also precipitated although with a very weak signal.

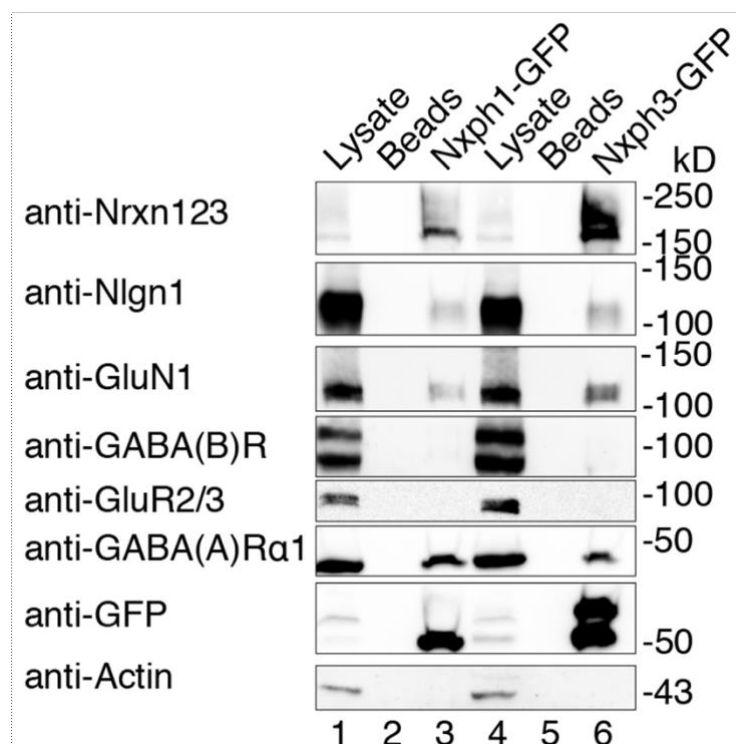
3.4 GluN1 binds to neurexins in adult brains

After I validated that known binding partners of neurexins and GABA_BR could be pulled from Nxph3-GFP^{tg/-} brains by Fc-tagged neurexins, in a search for new binding partners of neurexophilin/neurexin complex I decided to try a different approach. Here, I performed a pull down with the GFP-trap, which is a specific nanobody coupled to magnetic agarose beads that binds to GFP-tagged proteins and allows their immunoprecipitation from biological material, i.e., from the brain tissue lysate. Performed pull down from transgenic animals hopefully could precipitate Nxph3-GFP together with some new binding partners of Nxph3/ α -neurexins complex, i.e., previously tested GABA_BR and NMDAR. Moreover, since my recombinant experiments revealed that although mature Nxph1 and Nxph3 share the same binding epitope to LNS2 domain of Nr_{xn1} α , they do differ in molecular size (Fig. 3.1). Another difference between these two neurexophilins is that Nxph1 and Nxph3 are present in two distinct subpopulations of synapses, since Nxph1 is present in inhibitory neurons, while Nxph3 is expressed in excitatory neurons (Petrenko *et al.*, 1996, Beglopoulos *et al.*, 2005). Different molecular weight and synapse localization suggest that Nxph1 and Nxph3 might be parts of distinct protein clusters and might have different binding properties. Therefore, to investigate if Nxph1 and Nxph3 have different binding partners I also performed the GFP-trap pull down from Nxph1-GFP^{tg/-} mouse line, that overexpress Nxph1-GFP in the neocortical layer 6b, where Nxph1 is normally not expressed (Born *et al.*, 2014). In my research I used lysates obtained from adult (10-16 weeks old) transgenic Nxph1-GFP^{tg/-} and Nxph3-GFP^{tg/-} mice forebrains and each pulls down was performed from lysate that represents half of a brain. Instead of testing all the potential novel partners of neurexins like before (Fig. 3.5), I started with a smaller experiment, which was focused on the detection of GABA_BR and NMDAR from adult brains.

Nxph1-GFP was detected as two 52 and 60 kD bands in brain lysate (Fig. 3.6, anti-GFP, lane 1) but only the lower band was enriched in a pull-down (Fig. 3.6, lane 3).

Results

Nxph3-GFP was also detected in the lysate as two bands of 52 kD and 60 kD (Fig. 3.6, lane 4), but precipitated as two 52 kD and 65 kD bands (Fig. 3.6, lane 6, explained in the paragraph 3.1.3). The immunoprecipitated signals of Nxph1-GFP and Nxph3-GFP and a double band of Nxph3-GFP were already described above (Table 1). α -Neurexins immunoprecipitated with Nxph1-GFP and Nxph3-GFP, as expected from previous studies that neurexophilins stay in a tight complex with α -neurexins (Petrenko *et al.*, 1996). Neurexins were detected as 150-250 kD signals in brain lysates (Fig. 3.6, lanes 1 and 4) and they got extensively enriched by the GFP-trap (Fig. 3.6, lanes 3 and 6). Neuroligin 1 was pulled down in this experiment as a ~120 kD band, as expected from previous studies (Ichtchenko *et al.*, 1996), but without an enrichment (Fig. 3.6, lanes 3 and 6). GABA_AR α 1 subunit was detected in brain lysates as a 47 kD band and was successfully precipitated with GFP-tagged neurexophilins (Fig. 3.6, lanes 3 and 6). After I validated these already known partners of neurexins could be precipitated from both transgenic brains by the GFP-trap, I focused on GluN1 subunit of NMDAR. GluN1 was detected in both Nxph1-GFP^{tg/-} and Nxph3-GFP^{tg/-} brain lysates around 120 kD (Fig. 3.6, lanes 1 and 4) and was successfully pulled down with both Nxph1-GFP and Nxph3-GFP (Fig. 3.6, lanes 3 and 6) but without an enrichment. The positive result from NMDAR encouraged me to test also AMPAR, which is another type of glutamate receptor. Although AMPA



Results

receptor subunits GluR2 and GluR3 were both detected as a double signal at 100 kD in lysates (Fig. 3.6, lanes 1 and 4), GluR2/3 were pulled down neither from *Nxph1-GFP^{tg/-}* nor *Nxph3-GFP^{tg/-}* brains (Fig. 3.6, lanes 3 and 6). In case of GABA_BR, it was unfortunately not immunoprecipitated from the adult brain, although it was present in the lysates of both mice lines as a double ~100 kD band. Actin signals at 43 kD indicate equality of both lysate immunodetection (Fig. 3.6, lanes 1 and 4). Still, it was not pulled down (Fig. 3.6, lanes 3 and 6), which indicates no contamination and no unspecific binding to magnetic beads. Essentially, none of the listed proteins were pulled down by controls which are magnetic beads without GFP-specific nanobody (Fig. 3.6, lanes 2 and 5).

To sum it up, a GFP-trap pulls down from transgenic *Nxph1-GFP^{tg/-}* and *Nxph3-GFP^{tg/-}* brains revealed two main observations. First, *Nxph1-GFP* and *Nxph3-GFP* were successfully precipitated together with known partners of neurexins, including

Figure 3.6. α -Nrxn/Nxph-GFP pulled down NMDAR from adult mice brains. Brain lysates from transgenic *Nxph1-GFP^{tg/-}* and *Nxph3-GFP^{tg/-}* show intense protein levels of selected postsynaptic receptors (lanes 1 and 4, 2nd-6th panels from top), while neurexin and neurexophilins are hardly detected (1st and 7th panel). Total amounts of proteins in the lysates of *Nxph1-GFP^{tg/-}* and *Nxph3-GFP^{tg/-}* are comparable as indicated by actin levels (lane 1 and 4; lowest panel; anti-actin Sigma 1:000, Rabbit) as well as amounts of individual proteins. GFP-trap immunoprecipitation successfully pulled down *Nxph1-GFP* (lane 3, 7th panel, anti-GFP, Abcam 1:3000, Rabbit) and *Nxph3-GFP* (lane 6) in complex with α Neurexins (lane 3 and 6, 1st panel; anti-Nrxn123, Synaptic Systems 1:500, rabbit), Nlgn1 (lane 3 and 6, 2nd panel; anti-Nlgn1; Synaptic systems 1:5000, mouse), GABA_AR (lane 3 and 6, 6th panel; anti-GABA(A)R α 1; Synaptic Systems 1:500, Rabbit) and NMDAR (lane 3 and 6, 3rd panel; Anti-GluN1; Synaptic Systems 1:250, mouse) and a very weak signal for GABA_BR (lane 3 and 6, 4th-panel anti-GABA(B)R R1; Santa Cruz 1:1000, Rabbit) but not AMPAR (lane 3 and 6, 5th panel; Chemicon 1:1000, Rabbit). As expected, signals for Nrxns and Neurexophilins show enrichment of bound proteins in precipitates (lanes 3 and 6, 1st and 7th panels) compared to lysates (lanes 1 and 4). Note, that the lysates of neurexophilins show two bands at about 50 kD and 60 kD and that *Nxph1-GFP* precipitates only as a 50 kD protein, while both fragments of *Nxph3-GFP* were bound to beads. Interestingly, the levels of bound receptors were lower than in lysates, although 100-times more volume of lysate was used for the pull-down. Nearly, none of the proteins was pulled down by a control (lane 2 and 5). Some samples were treated differently from my standard method (boiled) as samples for GluN1 were boiled with 8M urea, GABA(A)R and GABA(B)R were not boiled. Panels are arranged according to the molecular weight of proteins (kD).

Results

Nlgn1 and GABA_AR (Fig. 3.6, lanes 3 and 6). Second, GluN1 subunit of NMDAR was immunoprecipitated from both transgenic mice lines. Although the amount of pulled GluN1 was not enriched, the control remained empty, which I saw in three biological replications. This result together with the recombinant experiment with the GFP-tagged GluN1 shows that NMDAR might be a novel binding partner of neurexins.

Quantitative *in vitro* receptor autoradiography shown that GABA_BR densities were significantly lower in 90-day old rats compared to newborns in the olfactory bulb and striatum (Behuet *et al.*, 2019). Therefore, I asked if GABA_B receptor and other synaptic proteins could be precipitated easier from younger mice brains. I performed

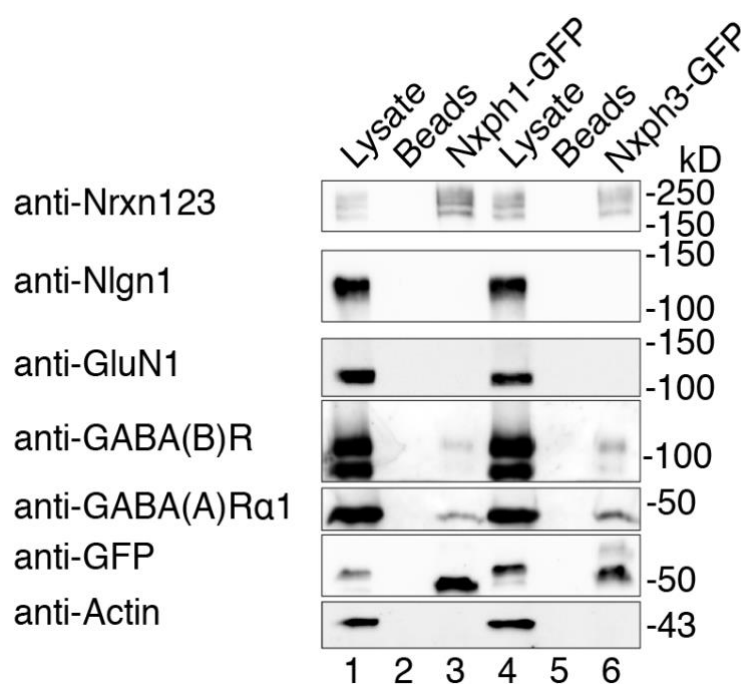


Figure 3.7. Neurexins pulled GABA_BR from P7 mice brains. Brain lysates from transgenic Nxph1-GFP^{tg/-} and Nxph3-GFP^{tg/-} show strong protein levels of selected postsynaptic receptors (lanes 1 and 4, 2nd-5th panels from top), while neurexin, neurexophilins are hardly detected (1st, 2nd and 6th panel). Total amounts of proteins in the lysates of Nxph1-GFP^{tg/-} and Nxph3-GFP^{tg/-} are comparable as indicated by actin levels (lane 1 and 4; lowest panel) as well as amounts of individual proteins. GFP-trap immunoprecipitation pulled down Nxph1-GFP (lane 3, 6th panel) and Nxph3-GFP (lane 6) in complex with α Neurexins (lane 3 and 6, 1st panel), however not as strong as on Fig. 3.7 in the adult experiment. GABA_BR (lane 3 and 6, 4th panel) and GABA_AR (lane 3 and 6, 5th panel) were also immunoprecipitated but not Nlgn1 (lane 3 and 6, 2nd panel) and GluN1 (lane 3 and 6, 3rd panel). None of the listed proteins was pulled down by a control (lane 2 and 5). Details of antibodies were already shown in Fig 3.5. Panels are arranged according to the molecular weight of proteins (kD).

Results

GFP-trap pull down on lysates obtained from 7 days old (P7) mice brains to investigate if Nxph/Nrxn complexes could precipitate different synaptic proteins than from the adult tissue. Moreover, younger neurones are less myelinated, which could help to release more synaptic receptors from cell membranes during lysis and easier purification.

First, I again tested if GFP-tagged neurexophilins, α -neurexins and the known partners of neurexins immunoprecipitate with GFP-trap. Nxph1-GFP was successfully pulled down as a single 53 kD band (Fig. 3.7, lane 3) and Nxph3-GFP as a double 52 and 65 kD band (Fig. 3.7, lane 6), although the upper band is weaker than in adult pull-down (Fig. 3.6). The reason for this difference in signal intensity might be that in younger cells, more Nxph3-GFP molecules are being proteolytically processed, giving more mature Nxph3-GFP (Table 1). Although α -Neurexins and GABA_AR α 1 were precipitated with both Nxph1-GFP and Nxph3-GFP (Fig. 3.7, lanes 3 and 6), Nlgn1 was detected only in both brain lysates (Fig. 3.7, lanes 1 and 4) but not precipitated (Fig. 3.7, lanes 3 and 6). This result might suggest that Nlgn1 do not form a major complex with Nxph-GFP/ α -neurexins in 7 days old mice brains, therefore was not precipitated by the GFP-trap.

After I gained knowledge of which partners of neurexins could be immunoprecipitated from P7 brains, I again tested synaptic receptors starting with GABA_B receptor. In contrast to adult pull-down (Fig. 3.6), GABA_BR was pulled from both Nxph1-GFP^{tg/-} and Nxph3-GFP^{tg/-} P7 brains (Fig. 3.7, lanes 4 and 6). This result is interesting because although binding between neurexins and GABA_BR has never been reported, there are reports of functional crosstalk between GABA_BR and neurexins. As previously mentioned, impaired facilitation of evoked postsynaptic currents at excitatory synapses in Nxph1-GFP brain slices could partially be rescued by the GABA_BR-specific blocker treatment (Born *et al.*, 2014). Moreover, the *Gabbr1* knock-out gene in a single parvalbumin-positive neocortical interneuron resulted in increased dynamics of β -neurexins at presynaptic terminals, which stayed insensitive to the GABA_BR antagonist (Fu and Huang, 2010). These results indicate that GABA_BR might be a novel binding partner of neurexins. Although GluN1 is present in the brain lysate of both mice lines (Fig. 3.7, lanes 1 and 4), it was pulled down neither with Nxph1-GFP nor with Nxph3-GFP (Fig. 3.7, lanes 3 and 6). The lack of binding of GluN1 to neurexins in P7 brains suggests that although GluN1 is expressed

Results

in virtually all neurones and during all stages of development (Monyer *et al.*, 1994), it starts to form a complex with neurexins after the seventh day of postnatal life. Essentially, actin is present in both lysates in equal amount (lanes 1 and 4) and was pulled down neither by Nxph1-GFP nor by Nxph3-GFP.

In summary, performed GFP-trap pull-downs from P7 and adult animals show different results. First, GluN1 subunit of NMDAR was immunoprecipitated by GFP-tagged neurexophilins from both Nxph1-GFP^{tg/-} and Nxph3-GFP^{tg/-} mice lines but only from adult brains (Fig. 3.6), while GABA_BR was pulled only from P7 animals (Fig. 3.7). Although the amount of pulled GluN1 and R1 of GABA_BR was not enriched, the control remained empty, which I saw in three biological replicates. It shows that interaction of GluN1 and R1 with neurexin/neurexophilin complexes was specific and suggests that NMDAR and GABA_BR might be novel binding partners of neurexins. Second, Nlgn1 was precipitated only from adult and not from P7 brain lysates, but still without an enrichment, which is characteristic for Nrnx-Nlgn pull-downs (Ichtchenko *et al.*, 1996). GABA_AR was pulled from both mice lines of both ages, but the intensity of pulled signals is even higher than for Nlgn1. Third, these results do not show differences in binding partners or intensity signals between pull-downs from Nxph1-GFP^{tg/-} and Nxph3-GFP^{tg/-}. Interestingly, GluN1 of NMDAR and $\alpha 1$ of GABA_AR were pulled from both Nxph1-GFP^{tg/-} and Nxph3-GFP^{tg/-} brains. Nxph1 is normally restricted to inhibitory synapses (Born *et al.*, 2014), but Nxph1-GFP pulled down the GluN1 of NMDAR, which is exclusively present in excitatory synapses only. Nxph3 normally occurs in excitatory synapses (Beglopoulos *et al.*, 2005), but Nxph3-GFP pulled GABA_AR $\alpha 1$, which is a characteristic receptor for inhibitory synapses. It can be explained by the fact that both Nxph1-GFP and Nxph3-GFP were expressed in both brains the neocortical layer 6b and their expression was not synapse-specific (Born *et al.*, 2014, Blanque, 2015). Since I did not see any differences between results obtained from Nxph1-GFP^{tg/-} and Nxph3-GFP^{tg/-} mice lines, I performed my next experiments on Nxph3-GFP^{tg/-} mice only.

3.5 NMDAR, GABA_BR, LRRTM2, Nlgn1, mGluR3 and mGluR5 interact with Nxph3-GFP/ α Nrnx complex during different stages of development

GFP-trap experiments showed that GluN1 subunit of the NMDA receptor could be immunoprecipitated from adult brains together with Nxph/Nrnx complex (Fig. 3.6). In

Results

contrast, R1 subunit of GABA_BR was pulled only from P7 brain lysates (Fig. 3.7). To validate if NMDAR forms a transsynaptic cluster with Nxph3/ α Nrxn complex, I wanted to test if also GluN2A and GluN2B could be pulled with GFP-tagged neurexophilins from adult Nxph3-GFP^{tg/-} brain lysate. Beside of NMDAR, I wanted to validate if GABA_BR and other synaptic receptors could also be precipitated from adult brains.

Nxph3-GFP and α -neurexins precipitated together as expected (Fig. 3.8, lane 3). Both Nlgn1 and Nlgn2 were pulled down, but only Nlgn2 was precipitated with an enrichment. Although Nlgn3 was immunodetected as a ~130 kD band in the lysate, it was not precipitated by the GFP-trap. This result is surprising because it has been reported that Nlgn3 is a binding partner of neurexins (Ichtchenko *et al.*, 1996). As expected, Nxph3-GFP again precipitated GABA_AR α 1 subunit (Fig. 3.8, lane 3). To test more partners of neurexins, I also checked my samples on the presence of LRRTM2, but it was not detected in the pull-down samples either (Fig. 3.8, lane 3).

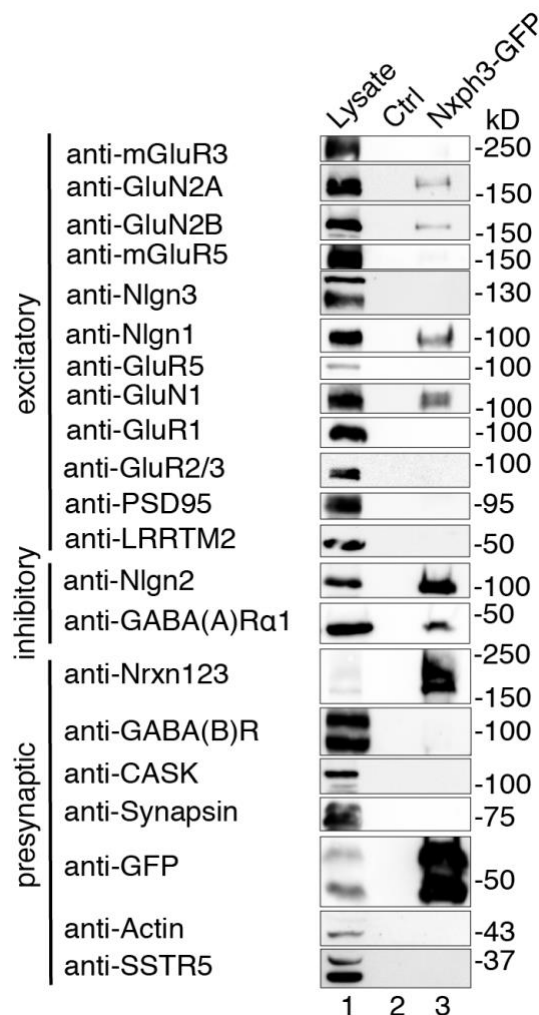
To validate if NMDAR interacts with Nxph3/ α -Nrxn complex in adult brains, I tested not only GluN1 but also GluN2A and GluN2B subunits of NMDAR. Nxph3-GFP successfully co-precipitated GluN1, GluN2A and GluN2B (Fig. 3.8, lane 3). Although visible signals were not enriched in comparison to signals from the lysate (Fig. 3.8, lane 1), precipitated GluN1, GluN2A and GluN2B give more evidence that NMDAR is indeed a novel binding partner of neurexins. In contrast to these results, GABA_B receptor R1 subunit again could not be immunoprecipitated from adult brain lysate (Fig. 3.9, lane 3). Since it has been shown that PSD95 interacts with NMDAR intracellularly in the two-hybrid system (Kornau *et al.*, 1995) and PSD95 coimmunoprecipitates with Nlgn1 by immobilized neurexins (Irie, 1997), I also asked if postsynaptic density protein 95 (PSD95) could be precipitated with Nxph3-GFP. PSD95 was detected in the lysate as a 95 kD band (lane 1); however, was not pulled down with Nxph3-GFP (Fig. 3.8, lane 3). Testing other glutamate receptors did not show positive results as both AMPA receptor subunits, kainite receptor GluR₅, and metabotropic glutamate receptors mGluR3 and mGluR5 were not pulled down in this experiment. SSTR5 also did not show a positive result of binding. Calcium/calmodulin-activated serine kinase (CASK) was identified as an intracellular binding partner of neurexins by the recombinant pull-down and a pull-down from subfractionated synaptic plasma membranes of a brain homogenate (Butz, Okamoto and

Results

Südhof, 1998). Although CASK was detected as a ~100 kD band in the lysate (Fig. 3.8, lane 1), it was not immunoprecipitated with Nxph3-GFP (Fig. 3.8, lane 3). Synapsin, a presynaptic protein which is an essential factor in neurotransmitter release was also not immunoprecipitated (lane 3), although it is visible in the lysate as a 75 kD band (Fig. 3.8, lane 1). Actin was again not pulled with Nxph3-GFP (lane 3). None of the proteins tested in these experiments was precipitated by the control (Fig. 3.8, lane 2).

In summary, beside of standard neurexin partners (Nlgn1, Nlgn2, GABA_AR) and all tested NMDAR subunits (GluN1, GluN2A, GluN2B) but neither GABA_BR nor LRRTM2 were pulled down by the GFP-trap from adult brains.

To validate that GABA_B R1 interacts with Nxph3-GFP/Nrxn complex, I repeated GFP-trap pull-down from P7 Nxph3-GFP^{tg/-} brain lysates. To investigate if other synaptic proteins interact with Nxph3/ α Nrxn complex in 7 days old animals, I also tested the same synaptic proteins as in adult GFP-trap pull-down (Fig. 3.8). Nxph3-



Results

GFP and α -neurexins are abundantly co-immunoprecipitated from P7 brain lysates (Fig. 3.9, lane 3). Out of all three tested neuroligins, only Nlgn2 was pulled down with an enrichment, while Nlgn1 and Nlgn3 were not precipitated (Fig. 3.9, lane 3). GABA_AR co-immunoprecipitated with Nxph3-GFP and interestingly, LRRTM2 was also pulled down in this experiment (Fig. 3.9, lane 3). R1 subunit of GABA_BR was successfully pulled with Nxph3-GFP (Fig. 3.9, lane 3), which validated that GABA_B receptor interacts with Nxph3/Nrxn complex in P7 brains. Interestingly, metabotropic glutamate receptors mGluR3 and mGluR5 (Fig. 3.9, lane 3) were also precipitated from P7 brain lysates. As expected from the first GFP-trap experiment from the P7 brains, all NMDAR subunits (GluN1, GluN2A and GluN2B) were not pulled with Nxph3-GFP (lane 3), which validated that NMDAR can be precipitated from adult brain homogenates only. GluR1 and GluR2/3 of AMPAR, kainite receptor (GluR₅), SSTR5 receptor, PSD95, CASK, synapsin and actin again did not show positive result from P7 brains either.

Here, I performed GFP-trap pull down from adult and P7 Nxph3-GFP^{tg/-} brain homogenates. In this experiment I validated that all subunits of NMDAR interact with neurexins while being pulled with Nxph3/ α Nrxn complex from adult brain homogenates. Interestingly, although GluN1, GluN2A, and GluN2B expression are

Figure 3.8. Searching for new potential binding partners of Nxph3 in adult Nxph3-GFP^{tg/-} mice. Brain lysates from transgenic Nxph3-GFP^{tg/-} adult mice show strong protein levels in all panels (lane 1), while GluR5 (7th excitatory panel), neurexins (1st presynaptic panel), neurexophilins (4th presynaptic panel) and actin (5th presynaptic panel) are hardly detected. GFP-trap pulled down Nxph3-GFP (lane 3, 4th presynaptic panel) in complex with α -neurexins (lane 3, 1st presynaptic panel), Nlgn1 (lane 3, 6th excitatory panel), Nlgn2 (lane 3, 1st inhibitory panel), NMDAR subunits: GluN2A (lane 3, 2nd excitatory panel), GluN2B (lanes 3, 3rd excitatory panel), GluN1 (lanes 3, 8th excitatory panel), GABA_AR (lane 3, 2nd inhibitory panel) but not mGluR3 (lane 3, 1st excitatory panel), mGluR5 (lane 3, 4th excitatory panel), Nlgn3 (lane 3, 5th excitatory panel), GluR5 (lane 3, 7th excitatory panel), AMPAR subunits: GluR1 (lane 3, 9th excitatory panel), GluR2/3 (lane 3, 10th excitatory panel), PSD95 (lane 3, 11th excitatory panel; anti-PSD95 Neuromab 1:1000, mouse), LRRTM (lane 3, 12th excitatory panel), GABA_BR (lane 3, 1st presynaptic panel), CASK (lane 3, 2nd presynaptic panel; anti-CASK Abnova 1:250, Rabbit), actin (lane 3, 5th presynaptic panel) and SSTR5 (lane 3, 6th presynaptic panel). None of the listed proteins was pulled down by control (lane 2). Details of some antibodies can be found on Fig. 5.

Results

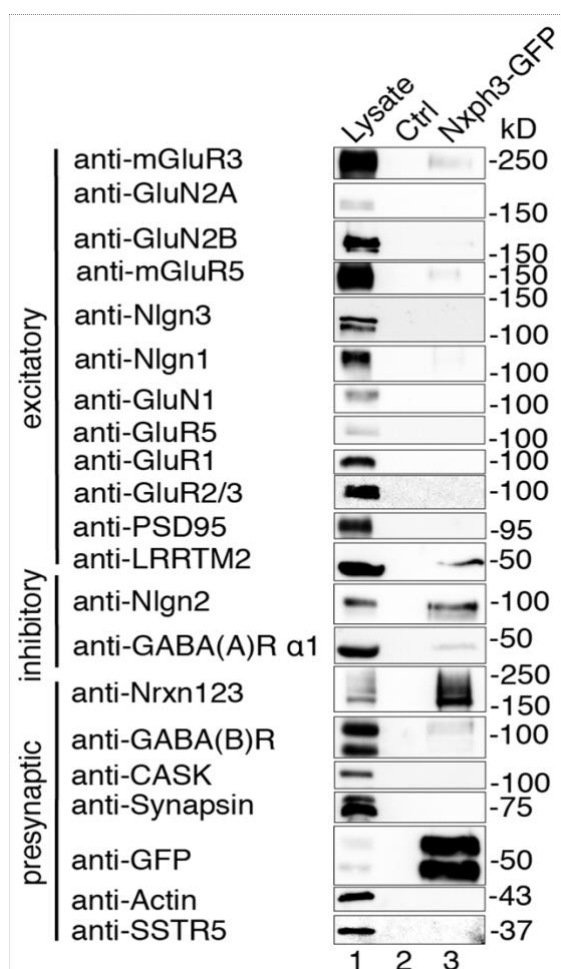


Figure 3.10. GluN1-GFP binds to Neurexins. Fc-tag fusion proteins consisting of Nxph3-Fc (lane 3), Nxph3-Fc with the extracellular domain of Nrnx1 α (Nrnx1 α ECD) (lane 4), Nrnx1 α -Fc (lane 5), Nrnx1 β -Fc (lane 6), Nrnx1 β D137A-Fc (lane 7) and a control Fc-tag (lane 2) were immobilized on protein A beads and used in pull-down experiments with lysates of HEK293 cells expressing GluN1-GFP (lane 1). GluN1-GFP was immunodetected by anti-GFP (upper panel, Abcam 1:3000, Rabbit) and anti-GluN1 (lower panel, Synaptic Systems 1:250, mouse) antibodies. GluN1-GFP was pulled down predominantly by Nrnx1 β -Fc (lane 6) and Nrnx1 α -Fc (lane 5), but neither by Nrnx1 β D137A-Fc (lane 7) nor by a control (lane 2). Nxph3-Fc (lane 3) and Nxph3-Fc+Nrxn1 α ECD (lane 4) pulled down GluN1-GFP in a very weak manner (1st and 2nd panels). Input is visible as a Ponsou S staining picture, which shows an equal amount of each fusion protein used.

high in P7 animals (Fig. 3.9, lane 1), none of these subunits was immunoprecipitated by the GFP-trap from 7 days old brain lysates. Besides NMDAR, I also discovered that GABA_BR, mGluR3 and mGluR5 interact with neurexins since they were all

Results

pulled down from P7 *Nxph3-GFP^{tg/-}* brain homogenates (Fig. 3.9, lane 3), but not from adults (Fig. 3.8, lane 3). Another surprising result is that *Nlgn1* could be immunoprecipitated from adult *Nxph3-GFP^{tg/-}* brains only (Fig. 3.8, lane 3), while *LRRTM2* was pulled only from P7 brain lysates (Fig. 3.9, lane 3).

Table 3. Synaptic receptors successfully co-sedimented by the GFP-trap from adult and P7 *Nxph3-GFP^{tg/-}* brain lysates (Fig. 3.9 and 3.10). References confirm proper immunodetected molecular weight.

Synaptic receptor	Molecular weight [kD]	Adult	P7
<i>Nlgn1</i>	120 (Ichtchenko <i>et al.</i> , 1996)	+	-
<i>Nlgn2</i>	100 (Ichtchenko <i>et al.</i> , 1996)	+	+
α Nrxns	150-250 (Hata, Slaughter and Südhof, 1993)	+	+
GABA _A R α 1	50 (Dunning <i>et al.</i> , 1999)	+	+
GluN1	120 (Akashi <i>et al.</i> , 2009)	+	-
GluN2A	150 (Akashi <i>et al.</i> , 2009)	+	-
GluN2B	150 (Akashi <i>et al.</i> , 2009)	+	-
GABA _B R1	100 (He <i>et al.</i> , 2001)	-	+
LRRTM2	50 (Ko <i>et al.</i> , 2009)	-	+
mGluR3	250 (Hayashi <i>et al.</i> , 1993)	-	+
mGluR5	150 (Hayashi <i>et al.</i> , 1993)	-	+

3.6 Recombinant GluN1-GFP binds to neurexins

To validate if the α -Nrxn/*Nxph3* complex or even *Nxph3* alone interact directly with the NMDA receptor I performed a recombinant pulldown. I expressed commercially available GFP-tagged GluN1 subunit of the NMDA receptor (Barria and Malinow, 2002) in HEK293 cells. I used cell lysate for in vitro binding experiments with Fc-tagged variants of neurexins and *Nxph3*. I again used HEK293 cells to produce Fc-tagged fusion proteins: *Nxph3*-Fc, *Nxph3*-Fc+Nrxn1 α ECD, Nrxn1 α -Fc, Nrxn1 β -Fc, Nrxn1 β D137A-Fc and Fc. Fc-tagged mature neurexophilin 3 (*Nxph3*-Fc) was

Results

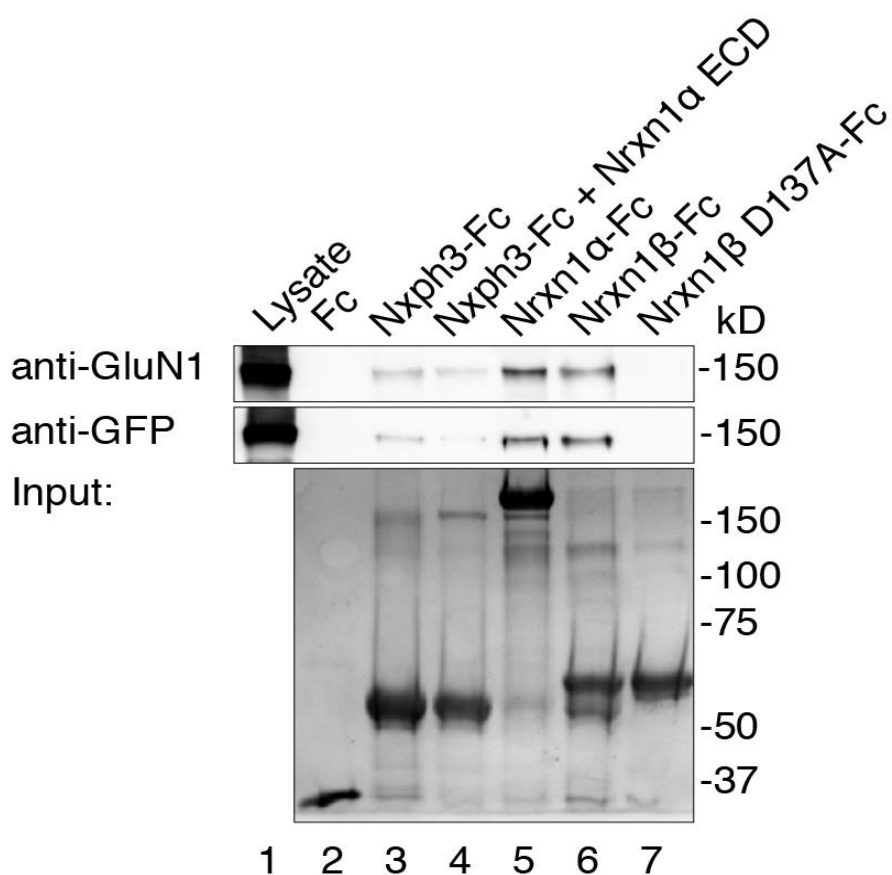


Figure 3.9. The Nxph3-GFP/ α -Nrnx complex binds to GABA_BR, LRRTM2, mGluR3 and mGluR5 but not to NMDAR in P7 Nxph3-GFP^{tg} brain. Brain lysates from transgenic Nxph3-GFP^{tg} P7 mice show strong protein levels in all panels (lane 1), while GluN2A (2nd excitatory panel), GluN1 (7th excitatory panel), GluR5 (8th excitatory panel) and neurexophilins (4th presynaptic panel) are hardly detected. GFP-trap pulled down Nxph3-GFP (lane 3, 4th presynaptic panel) in complex with α -neurexins (lane 3, 1st presynaptic panel), Nlgn2 (lane 3, 1st inhibitory panel), LRRTM (lane 3, 12th excitatory panel), mGluR3 (lane 3, 1st excitatory panel), mGluR5 (lane 3, 4th excitatory panel), GABA_AR (lane 3, 2nd inhibitory panel) and GABA_BR (lane 3, 1st presynaptic panel), but not Nlgn1 (lane 3, 6th excitatory panel), Nlgn3 (lane 3, 5th excitatory panel), NMDAR subunits: GluN2A (lane 3, 2nd excitatory panel), GluN2B (lanes 3, 3rd excitatory panel) and GluN1 (lanes 3, 7th excitatory panel). In addition, GluR5 (lane 3, 8th excitatory panel), NMDAR subunit: GluR1 (lane 3, 9th excitatory panel) and GluR2 (lane 3, 10th excitatory panel) were not detected. Input (input, lane 3) or together with extracellular domain (ECD) of Nrnx1 α (lane 4). Neurexophilins are only capable of reaching the presynaptic site when they secrete with neurexins, which was shown in cell culture experiments (Neupert *et al.*, 2015). However, when fused to Fc-tag, they are efficiently being secreted outside the cell as isolated proteins (Reissner *et al.*, 2014). Besides of WT Nrnx1 β -Fc, I also tested if Nrnx1 β D137A-Fc binds to GluN1-GFP (input, lane 7) in a calcium-dependent way. D137A mutation disturbs calcium-coordination site on LNS6/ β Nrnx, which impairs binding to neuroligins and α -dystroglycan and shows

Results

that interaction of neurexins with these partners occurs in a Ca^{2+} -dependent manner (Fairless *et al.*, 2008; Reissner *et al.*, 2014). All constructs were secreted to the medium, immobilized on protein A beads and visualized using coomassie staining (Fig. 3.10)

Since recombinant GluN1 is GFP-tagged, I could detect its presence with two antibodies: anti-GluN1 (Fig. 3.10, lower panel) and anti-GFP (Fig. 3.10, upper panel). Both antibodies see GluN1-GFP in the lysate with a molecular weight of ~150kD (Fig. 3.10, both panels, lane 1), which corresponds to the previously reported observed molecular weight of 150 kD (Barria *et al.*, 2002). Surprisingly, Nrnx1 α -Fc (Fig. 3.10, lane 5) and Nrnx1 β -Fc (Fig. 3.10, lane 6) successfully pulled down GluN1-GFP, but without an enrichment. In contrast to these results, Nrnx1 β -Fc carrying a point mutation D137A completely abolished binding to GluN1-GFP (Fig. 3.10, lane 7), which suggests that binding of GluN1-GFP to LNS6/ β Nrxn occurs calcium-dependently. In case of Nxph3-Fc (Fig. 3.10, lane 3) alone and Nxph3-Fc+Nrxn1 α ECD (Fig. 3.10, lane 4) the binding to GluN1-GFP is also visible, but it is weaker than the one shown with Nrnx1 α -Fc and Nrnx1 β -Fc (Fig. 3.10, lanes 5 and 6). Fc-tag alone did not pull down GluN1-GFP (lane 2), which indicates that visible signals of GluN1-GFP pulled with Nxph3-Fc (Fig. 3.6, lane 3), Nxph3-Fc+Nrxn1 α ECD (Fig. 3.10, lane 4) Nrnx1 α -Fc (Fig. 3.10, lane 5) and Nrnx1 β -Fc (Fig. 3.10, lane 6) were not specific.

These results show that recombinant GluN1-GFP subunit of NMDAR directly interacts with neurexins *in vitro* because GluN1-GFP was precipitated with Nrnx1 α -Fc (Fig. 3.10, lane 5) and Nrnx1 β -Fc (Fig. 3.10, lane 6). It seems that α LNS6/Nrxn β domains of neurexins are mainly responsible for this interaction since Nrnx1 α -Fc and Nrnx1 β -Fc (Fig. 3.10, lanes 5 and 6) precipitated three times more GluN1-GFP than Nxph3-Fc (Fig. 3.10, lane 3) (ImageJ analysis). Nxph3-Fc+Nrxn1 α ECD (Fig. 3.10, lane 4) also precipitated GluN1-GFP, but 7-times less than Nrnx1 α -Fc (Fig. 3.10, lane 5). It can be explained by the fact that input used in the experiment was adjusted to Fc-tagged proteins (in this case Nxph3-Fc) and therefore ten times less Nrnx1 α ECD was used (Fig. 3.10, input, lane 4, 150 kD band) than Nrnx1 α -Fc (Fig. 3.10, input, lane 5, 180 kD band). Another interesting observation is that although the expression of GluN1-GFP in HEK293 cells is very high (Fig. 3.10, lane 1), none of the Fc-tagged proteins was able to enrich GluN1-GFP in precipitates. From the other hand, there is

Results

no observed binding to Nrnx1 β D137A-Fc and to the control, which suggests that obtained pull-down signals of GluN1-GFP do not show impurities and are not a result of unspecific binding of the anti-GluN1 and anti-GFP antibodies. Also, D137A point mutation on Nrnx1 β -Fc completely abolished binding to GluN1-GFP (Fig. 3.10, lane 7), which shows that neurexins require Ca²⁺ ions in their calcium-coordination site to bind to GluN1-GFP, which is characteristic for many other neurexin partners, i.e., neuroligins (Reissner *et al.*, 2008). Interestingly, the same set of Fc-tagged proteins (Nrnx1 β -Fc, Nrnx1 α -Fc, Nxph3-Fc+Nrxn1 α ECD) from the previous experiment (Fig. 3.10) was not able to pull down GluN1 and other NMDAR subunits from the brain lysate (Fig. 3.5). It suggests that different biochemical techniques are required to show binding of NMDAR to neurexins.

Results

Discussion

Neurexophilins are specific ligands of α -Neurexins, presynaptic cell adhesion proteins. Although the neurexophilin/ α -neurexin complex has been intensively studied, many questions about its function remained unanswered. First, I showed that all neurexophilin family members interact to the same binding epitope of Nrnx1 α . Second, I wanted to further investigate the functions of neurexophilins by finding novel binding partners of Nxph1 and Nxph3. Although both neurexophilins bind to the same interface on Neurexin1 α , they are expressed in different localisations: Nxph1 in inhibitory terminals and Nxph3 excitatory terminals (Petrenko *et al.*, 1996, Beglopoulos *et al.*, 2005), which could determine distinct binding partners in synapses. To screen synaptic proteins in complex with these two neurexophilins, I performed brain pulldown experiments from transgenic Nxph1-GFP^{tg/-} and Nxph3-GFP^{tg/-} mice brain lysates.

4.1 All neurexophilins bind to the same epitope of Nrnx1 α

In the first part of my PhD project, I focused on determining the binding epitope of the Nxph1 α LNS2 domain to neurexophilins (Fig. 3.2). My results showed that LNS2 I401D impaired the binding to all neurexophilins. The crystal structure of the LNS2-Nxph1 complex recently revealed that Ile-401 interacts with the hydrophobic binding pocket of Nxph1 formed by Tyr-249 and Leu-251 (Fig. 1.3) (Reissner *et al.*, 2014). Co-immunoprecipitation validated the interface with point mutations of selected residues (I401, T405 and Y407) of the LNS2 β 10 strand (Wilson *et al.*, 2019). Mutating these residues to glutamine showed reduced binding to Nxph1 (Wilson *et al.*, 2019), but I401D mutation also showed the same effect in screening mutagenesis by coexpressed constructs (Reissner *et al.*, 2014). This means that interaction between neurexophilins and LNS2 domain requires hydrophobicity on I401 position of Nrnx1 α LNS2 (Fig. 1.3). The binding of all neurexophilins to LNS2 carrying T404P mutation was impaired (Fig. 3.2). As revealed by the crystal structure, both Nxph1 and LNS2 are composed mainly of β -strands, and the interface of the Nxph1-LNS2 complex is formed by anti-parallel β -sheet extensions mediated by interactions between β ₁ and β ₈ of Nxph1 and β ₁₀ and β ₇ of LNS2 (Wilson *et al.*, 2019). Site-directed mutagenesis of one of the central residues of β -10 in the LNS2 domain to proline (T404P) completely

Discussion

impaired binding to all neurexophilins (Fig. 3.2) Taken together, I demonstrated that all neurexophilins bind to the same binding epitope of the Nrnx1 α LNS2 domain.

Interestingly, mutation of Val-358, another hydrophobic residue close to the Nxph1 binding epitope of Nrnx1 α LNS2, demonstrated reduced binding to Nxph4 (Fig. 3.3). I also discovered that while Nxph1 binding to Nrnx1 α retained on the same level at all salt concentrations, Nxph4 binding was strongly impaired at 500mM NaCl (Fig. 3.3). The difference between Nxph4 and the other three neurexophilins is that it contains an extra 50 glycine- and proline-rich residues long loop that connects β 4 and β 5 in analogy to Nxph1 (Wilson *et al.*, 2019). The additional loop might cause steric changes in Nxph4 structure, which could cause the binding of Nxph4 was almost wholly abolished to 1 α V358D-Fc and partially impaired to 1 α L402D-Fc (Fig. 1.3). This additional unique feature of Nxph4 also could be a reason for a change in binding affinity to WT LNS2. Initially it was showed that Nrnx1 α and Nxph4 do not interact with each other, since immobilized α -latrotoxin failed to purify Nrnx-Nxph4 complex from mice brain lysates (Missler *et al.*, 1998). Recently it was reported that Nxph4 interacts with α -neurexins *in vivo*, not only with LNS2 but also with LNS4 domain (Meng *et al.*, 2019). 50 residues long loop might alter the binding of Nxph4 to neurexins and their postsynaptic binding partners. This unique feature of Nxph4 might also give a specific function of Nxph4. It was reported that Nxph4 is a secreted glycoprotein, which interacts with GABA_AR (Meng *et al.*, 2019) and it is expressed in inhibitory neurons of the hindbrain (Zeisel *et al.*, 2018), which means that it might have an important role in this specific brain region.

4.2 NMDAR is a novel binding partner of neurexins

NMDA receptors (N-methyl-D-aspartate receptors) are mainly postsynaptic, glutamate-gated cation-passing channels that play a significant role in neurotransmission in excitatory (glutamatergic) synapses. In my research I discovered that this important glutamate receptor makes a physical interaction with neurexin/neurexophilin complex. I showed that not only GluN1, but also other NMDAR subunits were precipitated with Nxph3-GFP, including GluN2A and GluN2B (Fig. 3.9). Although obtained signals are not enriched (Fig. 3.9, lane 3), the control remained empty, which shows that binding of neurexins to GluN1, GluN2A and GluN2B was specific. Moreover, I proved in the recombinant study that neurexins do not need neurexophilins to bind to GFP-tagged NMDA receptor subunit

Discussion

GluN1 (Fig. 3.10). Although a pulldown with Nxph3-Fc showed a signal of GluN1-GFP, it is still very weak, and it seems that neurexins and LNS6/LNS β domains are responsible for the interaction with the GluN1 subunit (Fig. 3.6). This domain has already been identified as a hot spot for many other interactors of neurexins, i.e., neuroligins, LRRTMs and cerebellins (Table 2). The binding of α LNS6/ β Nrxn to neurexin partners is controlled by alternative splice site SS#4, while most of the proteins prefer to bind to the isoform, which does not contain an insert (SS#4-) and I also used this variant in my recombinant experiment (Fig. 3.10). It has been shown that alternative splicing of neurexins regulates postsynaptic NMDAR responses. Neurexin 1 carrying SS#4 insert enhances NMDAR responses, while neurexin 3 with this insert does not alter NMDAR responses (Dai *et al.*, 2019). The interaction between neurexins and NMDAR occurs Ca²⁺-dependently since a Nrxn1 β -Fc with a mutation in the calcium-coordination site (Nrxn1 β D137A-Fc) completely abolished binding to GluN1-GFP just like it was shown for Nlgn1, Nlgn2 and α -DAG (Reissner *et al.*, 2008; Reissner *et al.*, 2014). Obtained signals of pulled GluN1-GFP were not enriched, which suggests that the binding between neurexins and NMDAR is not irreversible like in the case of neurexin-neuroligin interactions (Ichtchenko *et al.*, 1995). This could also explain why I could not precipitate any of the NMDAR subunits by Fc-tagged neurexins (Fig. 3.5). Another explanation for obtained weak pulldown signals might be incorrect NMDAR-Nrxn binding conditions, although I performed all experiments in buffers imitating physiological environment in the synaptic cleft.

The functional crosstalk between neurexins and NMDAR was demonstrated before. A triple knock-out of neurexins in mice showed a reduction of NMDAR-mediated postsynaptic currents, which indicates that neurexins are required for regular activity of NMDA receptors (Kattenstroth *et al.*, 2003). Moreover, neurexins mediate postsynaptic glutamate differentiation in contacting neurons and induce clustering of GluN1 subunit of NMDAR (Graf *et al.*, 2004). As demonstrated in a different PhD project from our group, the electrophysiological recordings performed on the same Nxph3-GFP^{tg/-} mice brain slices showed altered NMDAR responses (Wang, 2014). Since neurexophilins are in a tight complex with the LNS2 domain of α -neurexins (Missler *et al.*, 1998) and the dissociation of α Nrxn/Nxph complexes occurs only in near denaturing conditions (Petrenko *et al.*, 1996), it is likely that the Nxph3/ α Nrxn complex mediates observed altered synaptic transmission in Nxph3- GFP^{tg/-} mice.

4.3 NMDAR interacts with α -neurexin/neurexophilin complex in mature brains

Another interesting observation is that NMDAR subunits could be pulled down from adult (10-16 weeks old) animals but not from young P7 mice. However, NMDAR subunits are already expressed at this stage of life. GluN1 is expressed in virtually all neurons, and during all developmental stages, GluN2B occurs prenatally, while GluN2A mRNA is first detected near birth (Monyer *et al.*, 1994). Lack of visible NMDAR signals in samples obtained by GFP-trap from P7 brains suggests that although GluN1, GluN2A and GluN2B are present in cells, they start interacting with neurexins after the seventh day of postnatal life. This point of time is interesting because mice begin to open their eyes between P12 and P14 (Hoy and Niell, 2015). The eye-opening was shown to be the period of fast synaptogenesis in the primary visual cortex (Blue and Parnavelas, 1983). A conditional knockout of GluN1 subunit introduced in retinal ganglion cells of P1-P3 animals led to a reduction in expansion of the dendritic field size, dendritic elongation, and the number of the dendritic protrusions in retinal ganglion cells before eye-opening (Elias *et al.*, 2018). Interestingly, when the same mice were reared in the darkness, the number of dendritic protrusions and the size of the dendritic field did not change after eye-opening (Elias *et al.*, 2018). This study demonstrates a correlation between a visual experience that leads to eye-opening and the NMDAR mediated dendritic development. It cannot be excluded that the formation of new synapses during eye-opening requires interaction between neurexins and the NMDA receptor. That is why the physical interaction between these two proteins was not visible on the pull-downs performed on brain lysates of 7-day old mice; since it probably started to occur after eye-opening between P12 and P14, more synaptic connections were formed.

4.4 Other age-dependent interactions

The binding between NMDAR and neurexins was not the only age-dependent interaction observed in experiments with the GFP-trap. Nlgn1 was precipitated from adult (Fig. 3.6 and 3.8) but not from P7 brains (Fig. 3.7 and 3.9), although Nlgn1 is already expressed as visible in the brain lysates on immunoblots. One possible explanation for the lack of Nlgn1 immunoprecipitated from P7 brains is that α -neurexins without GFP-tagged neurexophilins could “occupy” most of the Nlgn1 molecules since free neurexins including α - and β -neurexins might sterically better access to Nlgn1. However, it has been reported that the presence of Nxph1 does not

Discussion

disturb binding to neuroligins in recombinant pulldowns (Reissner *et al.*, 2014). Also, the lack of the high enrichment in Nlgn1 brain pulldown samples characteristic for Nrxn-Nlgn interactions (Ichtchenko *et al.*, 1995) suggests that overexpression of Nxph3-GFP may disturb the interaction with neurexins in these brains. However, this hypothesis can be excluded because it could pull down Nlgn1 in a high amount from Nxph3-GFP^{tg/-} adult brains by the Fc-tagged neurexins (Fig. 3.5). It is also possible that GFP-tagged neurexophilin- α Nrxn complexes in Nxph1-GFP^{tg/-} and Nxph3-GFP^{tg/-} brains prefer binding to distinct postsynaptic partners than Nlgn1, i.e., Nlgn2 and LRRTM2 that were already visible in the P7 brain pulldown (Fig. 3.7 and 3.9). Nlgn1, Nlgn2 and LRRTM2 are all expressed already during embryonic development (Song *et al.*, 1999; Varoqueaux, Jamain and Brose, 2004; Haines and Rigby, 2007), which shows that although they are all present in P7 brains, Nlgn1 do not get in touch with neurexin/Nxph3 complexes at this stage. Also, although it was previously reported that Nlgn1, NMDAR and PSD95 interact together (Frank *et al.*, 2016), it was impossible to pulldown PSD95 from transgenic brains. That result is also interesting since both Nlgn1 and NMDAR could be pulled from adult brains.

Another attractive new identified binding partner of the neurexin-neurexophilin complex is GABA_BR. Nxph1-GFP and Nxph3-GFP pulled GABA_BR from transgenic P7 brains (Fig. 3.7 and 3.9) but not from adults (Fig. 3.6 and 3.8), although signals for anti-GABA_BR are both intense in both P7 and adult brain lysates. This result again suggests an age-dependency of this complex relationship, which is opposite to observed NMDAR-neurexin binding that was gained during postnatal development after seven days of age. As in GluN1, GluN2A and GluN2B, it was not possible to achieve a robust binding signal of anti-GABA_BR in GFP-trap samples (Fig. 3.6 and 3.8), suggesting the Nrxn/Nxph-GABA_BR transient weak nature of this interaction or not proper binding conditions used in the experiment. A functional crosstalk between Nxph/Nrxn complex and GABA_BR has been reported. Electrophysiological recordings from both Nxph1-GFP^{tg/-} and Nxph3-GFP^{tg/-} brain slices showed a reduced frequency of mini excitatory postsynaptic currents (mEPSCs), which were rescued to WT levels by GABA_BR-specific blockers (Born *et al.*, 2014). Progressive decay in postnatal development raises questions if Nxph/Nrxn-GABA_BR complex is formed during the embryonic state and starts to disappear after birth. Moreover, it was also reported that the GABA_AR γ 2 subunit interacts with the R1 subunit of the GABA_B receptor and promotes R1 subunit expression in the absence of R2 subunits (Frangaj

Discussion

and Fan, 2018). The $\gamma 2$ subunit of GABA_AR associates with functional R1/R2 heterodimers and promotes GABA_BR internalization in response to agonist stimulation (Frangaj and Fan, 2018). α Neurexin/neurexophilin complex was shown to interact with both GABA_AR $\alpha 1$ and GABA_B receptors in P7 brains (Fig. 3.9). However, the immunodetected signal of binding to GABA_B receptors are completely impaired in adult animals (10-16 weeks old), while the binding signal to GABA_AR $\alpha 1$ become stronger in older brains (Fig. 3.8) Same time immunodetected signals for both receptors in brain lysates from P7 and adult brain lysates have the same intense level. Interestingly, although Nxph3-GFP was shown to be present mostly in excitatory neurons (Blanque, 2015) it pulled GABA_AR $\alpha 1$, which is a receptor present mostly in inhibitory neurons. However, it was shown that Nrxns together with $\alpha 2\delta-2$ can modulate postsynaptic GABA_AR abundance, which can lead to a mismatched localization of GABA_AR in glutamatergic neurons (Geisler *et al.*, 2019). Combining these pieces of information suggests that α Neurexins with neurexophilins, GABA_AR and GABA_BR are in a multiplex formed early in development and later dismiss GABA_BR from physical contact with other members. However, this interaction requires further investigation and more shreds of evidence.

Metabotropic glutamate receptors (mGluRs) and ionotropic glutamate receptors (iGluRs), i.e., NMDAR, AMPAR, are responsible for glutamate signalling in the nervous system. iGluRs are ligand-gated ion channels producing glutamate-evoked currents, and mGluRs are G-protein coupled receptors (GPCRs) that mediate signalling processes via G protein signalling (Reiner and Levitz, 2018). The best described binding partners of mGluRs are scaffold proteins that interact via PDZ domains with C-terminal domains (CTDs) of mGluRs, i.e., PSD-95, HOMER, SHANK and DLGAP (Tu *et al.*, 1999). Although there is no evidence of trans-synaptic interactions of metabotropic glutamate receptors with presynaptic proteins, there are reports of an interaction between metabotropic glutamate receptors and NMDAR (Perroy *et al.*, 2008, Moutin *et al.*, 2012). Functional measurements in HEK293 cells and bioluminescence resonance energy transfer (BRET) studies showed a dynamic interaction between CTDs of mGluR5 and NMDAR composed of GluN1/GluN2B subunits, which resulted in bidirectional inhibition (Perroy *et al.*, 2008). There are also reports of functional crosstalk between mGluR5 and NMDAR in dendritic spines of hippocampal neurons showed in BRET studies (Moutin *et al.*,

Discussion

2012). However, more studies must be performed to see whether these phenomena are relevant in physiological conditions.

In summary, GABA_BR, LRRTM2, mGluR3, and mGluR5 could be precipitated from the P7 animals (Fig. 3.7 and 3.9) while Nlgn1 and NMDAR were pulled only from the adult brain (Fig. 3.6 and 3.8). These results are in contrast with experiment using Fc-tagged recombinant neurexins -1 β and -1 α and Nxph3/Nrxn1 α complex (Fig. 3.5) and the same Nxph3-GFP^{tg/-} adult mice brains, in which it was possible to precipitate Nlgn1, Nlgn2, LRRTM2 and GABA_BR but not NMDAR, mGluR3 and mGluR5. It shows that it is only possible to pull down these receptors using GFP-trap that directly pulled Nxph3-GFP from its synaptic complexes. These proteins are expressed already in P7 in a high amount, which was visible in the brain lysate input on every immunoblot (Fig. 3.6-3.9). However, they interact with Nxph/Nrxn complexes at different point of life. These results suggest that there is a molecular switch that changes the binding properties of the α Nrxn/Nxph3-GFP complex after the seventh day of age. In my model, at first Nrxn/Nxph complex interact with LRRTM2, GABA_BR, mGluR3 and mGluR5 in excitatory synapses. mGluR3 and mGluR5 are the glutamate receptors that could be involved in the excitatory neurotransmission till NMDAR starts to play a leading role after seven days of life (Fig. 4.1). At this stage, Nlgn1 is also involved in the interaction with neurexins, while interaction with LRRTM2, GABA_BR and mGluR3 and mGluR5 get lost. For instance, Nlgn1 was shown to be present in embryonic rat brains and increases its expression at birth to peak at postnatal days 5-8 and later again in adulthood (Song *et al.*, 1999), which also fits to my model in which Nlgn1 starts to interact with neurexins after P7 where there is more Nlgn1 present in synapses. Moreover, it was shown that NMDA receptors are present in the brain together with other synaptic proteins as two supermolecular complexes of 0.8MDa and 1.5MDa size (Frank *et al.*, 2016). Interestingly, 0.8MDa complexes were observed at all ages of mice, while 1.5MDa increased significantly after P16. It was shown that 1.5MDa complexes contained NMDAR and Neurexin1 α and Nlgn1, which also fits my model in which all these proteins start to interact with each other in developing mature forebrain.

Discussion

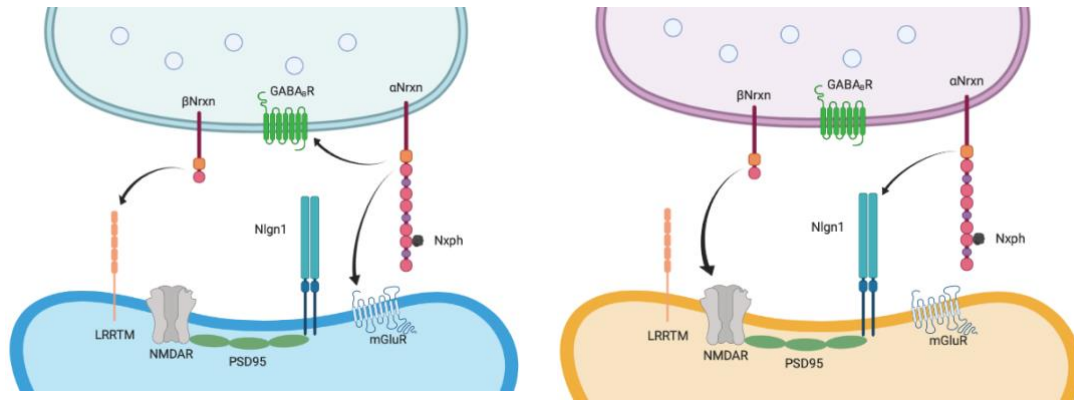


Figure 4.1. Model explaining age-dependent interactions between neurexins and their binding partners in excitatory synapses of *Nxph3-GFP^{tg/-}* brain. Simplified model of the synaptic cleft includes only these proteins that were pulled together with *Nxph3-GFP* from both P7 (left) and adult 16 weeks old (right) brain lysates including: Neurexins, LRRTM, NMDAR, GABA_BR, Nlgn1 and mGluR. Neurexins are shown in two isoforms: long α Nrxn and short β Nrxn. Neurexins recruit LRRTM2, GABA_BR, mGluR3, mGluR5 in P7 transgenic brains (Left) but later in postnatal development start to interact with Nlgn1 and NMDAR (Right).

4.5 Limitations and recommendations

Here I would like to explain what limitations I faced while working with synaptic receptors. First, I would like to point to the low-intensity signals of pulled proteins compared to signals obtained in the lysates in all the performed immunoblots. All the pulldown signals from *Nxph3-GFP^{tg/-}* and *Nxph1-GFP^{tg/-}* brains were obtained by immunoprecipitation from brain lysate that represents half of the transgenic mouse forebrain. In contrast, signals in brain lysates on immunoblots were detected from only 0,37% of the total lysate volume used for each pulldown lane. In other words, signals in input represent 135 times less lysate than was used for the pulldown. The only enriched signals from GFP-trap are *Nxph1-GFP* (Fig. 3.7 and 3.8) and *Nxph3-GFP* (Fig. 3.7-3.10) that were pulled from half a brain but did not pull any of the synaptic receptors profusely. Even Nlgn1 and Nlgn2, which bind to neurexins irreversibly, were not precipitated with an enrichment characteristic for this interaction (Ichtchenko *et al.*, 1995, Ichtchenko *et al.*, 1996), like in the pulldown with the Fc-tagged neurexins (Fig. 3.5). On the other hand, signals of GFP-tagged neurexophilins are very enriched. Still, we must remember that we are pulling them from the brain lysate. We do not know how many molecules from this pull interact

Discussion

with all immunoprecipitated synaptic receptors. It seems that only a low number of pulled GFP-neurexophilin/ α Nrxn complex interact with pulled proteins, and the interaction can also be very transient. Although obtained immunodetection signals of pulled NMDAR, GABA_BR, Nlgns, LRRTM2 and mGluRs are relatively weak, the control is always empty, which points to the specificity of the interaction. I saw the same results in three biological replicates, highlighting NMDAR, GABA_BR, mGluR3 and mGluR5 are novel partners of the neurexin/neurexophilin complex.

Results from the recombinant pulldown also did not give an enrichment of pulled GluN1-GFP (Fig. 3.6). The very intense signals of GluN1-GFP were obtained from 15 μ l of cell lysate, which is an equivalent of 1/20 of a single HEK293 cells plate transfected with GluN1-GFP. For pulldown, every Fc-tagged fusion protein bounded to protein A (Fig. 3.6, lanes 2-7) were incubated with cell lysate prepared from 2,5 HEK293 plates transfected with GluN1-GFP, which is in total 75 times more lysate volume then loaded in lane 1. Nrxn1 β -Fc successfully pulled down GluN1-GFP (Fig. 3.6, lane 6, lower panel). However, the band obtained from 2,5 plates of cell lysate in lane six is five times weaker than lysate loaded in lane 1. Nrxn1 β -Fc binds to GluN1 probably better because Nrxn1 β is a smaller analogue of Nrxn1 α , which contains only one LNS domain (LNS6/ β Nrxn) and therefore molarity of Nrxn1 β -Fc used in the input (lane 6) is higher than the one of Nrxn1 α -Fc (lane 5), as explained in the paragraph 3.3. As a result, the Nrxn1 α ECD complex binds to GluN1-GFP but in a weaker manner because there are fewer molecules of Nrxn1 α ECD (Fig. 3.6, input, lane 4, ~150 kD) than Nrxn1 β -Fc (input, lane 6, ~50 kD). However, although lysis conditions were good enough to release many GluN1-GFP from HEK293 cells membranes (Fig. 3.6, both panels, lane 1), it was still not enough to pull down GluN1-GFP in an enriched manner. One explanation for this is that only a specific fraction of GluN1-GFP molecules bind to neurexins. GluN1 subunit has ten N-glycosylation sites (Sanz-Clemente, Nicoll and Roche, 2013). It is possible that all the intense GluN1-GFP band in the lysate (Fig. 3.6, lane 1) represent a variation of N-glycosylated fractions and probably only the fully N-glycosylated molecule can bind to neurexins. To further validate the interaction of neurexins with the GluN1 subunit, the experiment could be designed oppositely with Fc-tagged extracellular parts GluN1 interacting with full-length neurexins, which would also be easier to detect the binding epitope of GluN1 to neurexins.

Discussion

Another difficulty that I faced was the preparation of brain samples. To detect all of the synaptic receptors from brain lysates, I had to prepare samples in three different conditions. Detection of most of the proteins requires boiling of lysates and purified pulldown samples in sample buffer at 99°C for 5 to 10 minutes. However, some receptors required different sample preparation steps, which lead to more tissue material to be used to detect all proteins of interest. To immunodetect GABA_AR α 1, GABA_BR R1, mGluR3, mGluR5, PSD95 and synapsin with a proper molecular weight, samples could not be boiled. Boiling at 99°C, in this case, caused a formation of protein clusters, which did not migrate through polyacrylamide gels. Protein denaturation had to be performed by rotation of brain samples mixed with sample buffer at RT for 20 minutes. GluN1 of NMDAR could only be immunodetected in the presence of 8 M urea in the sample buffer and after boiling. The presence of urea strongly denatures NMDAR and exposes antibody binding epitope, which allows immunodetection of GluN1. In summary, to detect all listed synaptic proteins, I had to prepare brain samples in three different ways. First, samples boiled in 2x sample buffer at 99°C for 5 min to detect most of the synaptic receptors. Second, samples boiled in sample buffer supplemented with 8 M urea to detect GluN1; Third, non-boiled samples prepared by a rotation at RT for 20 min in same sample buffer to detect GABA_AR α 1 and GABA_BR R1 (see more details in materials and methods).

4.6 Conclusion and outlook

This doctoral study focused on neurexophilins and their complex with α -neurexins. First, I confirmed that all four neurexophilins bind to the same binding epitope of Nr_{xn}1 α . This result was not a surprise since protein sequences of neurexophilins are homologous, and they do not show many differences. The only neurexophilin that stands out is Nxph4, which behaved slightly different and showed some impairment in binding to mutated residues close to the previously determined binding epitope of Nr_{xn}1 α to Nxph1 (Reissner *et al.*, 2014; Wilson *et al.*, 2019). The reason for this behavior is probably a unique fifty residues long loop not present in Nxph1, Nxph2, nor Nxph3 (Wilson *et al.*, 2019), that sterically hinders the binding of Nxph4 to Nr_{xn}1 α . I showed that this feature of Nxph4 causes a lower stability to Nr_{xn}1 α than Nxph1, which was demonstrated to be in a tight complex with Nr_{xn}1 α that could be destroyed only under strongly denaturing conditions (Ichtienko *et al.*, 1995).

Discussion

In the second part of my thesis, I searched for novel binding partners of Neurexophilin/ α Neurexin complex. Using transgenic mice that overexpress Nxph1-GFP and Nxph3-GFP in brain areas that Nxph1 or Nxph3 do not occur naturally. I showed that the Nxph/ α Nrxn complex was able to immunoprecipitate NMDA, GABA_B, mGluR3 and mGluR5 receptors. Although there were some reports of functional cross-talks between neurexins and NMDAR (Dai *et al.*, 2019), it has never been reported before that this primary glutamate receptor physically interacts with neurexins. I confirmed in a recombinant study that the LNS6/ β Nrxn domain of neurexins is responsible for binding to the GluN1 subunit of NMDAR. The interaction occurs in a Ca²⁺-dependent manner, which is characteristic of most interactions between neurexins and their binding partners (Table 2). Interestingly, the NMDAR-Neurexin interaction could be observed in a pulldown performed on sixteen-week-old mice brains but not on seven days old animals, suggesting that these two proteins start to interact with each other in the second postnatal week or later. On the other way around to NMDAR, I discovered that GABA_BR, mGluR3 and mGluR5 interact with the Nxph/ α Nrxn complex in 7 days old animals but not adults. It suggests that neurexins and neurexophilins are involved in an age-dependent molecular switch that happens during the maturation of synapses.

Discussion

References

Akanno, E. C., Chen, L., Abo-Ismael, M. K., Crowley, J. J., Wang, Z., Li, C., Basarab, J. A., MacNeil, M. D., & Plastow, G. S. (2018). Genome-wide association scan for heterotic quantitative trait loci in multi-breed and crossbred beef cattle 06 Biological Sciences 0604 Genetics. *Genetics Selection Evolution*, *50*(1). <https://doi.org/10.1186/s12711-018-0405-y>

Akashi, K., Kakizaki, T., Kamiya, H., Fukaya, M., Yamasaki, M., Abe, M., Natsume, R., Watanabe, M., & Sakimura, K. (2009). NMDA Receptor GluN2B (GluR 2/NR2B) Subunit Is Crucial for Channel Function, Postsynaptic Macromolecular Organization, and Actin Cytoskeleton at Hippocampal CA3 Synapses. *Journal of Neuroscience*, *29*(35). <https://doi.org/10.1523/JNEUROSCI.5531-08.2009>

Ali, G., Lee, K., Andrade, P. B., Basit, S., Santos-Cortez, R. L. P., Chen, L., Jelani, M., Ansar, M., Ahmad, W., & Leal, S. M. (2011). Novel autosomal recessive nonsyndromic hearing impairment locus DFNB90 maps to 7p22.1-p15.3. *Human Heredity*, *71*(2), 106–112. <https://doi.org/10.1159/000320154>

Anderson, G. R., Aoto, J., Tabuchi, K., Földy, C., Covy, J., Yee, A. X., Wu, D., Lee, S.-J., Chen, L., Malenka, R. C., & Südhof, T. C. (2015). β -Neurexins Control Neural Circuits by Regulating Synaptic Endocannabinoid Signaling. *Cell*, *162*(3). <https://doi.org/10.1016/j.cell.2015.06.056>

Andreyeva, A., Leshchyns'ka, I., Knepper, M., Betzel, C., Redecke, L., Sytnyk, V., & Schachner, M. (2010). CHL1 Is a Selective Organizer of the Presynaptic Machinery Chaperoning the SNARE Complex. *PLoS ONE*, *5*(8). <https://doi.org/10.1371/journal.pone.0012018>

Aoto, J., Földy, C., Ilcus, S. M. C., Tabuchi, K., & Südhof, T. C. (2015). Distinct circuit-dependent functions of presynaptic neurexin-3 at GABAergic and glutamatergic synapses. *Nature Neuroscience*, *18*(7). <https://doi.org/10.1038/nn.4037>

References

- Aoto, J., Martinelli, D. C., Malenka, R. C., Tabuchi, K., & Südhof, T. C. (2013). XPresynaptic neurexin-3 alternative splicing trans-synaptically controls postsynaptic AMPA receptor trafficking. *Cell*, *154*(1), 75. <https://doi.org/10.1016/j.cell.2013.05.060>
- Araç, D., Boucard, A. A., Özkan, E., Strop, P., Newell, E., Südhof, T. C., & Brunger, A. T. (2007). Structures of Neuroligin-1 and the Neuroligin-1/Neurexin-1 β Complex Reveal Specific Protein-Protein and Protein-Ca²⁺ Interactions. *Neuron*, *56*(6). <https://doi.org/10.1016/j.neuron.2007.12.002>
- Baez, M. V., Cercato, M. C., & Jerusalinsky, D. A. (2018). NMDA receptor subunits change after synaptic plasticity induction and learning and memory acquisition. In *Neural Plasticity* (Vol. 2018). Hindawi Limited. <https://doi.org/10.1155/2018/5093048>
- Balasubramanian, S., Teissère, J. A., Raju, D. v., & Hall, R. A. (2004). Hetero-oligomerization between GABAA and GABAB Receptors Regulates GABAB Receptor Trafficking. *Journal of Biological Chemistry*, *279*(18), 18840–18850. <https://doi.org/10.1074/jbc.M313470200>
- Barberis, A. (2020). Postsynaptic plasticity of GABAergic synapses. *Neuropharmacology*, *169*, 107643. <https://doi.org/10.1016/j.neuropharm.2019.05.020>
- Barria, A., & Malinow, R. (2002). Subunit-Specific NMDA Receptor Trafficking to Synapses. *Neuron*, *35*(2). [https://doi.org/10.1016/S0896-6273\(02\)00776-6](https://doi.org/10.1016/S0896-6273(02)00776-6)
- Beglopoulos, V., Montag-Sallaz, M., Rohlmann, A., Piechotta, K., Ahmad, M., Montag, D., & Missler, M. (2005). Neurexophilin 3 Is Highly Localized in Cortical and Cerebellar Regions and Is Functionally Important for Sensorimotor Gating and Motor Coordination. *Molecular and Cellular Biology*, *25*(16), 7278–7288. <https://doi.org/10.1128/mcb.25.16.7278-7288.2005>
- Behuet, S., Cremer, J. N., Cremer, M., Palomero-Gallagher, N., Zilles, K., & Amunts, K. (2019). Developmental Changes of Glutamate and GABA Receptor Densities in Wistar Rats. *Frontiers in Neuroanatomy*, *13*. <https://doi.org/10.3389/fnana.2019.00100>

References

- Beique, J.-C., Lin, D.-T., Kang, M.-G., Aizawa, H., Takamiya, K., & Huganir, R. L. (2006). Synapse-specific regulation of AMPA receptor function by PSD-95. *Proceedings of the National Academy of Sciences*, *103*(51). <https://doi.org/10.1073/pnas.0608492103>
- Ben-Ari, Y. (2014). The GABA excitatory/inhibitory developmental sequence: A personal journey. In *Neuroscience* (Vol. 279, pp. 187–219). Elsevier Ltd. <https://doi.org/10.1016/j.neuroscience.2014.08.001>
- Bennett, M. V. L., & Zukin, R. S. (2004). Electrical Coupling and Neuronal Synchronization in the Mammalian Brain. *Neuron*, *41*(4). [https://doi.org/10.1016/S0896-6273\(04\)00043-1](https://doi.org/10.1016/S0896-6273(04)00043-1)
- Benson, D. L., & Huntley, G. W. (2012). Synapse adhesion: a dynamic equilibrium conferring stability and flexibility. *Current Opinion in Neurobiology*, *22*(3). <https://doi.org/10.1016/j.conb.2011.09.011>
- Biederer, T., & Südhof, T. C. (2000). Mints as adaptors. Direct binding to neuexins and recruitment of Munc18. *Journal of Biological Chemistry*, *275*(51), 39803–39806. <https://doi.org/10.1074/jbc.C000656200>
- Biederer, T., & Südhof, T. C. (2001). CASK and Protein 4.1 Support F-actin Nucleation on Neuexins. *Journal of Biological Chemistry*, *276*(51). <https://doi.org/10.1074/jbc.M105287200>
- Bishop, D. V., & Scerif, G. (2011). Klinefelter syndrome as a window on the aetiology of language and communication impairments in children: The neuroligin-neurexin hypothesis. *Acta Paediatrica, International Journal of Paediatrics*, *100*(6), 903–907. <https://doi.org/10.1111/j.1651-2227.2011.02150.x>
- Biswas, S., Russell, R. J., Jackson, C. J., Vidovic, M., Ganeshina, O., Oakeshott, J. G., & Claudianos, C. (2008). Bridging the Synaptic Gap: Neuroligins and Neurexin I in *Apis mellifera*. *PLoS ONE*, *3*(10). <https://doi.org/10.1371/journal.pone.0003542>
- Blein, S., Ginham, R., Uhrin, D., Smith, B. O., Soares, D. C., Veltel, S., McIlhinney, R. A. J., White, J. H., & Barlow, P. N. (2004). Structural Analysis of the Complement Control Protein

References

(CCP) Modules of GABAB Receptor 1a. *Journal of Biological Chemistry*, 279(46). <https://doi.org/10.1074/jbc.M406540200>

Blue, M. E., & Parnavelas, J. G. (1983). The formation and maturation of synapses in the visual cortex of the rat. II. Quantitative analysis. *Journal of Neurocytology*, 12(4). <https://doi.org/10.1007/BF01181531>

Born, G., Breuer, D., Wang, S., Rohlmann, A., Coulon, P., Vakili, P., Reissner, C., Kiefer, F., Heine, M., Pape, H. C., & Missler, M. (2014). Modulation of synaptic function through the a-neurexin-specific ligand neurexophilin-1. *Proceedings of the National Academy of Sciences of the United States of America*, 111(13). <https://doi.org/10.1073/pnas.1312112111>

Boucard, A. A., Chubykin, A. A., Comoletti, D., Taylor, P., & Südhof, T. C. (2005). A splice code for trans-synaptic cell adhesion mediated by binding of neuroligin 1 to α - and β -neurexins. *Neuron*, 48(2), 229–236. <https://doi.org/10.1016/j.neuron.2005.08.026>

Boucard, A. A., Ko, J., & Südhof, T. C. (2012a). High Affinity Neurexin Binding to Cell Adhesion G-protein-coupled Receptor CIRL1/Latrophilin-1 Produces an Intercellular Adhesion Complex. *Journal of Biological Chemistry*, 287(12). <https://doi.org/10.1074/jbc.M111.318659>

Boucard, A. A., Ko, J., & Südhof, T. C. (2012b). High affinity neurexin binding to cell adhesion G-protein-coupled receptor CIRL1/latrophilin-1 produces an intercellular adhesion complex. *Journal of Biological Chemistry*, 287(12), 9399–9413. <https://doi.org/10.1074/jbc.M111.318659>

Bourne, J. N., & Harris, K. M. (2008). Balancing Structure and Function at Hippocampal Dendritic Spines. *Annual Review of Neuroscience*, 31(1). <https://doi.org/10.1146/annurev.neuro.31.060407.125646>

Brito-Moreira, J., Lourenco, M. v., Oliveira, M. M., Ribeiro, F. C., Ledo, J. H., Diniz, L. P., Vital, J. F. S., Magdesian, M. H., Melo, H. M., Barros-Aragão, F., de Souza, J. M., Alves-Leon, S. v., Gomes, F. C. A., Clarke, J. R., Figueiredo, C. P., de Felice, F. G., & Ferreira, S. T. (2017). Interaction of amyloid- β (A β) oligomers with neurexin 2 α and neuroligin 1

References

mediates synapse damage and memory loss in mice. *Journal of Biological Chemistry*, 292(18). <https://doi.org/10.1074/jbc.M116.761189>

Bustos, F. J., Varela-Nallar, L., Campos, M., Henriquez, B., Phillips, M., Opazo, C., Aguayo, L. G., Montecino, M., Constantine-Paton, M., Inestrosa, N. C., & van Zundert, B. (2014). PSD95 Suppresses Dendritic Arbor Development in Mature Hippocampal Neurons by Occluding the Clustering of NR2B-NMDA Receptors. *PLoS ONE*, 9(4). <https://doi.org/10.1371/journal.pone.0094037>

Butz, S., Okamoto, M., & Südhof, T. C. (1998). A Tripartite Protein Complex with the Potential to Couple Synaptic Vesicle Exocytosis to Cell Adhesion in Brain. *Cell*, 94(6). [https://doi.org/10.1016/S0092-8674\(00\)81736-5](https://doi.org/10.1016/S0092-8674(00)81736-5)

Chen, F., Venugopal, V., Murray, B., & Rudenko, G. (2011). The Structure of Neurexin 1 α Reveals Features Promoting a Role as Synaptic Organizer. *Structure*, 19(6). <https://doi.org/10.1016/j.str.2011.03.012>

Chen, L. Y., Jiang, M., Zhang, B., Gokce, O., & Südhof, T. C. (2017). Conditional Deletion of All Neurexins Defines Diversity of Essential Synaptic Organizer Functions for Neurexins. *Neuron*, 94(3). <https://doi.org/10.1016/j.neuron.2017.04.011>

Chen, X., Liu, H., Shim, A. H. R., Focia, P. J., & He, X. (2008). Structural basis for synaptic adhesion mediated by neuroligin-neurexin interactions. *Nature Structural & Molecular Biology*, 15(1). <https://doi.org/10.1038/nsmb1350>

Chen, Y., Chen, S. R., Chen, H., Zhang, J., & Pan, H. L. (2019). Increased $\alpha 2\delta$ -1-NMDA receptor coupling potentiates glutamatergic input to spinal dorsal horn neurons in chemotherapy-induced neuropathic pain. *Journal of Neurochemistry*, 148(2), 252–274. <https://doi.org/10.1111/jnc.14627>

Chittajallu, R., Wester, J. C., Craig, M. T., Barksdale, E., Yuan, X. Q., Akgül, G., Fang, C., Collins, D., Hunt, S., Pelkey, K. A., & McBain, C. J. (2017). Afferent specific role of NMDA receptors for the circuit integration of hippocampal neurogliaform cells. *Nature Communications*, 8(1). <https://doi.org/10.1038/s41467-017-00218-y>

References

- Clarris, H. J., Mckeown, S., & Key, B. (2002). Expression of neurexin ligands, the neuroligins and the neurexophilins, in the developing and adult rodent olfactory bulb. In *Int. J. Dev. Biol* (Vol. 46). www.ijdb.ehu.es
- Collingridge, G. L., Volianskis, A., Bannister, N., France, G., Hanna, L., Mercier, M., Tidball, P., Fang, G., Irvine, M. W., Costa, B. M., Monaghan, D. T., Bortolotto, Z. A., Molnár, E., Lodge, D., & Jane, D. E. (2013). The NMDA receptor as a target for cognitive enhancement. *Neuropharmacology*, *64*. <https://doi.org/10.1016/j.neuropharm.2012.06.051>
- Connors, B. W., & Long, M. A. (2004). Electrical synapses in the mammalian brain. In *Annual Review of Neuroscience* (Vol. 27, pp. 393–418). <https://doi.org/10.1146/annurev.neuro.26.041002.131128>
- Corlew, R., Wang, Y., Ghermazien, H., Erisir, A., & Philpot, B. D. (2007). Developmental Switch in the Contribution of Presynaptic and Postsynaptic NMDA Receptors to Long-Term Depression. *Journal of Neuroscience*, *27*(37). <https://doi.org/10.1523/JNEUROSCI.5494-06.2007>
- Cottrell, G. T., & Ferguson, A. v. (2004). Sensory circumventricular organs: central roles in integrated autonomic regulation. *Regulatory Peptides*, *117*(1). <https://doi.org/10.1016/j.regpep.2003.09.004>
- Crespo, K., Chauvet, C., Blain, M., Ménard, A., Roy, J., & Deng, A. Y. (2011). Normotension in Lewis and Dahl salt-resistant rats is governed by different genes. *Journal of Hypertension*, *29*(3), 460–465. <https://doi.org/10.1097/HJH.0b013e328341f1cc>
- Dai, J., Aoto, J., & Südhof, T. C. (2019). Alternative Splicing of Presynaptic Neurexins Differentially Controls Postsynaptic NMDA and AMPA Receptor Responses. *Neuron*, *102*(5). <https://doi.org/10.1016/j.neuron.2019.03.032>
- Davletov, B. A., Krasnoperov, V., Hata, Y., Petrenko, A. G., & Südhof, T. C. (1995). High Affinity Binding of α -Latrotoxin to Recombinant Neurexin Ia. *Journal of Biological Chemistry*, *270*(41). <https://doi.org/10.1074/jbc.270.41.23903>

References

- de Wit, J., Sylwestrak, E., O'Sullivan, M. L., Otto, S., Tiglio, K., Savas, J. N., Yates, J. R., Comoletti, D., Taylor, P., & Ghosh, A. (2009). LRRTM2 Interacts with Neurexin1 and Regulates Excitatory Synapse Formation. *Neuron*, 64(6). <https://doi.org/10.1016/j.neuron.2009.12.019>
- Decock, A., Ongenaert, M., Cannoodt, R., Verniers, K., de Wilde, B., Laureys, G., Roy, N. van, Berbegall, A. P., Bienertova-Vasku, J., Bown, N., Clément, N., Combaret, V., Haber, M., Hoyoux, C., Murray, J., Noguera, R., Pierron, G., Schleiermacher, G., Schulte, J. H., ... Vandesompele, J. (n.d.). Methyl-CpG-binding domain sequencing reveals a prognostic methylation signature in neuroblastoma. In *Oncotarget* (Vol. 7, Issue 2). www.impactjournals.com/oncotarget/
- Deng. (2019). $\alpha 2\delta$ -1-Bound Glutamate Receptors in Opioid Signaling. In *Anesthesiology* (Vol. 130).
- Deng, M., Chen, S. R., & Pan, H. L. (2019). Presynaptic NMDA receptors control nociceptive transmission at the spinal cord level in neuropathic pain. In *Cellular and Molecular Life Sciences* (Vol. 76, Issue 10, pp. 1889–1899). Birkhauser Verlag AG. <https://doi.org/10.1007/s00018-019-03047-y>
- DeWit, J., O'Sullivan, M. L., Savas, J. N., Condomitti, G., Caccese, M. C., Vennekens, K. M., Yates, J. R., & Ghosh, A. (2013). Unbiased discovery of Glypican as a receptor for LRRTM4 in regulating excitatory synapse development. *Neuron*, 79(4), 696–711. <https://doi.org/10.1016/j.neuron.2013.06.049>
- Dityatev, A. (2004). Polysialylated Neural Cell Adhesion Molecule Promotes Remodeling and Formation of Hippocampal Synapses. *Journal of Neuroscience*, 24(42). <https://doi.org/10.1523/JNEUROSCI.1702-04.2004>
- Dumas, T. C. (2005). Developmental regulation of cognitive abilities: Modified composition of a molecular switch turns on associative learning. *Progress in Neurobiology*, 76(3). <https://doi.org/10.1016/j.pneurobio.2005.08.002>

References

- Dunning, D. D., Hoover, C. L., Soltesz, I., Smith, M. A., & O'Dowd, D. K. (1999). GABA_A Receptor-Mediated Miniature Postsynaptic Currents and α -Subunit Expression in Developing Cortical Neurons. *Journal of Neurophysiology*, 82(6). <https://doi.org/10.1152/jn.1999.82.6.3286>
- Elegheert, J., Cvetkovska, V., Clayton, A. J., Heroven, C., Vennekens, K. M., Smukowski, S. N., Regan, M. C., Jia, W., Smith, A. C., Furukawa, H., Savas, J. N., de Wit, J., Begbie, J., Craig, A. M., & Aricescu, A. R. (2017). Structural Mechanism for Modulation of Synaptic Neuroligin-Neurexin Signaling by MDGA Proteins. *Neuron*, 95(4), 896-913.e10. <https://doi.org/10.1016/j.neuron.2017.07.040>
- Elias, E., Yang, N., Wang, P., & Tian, N. (2018). Glutamate Activity Regulates and Dendritic Development of J-RGCs. *Frontiers in Cellular Neuroscience*, 12. <https://doi.org/10.3389/fncel.2018.00249>
- Fabrichny, I. P., Leone, P., Sulzenbacher, G., Comoletti, D., Miller, M. T., Taylor, P., Bourne, Y., & Marchot, P. (2007). Structural Analysis of the Synaptic Protein Neuroligin and Its β -Neurexin Complex: Determinants for Folding and Cell Adhesion. *Neuron*, 56(6). <https://doi.org/10.1016/j.neuron.2007.11.013>
- Fairless, R., Masius, H., Rohlmann, A., Heupel, K., Ahmad, M., Reissner, C., Dresbach, T., & Missler, M. (2008). Polarized Targeting of Neurexins to Synapses Is Regulated by their C-Terminal Sequences. *Journal of Neuroscience*, 28(48). <https://doi.org/10.1523/JNEUROSCI.5294-07.2008>
- Faria, C., Miguéns, J., Antunes, J. L., Barroso, C., Pimentel, J., Martins, M. D. C., Moura-Nunes, V., & Roque, L. (2008). Genetic alterations in a papillary glioneuronal tumor: Case report. *Journal of Neurosurgery: Pediatrics*, 1(1), 99–102. <https://doi.org/10.3171/PED-08/01/099>
- Faryna, M., Konermann, C., Aulmann, S., Bermejo, J. L., Brugger, M., Diederichs, S., Rom, J., Weichenhan, D., Claus, R., Rehli, M., Schirmacher, P., Sinn, H. P., Plass, C., & Gerhauser, C. (2012). Genome-wide methylation screen in low-grade breast cancer identifies novel

References

epigenetically altered genes as potential biomarkers for tumor diagnosis. *FASEB Journal*, 26(12), 4937–4950. <https://doi.org/10.1096/fj.12-209502>

Fiala, G. J., Schamel, W. W. A., & Blumenthal, B. (2010). Blue native polyacrylamide gel electrophoresis (BN-PAGE) for analysis of multiprotein complexes from cellular lysates. *Journal of Visualized Experiments*, 48. <https://doi.org/10.3791/2164>

Forde, N., Mehta, J. P., McGettigan, P. A., Mamo, S., Bazer, F. W., Spencer, T. E., & Lonergan, P. (2013). Alterations in expression of endometrial genes coding for proteins secreted into the uterine lumen during conceptus elongation in cattle. *BMC Genomics*, 14. <https://doi.org/10.1186/1471-2164-14-321>

Frangaj, A., & Fan, Q. R. (2018). Structural biology of GABAB receptor. *Neuropharmacology*, 136. <https://doi.org/10.1016/j.neuropharm.2017.10.011>

Frank, R. A. W., Komiyama, N. H., Ryan, T. J., Zhu, F., O'Dell, T. J., & Grant, S. G. N. (2016). NMDA receptors are selectively partitioned into complexes and supercomplexes during synapse maturation. *Nature Communications*, 7(1). <https://doi.org/10.1038/ncomms11264>

Friedman, D., & Strowbridge, B. W. (2000). Functional Role of NMDA Autoreceptors in Olfactory Mitral Cells. *Journal of Neurophysiology*, 84(1). <https://doi.org/10.1152/jn.2000.84.1.39>

Fry, M., & Ferguson, A. v. (2007). The sensory circumventricular organs: Brain targets for circulating signals controlling ingestive behavior. *Physiology & Behavior*, 91(4). <https://doi.org/10.1016/j.physbeh.2007.04.003>

Fu, Y., & Huang, Z. J. (2010). Differential dynamics and activity-dependent regulation of δ - and ϵ -neurexins at developing GABAergic synapses. *Proceedings of the National Academy of Sciences*, 107(52). <https://doi.org/10.1073/pnas.1011233108>

Gamboa-Meléndez, M. A., Huerta-Chagoya, A., Moreno-Macías, H., Vázquez-Cárdenas, P., Ordóñez-Sánchez, M. L., Rodríguez-Guillén, R., Riba, L., Rodríguez-Torres, M., Guerra-

References

- García, M. T., Guillén-Pineda, L. E., Choudhry, S., del Bosque-Plata, L., Canizales-Quinteros, S., Pérez-Ortiz, G., Escobedo-Aguirre, F., Parra, A., Lerman-Garber, I., Aguilar-Salinas, C. A., & Tusié-Luna, M. T. (2012). Contribution of common genetic variation to the risk of type 2 diabetes in the Mexican Mestizo population. *Diabetes*, *61*(12), 3314–3321. <https://doi.org/10.2337/db11-0550>
- García-Chapa, E. G., Leal-Ugarte, E., Peralta-Leal, V., Durán-González, J., & Meza-Espinoza, J. P. (2017). Genetic Epidemiology of Type 2 Diabetes in Mexican Mestizos. In *BioMed Research International* (Vol. 2017). Hindawi Limited. <https://doi.org/10.1155/2017/3937893>
- Gasparini, S., Resch, J. M., Narayan, S. v., Peltekian, L., Iverson, G. N., Karthik, S., & Geerling, J. C. (2019). Aldosterone-sensitive HSD2 neurons in mice. *Brain Structure and Function*, *224*(1), 387–417. <https://doi.org/10.1007/s00429-018-1778-y>
- Geisler, S., Schöpf, C. L., Stanika, R., Kalb, M., Campiglio, M., Repetto, D., Traxler, L., Missler, M., & Obermair, G. J. (2019). Presynaptic $\alpha_2\delta$ -2 Calcium Channel Subunits Regulate Postsynaptic GABA_A Receptor Abundance and Axonal Wiring. *The Journal of Neuroscience*, *39*(14). <https://doi.org/10.1523/JNEUROSCI.2234-18.2019>
- Gerrow, K. (2006). Cell adhesion molecules at the synapse. *Frontiers in Bioscience*, *11*(1). <https://doi.org/10.2741/1978>
- Girard, F., Meszar, Z., Marti, C., Davis, F. P., & Celio, M. (2011). Gene expression analysis in the parvalbumin-immunoreactive PV1 nucleus of the mouse lateral hypothalamus. *European Journal of Neuroscience*, *34*(12), 1934–1943. <https://doi.org/10.1111/j.1460-9568.2011.07918.x>
- Gomez, A. M., Traunmüller, L., & Scheiffele, P. (2021). Neurexins: molecular codes for shaping neuronal synapses. *Nature Reviews Neuroscience*, *22*(3). <https://doi.org/10.1038/s41583-020-00415-7>

References

- Graf, E. R., Zhang, X., Jin, S.-X., Linhoff, M. W., & Craig, A. M. (2004). Neurexins Induce Differentiation of GABA and Glutamate Postsynaptic Specializations via Neuroligins. *Cell*, *119*(7). <https://doi.org/10.1016/j.cell.2004.11.035>
- Greger, I. H., Watson, J. F., & Cull-Candy, S. G. (2017). Structural and Functional Architecture of AMPA-Type Glutamate Receptors and Their Auxiliary Proteins. In *Neuron* (Vol. 94, Issue 4, pp. 713–730). Cell Press. <https://doi.org/10.1016/j.neuron.2017.04.009>
- Haines, B. P., & Rigby, P. W. J. (2007). Developmentally regulated expression of the LRRTM gene family during mid-gestation mouse embryogenesis. *Gene Expression Patterns*, *7*(1–2). <https://doi.org/10.1016/j.modgep.2006.05.004>
- Haklai-Topper, L., Soutschek, J., Sabanay, H., Scheel, J., Hobert, O., & Peles, E. (2011). The neurexin superfamily of *Caenorhabditis elegans*. *Gene Expression Patterns*, *11*(1–2). <https://doi.org/10.1016/j.gep.2010.10.008>
- Hall, B. J., Ripley, B., & Ghosh, A. (2007). NR2B Signaling Regulates the Development of Synaptic AMPA Receptor Current. *Journal of Neuroscience*, *27*(49). <https://doi.org/10.1523/JNEUROSCI.3793-07.2007>
- Harris, K. P., & Littleton, J. T. (2015). Transmission, development, and plasticity of synapses. *Genetics*, *201*(2), 345–375. <https://doi.org/10.1534/genetics.115.176529>
- Hata, Y., Slaughter, C. A., & Südhof, T. C. (1993). Synaptic vesicle fusion complex contains unc-18 homologue bound to syntaxin. *Nature*, *366*(6453). <https://doi.org/10.1038/366347a0>
- Hayashi, Y., Momiyama, A., Takahashi, T., Ohishi, H., Ogawa-Meguro, R., Shigemoto, R., Mizuno, N., & Nakanishi, S. (1993). Role of a metabotropic glutamate receptor in synaptic modulation in the accessory olfactory bulb. *Nature*, *366*(6456). <https://doi.org/10.1038/366687a0>
- He, X. B., Hu, J. H., Wu, Q., Yan, Y. C., & Koide, S. S. (2001). Identification of GABAB Receptor in Rat Testis and Sperm. *Biochemical and Biophysical Research Communications*, *283*(1). <https://doi.org/10.1006/bbrc.2001.4732>

References

- Hoffmann, H., Gremme, T., Hatt, H., & Gottmann, K. (2000). Synaptic Activity-Dependent Developmental Regulation of NMDA Receptor Subunit Expression in Cultured Neocortical Neurons. In *J. Neurochem* (Vol. 75).
- Holmes, D. S., & Quigley, M. (1981). A rapid boiling method for the preparation of bacterial plasmids. *Analytical Biochemistry*, *114*(1). [https://doi.org/10.1016/0003-2697\(81\)90473-5](https://doi.org/10.1016/0003-2697(81)90473-5)
- Hong, S. M., Omura, N., Vincent, A., Li, A., Knight, S., Yu, J., Hruban, R. H., & Goggins, M. (2012). Genome-wide CpG island profiling of intraductal papillary mucinous neoplasms of the pancreas. *Clinical Cancer Research*, *18*(3), 700–712. <https://doi.org/10.1158/1078-0432.CCR-11-1718>
- Hortopan, G. A., & Baraban, S. C. (2011). Aberrant expression of genes necessary for neuronal development and notch signaling in an epileptic mind bomb zebrafish. *Developmental Dynamics*, *240*(8), 1964–1976. <https://doi.org/10.1002/dvdy.22680>
- Hoy, J. L., & Niell, C. M. (2015). Layer-Specific Refinement of Visual Cortex Function after Eye Opening in the Awake Mouse. *Journal of Neuroscience*, *35*(8). <https://doi.org/10.1523/JNEUROSCI.3174-14.2015>
- Hu, C., Chen, W., Myers, S. J., Yuan, H., & Traynelis, S. F. (2016). Human GRIN2B variants in neurodevelopmental disorders. *Journal of Pharmacological Sciences*, *132*(2). <https://doi.org/10.1016/j.jphs.2016.10.002>
- Huh, K.-H., & Wenthold, R. J. (1999). Turnover Analysis of Glutamate Receptors Identifies a Rapidly Degraded Pool of the N-Methyl-d-aspartate Receptor Subunit, NR1, in Cultured Cerebellar Granule Cells. *Journal of Biological Chemistry*, *274*(1). <https://doi.org/10.1074/jbc.274.1.151>
- Ichtchenko, K., Hata, Y., Nguyen, T., Ullrich, B., Missler, M., Moomaw, C., & Südhof, T. C. (1995). Neuroligin 1: A splice site-specific ligand for β -neurexins. *Cell*, *81*(3). [https://doi.org/10.1016/0092-8674\(95\)90396-8](https://doi.org/10.1016/0092-8674(95)90396-8)

References

- Ichtchenko, K., Nguyen, T., & Südhof, T. C. (1996). Structures, Alternative Splicing, and Neurexin Binding of Multiple Neuroligins. *Journal of Biological Chemistry*, 271(5). <https://doi.org/10.1074/jbc.271.5.2676>
- Irie, M. (1997). Binding of Neuroligins to PSD-95. *Science*, 277(5331). <https://doi.org/10.1126/science.277.5331.1511>
- Jabeen, S., & Thirumalai, V. (2018). The interplay between electrical and chemical synaptogenesis. *J Neurophysiol*, 120, 1914–1922. <https://doi.org/10.1152/jn.00398.2018.-Neurons>
- Johnson, L. R., Battle, A. R., & Martinac, B. (2019). Remembering Mechanosensitivity of NMDA Receptors. In *Frontiers in Cellular Neuroscience* (Vol. 13). Frontiers Media S.A. <https://doi.org/10.3389/fncel.2019.00533>
- Jones, K. A., Borowsky, B., Tamm, J. A., Craig, D. A., Durkin, M. M., Dai, M., Yao, W.-J., Johnson, M., Gunwaldsen, C., Huang, L.-Y., Tang, C., Shen, Q., Salon, J. A., Morse, K., Laz, T., Smith, K. E., Nagarathnam, D., Noble, S. A., Branchek, T. A., & Gerald, C. (1998). GABAB receptors function as a heteromeric assembly of the subunits GABABR1 and GABABR2. *Nature*, 396(6712). <https://doi.org/10.1038/25348>
- Joo, J.-Y., Lee, S.-J., Uemura, T., Yoshida, T., Yasumura, M., Watanabe, M., & Mishina, M. (2011). Differential interactions of cerebellin precursor protein (Cbln) subtypes and neurexin variants for synapse formation of cortical neurons. *Biochemical and Biophysical Research Communications*, 406(4). <https://doi.org/10.1016/j.bbrc.2011.02.108>
- Kattenstroth, G., Tantalaki, E., Südhof, T. C., Gottmann, K., & Missler, M. (2004). Postsynaptic N-methyl-D-aspartate receptor function requires α -neurexins. *Proceedings of the National Academy of Sciences*, 101(8). <https://doi.org/10.1073/pnas.0308626100>
- Kehrer-Sawatzki, H., Schreiner, B., Tänzer, S., Platzer, M., Müller, S., & Hameister, H. (2002). Molecular Characterization of the Pericentric Inversion That Causes Differences Between Chimpanzee Chromosome 19 and Human Chromosome 17. In *Am. J. Hum. Genet* (Vol. 71).

References

- Kinzfogel, J., Hango, G., & Broxmeyer, H. E. (2011). *Neurexophilin 1 suppresses the proliferation of hematopoietic progenitor cells*. <https://doi.org/10.1182/blood-2010>
- Ko, J., Fuccillo, M. v., Malenka, R. C., & Südhof, T. C. (2009). LRRTM2 Functions as a Neurexin Ligand in Promoting Excitatory Synapse Formation. *Neuron*, 64(6). <https://doi.org/10.1016/j.neuron.2009.12.012>
- Koehnke, J., Katsamba, P. S., Ahlsen, G., Bahna, F., Vendome, J., Honig, B., Shapiro, L., & Jin, X. (2010). Splice form dependence of β -neurexin/neurologin binding interactions. *Neuron*, 67(1), 61–74. <https://doi.org/10.1016/j.neuron.2010.06.001>
- Kornau, H., Schenker, L., Kennedy, M., & Seeburg, P. (1995). Domain interaction between NMDA receptor subunits and the postsynaptic density protein PSD-95. *Science*, 269(5231). <https://doi.org/10.1126/science.7569905>
- Kraja, A. T., Borecki, I. B., Tsai, M. Y., Ordovas, J. M., Hopkins, P. N., Lai, C. Q., Frazier-Wood, A. C., Straka, R. J., Hixson, J. E., Province, M. A., & Arnett, D. K. (2013). Genetic analysis of 16 NMR-lipoprotein fractions in humans, the GOLDN study. *Lipids*, 48(2), 155–165. <https://doi.org/10.1007/s11745-012-3740-8>
- Kumar, A. (2015). NMDA receptor function during senescence: Implication on cognitive performance. In *Frontiers in Neuroscience* (Vol. 9, Issue DEC). Frontiers Media S.A. <https://doi.org/10.3389/fnins.2015.00473>
- LaConte, L. E. W., Chavan, V., Liang, C., Willis, J., Schönhense, E.-M., Schoch, S., & Mukherjee, K. (2016). CASK stabilizes neurexin and links it to liprin- α in a neuronal activity-dependent manner. *Cellular and Molecular Life Sciences*, 73(18). <https://doi.org/10.1007/s00018-016-2183-4>
- Lau, C. G., & Zukin, R. S. (2007). NMDA receptor trafficking in synaptic plasticity and neuropsychiatric disorders. In *Nature Reviews Neuroscience* (Vol. 8, Issue 6, pp. 413–426). <https://doi.org/10.1038/nrn2153>

References

- Lee, S.-J., Uemura, T., Yoshida, T., & Mishina, M. (2012). GluR 2 Assembles Four Neurexins into Trans-Synaptic Triad to Trigger Synapse Formation. *Journal of Neuroscience*, 32(13). <https://doi.org/10.1523/JNEUROSCI.5584-11.2012>
- Leshchyns'ka, I., & Sytnyk, V. (2016). Synaptic Cell Adhesion Molecules in Alzheimer's Disease. *Neural Plasticity*, 2016. <https://doi.org/10.1155/2016/6427537>
- Leshchyns'ka, I., Sytnyk, V., Richter, M., Andreyeva, A., Puchkov, D., & Schachner, M. (2006). The Adhesion Molecule CHL1 Regulates Uncoating of Clathrin-Coated Synaptic Vesicles. *Neuron*, 52(6). <https://doi.org/10.1016/j.neuron.2006.10.020>
- Li, T., Tian, Y., Li, Q., Chen, H., Lv, H., Xie, W., & Han, J. (2015). The neurexin/N-ethylmaleimide-sensitive factor (NSF) interaction regulates short term synaptic depression. *Journal of Biological Chemistry*, 290(29), 17656–17667. <https://doi.org/10.1074/jbc.M115.644583>
- Liu, Y. R., Hu, Y., Zeng, Y., Li, Z. X., Zhang, H. B., Deng, J. L., & Wang, G. (2019). Neurexophilin and PC-esterase domain family member 4 (NXPE4) and prostate androgen-regulated mucin-like protein 1 (PARM1) as prognostic biomarkers for colorectal cancer. *Journal of Cellular Biochemistry*, 120(10), 18041–18052. <https://doi.org/10.1002/jcb.29107>
- Losi, G., Prybylowski, K., Fu, Z., Luo, J., Wenthold, R. J., & Vicini, S. (2003). PSD-95 regulates NMDA receptors in developing cerebellar granule neurons of the rat. *The Journal of Physiology*, 548(1). <https://doi.org/10.1113/jphysiol.2002.034918>
- Lu, Z., Wang, Y., Chen, F., Tong, H., Reddy, M. V. V. S., Luo, L., Seshadrinathan, S., Zhang, L., Holthausen, L. M. F., Craig, A. M., Ren, G., & Rudenko, G. (2014). Calsyntenin-3 Molecular Architecture and Interaction with Neurexin 1 α . *Journal of Biological Chemistry*, 289(50). <https://doi.org/10.1074/jbc.M114.606806>
- Lübbert, M., Goral, R. O., Keine, C., Thomas, C., Guerrero-Given, D., Putzke, T., Satterfield, R., Kamasawa, N., & Young, S. M. (2019). Ca V 2.1 α 1 Subunit Expression Regulates Presynaptic Ca V 2.1 Abundance and Synaptic Strength at a Central Synapse. *Neuron*, 101(2), 260-273.e6. <https://doi.org/10.1016/j.neuron.2018.11.028>

References

- Marcotte, B. V., Guénard, F., Cormier, H., Lemieux, S., Couture, P., Rudkowska, I., & Vohl, M. C. (2017). Plasma triglyceride levels may be modulated by gene expression of IQCJ, NXP1, PHF17 and MYB in humans. *International Journal of Molecular Sciences*, *18*(2). <https://doi.org/10.3390/ijms18020257>
- Matsuda, K., Budisantoso, T., Mitakidis, N., Sugaya, Y., Miura, E., Kakegawa, W., Yamasaki, M., Konno, K., Uchigashima, M., Abe, M., Watanabe, I., Kano, M., Watanabe, M., Sakimura, K., Aricescu, A. R., & Yuzaki, M. (2016). Transsynaptic Modulation of Kainate Receptor Functions by C1q-like Proteins. *Neuron*, *90*(4). <https://doi.org/10.1016/j.neuron.2016.04.001>
- Matsuda, K., & Yuzaki, M. (2011a). Cbln family proteins promote synapse formation by regulating distinct neurexin signaling pathways in various brain regions. *European Journal of Neuroscience*, *33*(8). <https://doi.org/10.1111/j.1460-9568.2011.07638.x>
- Matsuda, K., & Yuzaki, M. (2011b). Cbln family proteins promote synapse formation by regulating distinct neurexin signaling pathways in various brain regions. *European Journal of Neuroscience*, *33*(8), 1447–1461. <https://doi.org/10.1111/j.1460-9568.2011.07638.x>
- McIlhinney, R. A. J., le Bourdellès, B., Molnár, E., Tricaud, N., Streit, P., & Whiting, P. J. (1998). Assembly intracellular targeting and cell surface expression of the human N-methyl-d-aspartate receptor subunits NR1a and NR2A in transfected cells. *Neuropharmacology*, *37*(10–11). [https://doi.org/10.1016/S0028-3908\(98\)00121-X](https://doi.org/10.1016/S0028-3908(98)00121-X)
- Mendez, P., de Roo, M., Poglia, L., Klausner, P., & Muller, D. (2010). N-cadherin mediates plasticity-induced long-term spine stabilization. *Journal of Cell Biology*, *189*(3). <https://doi.org/10.1083/jcb.201003007>
- Meng, X., McGraw, C. M., Wang, W., Jing, J., Yeh, S.-Y., Wang, L., Lopez, J., Brown, A. M., Lin, T., Chen, W., Xue, M., Sillitoe, R. v, Jiang, X., & Zoghbi, H. Y. (2019). Neurexophilin4 is a selectively expressed α -neurexin ligand that modulates specific cerebellar synapses and motor functions. *ELife*, *8*. <https://doi.org/10.7554/eLife.46773>

References

- Meyers, J. A., Sanchez, D., Elwell, L. P., & Falkow, S. (1976). Simple agarose gel electrophoretic method for the identification and characterization of plasmid deoxyribonucleic acid. *Journal of Bacteriology*, *127*(3). <https://doi.org/10.1128/JB.127.3.1529-1537.1976>
- Miller, M. T., Mileni, M., Comoletti, D., Stevens, R. C., Harel, M., & Taylor, P. (2011). The Crystal Structure of the α -Neurexin-1 Extracellular Region Reveals a Hinge Point for Mediating Synaptic Adhesion and Function. *Structure*, *19*(6). <https://doi.org/10.1016/j.str.2011.03.011>
- Missler, M., Hammer, R. E., & Sü, T. C. (1998a). *Neurexophilin Binding to-Neurexins A SINGLE LNS DOMAIN FUNCTIONS AS AN INDEPENDENTLY FOLDING LIGAND-BINDING UNIT**. <http://www.jbc.org/>
- Missler, M., Hammer, R. E., & Sü, T. C. (1998b). *Neurexophilin Binding to-Neurexins A SINGLE LNS DOMAIN FUNCTIONS AS AN INDEPENDENTLY FOLDING LIGAND-BINDING UNIT**. <http://www.jbc.org/>
- Missler, M., & Sü, T. C. (1998). *Neurexophilins Form a Conserved Family of Neuropeptide-Like Glycoproteins*.
- Missler, M., Südhof, T. C., & Biederer, T. (2012). Synaptic Cell Adhesion. *Cold Spring Harbor Perspectives in Biology*, *4*(4). <https://doi.org/10.1101/cshperspect.a005694>
- Missler, M., Zhang, W., Rohlmann, A., Kattenstroth, G., Hammer, R. E., Gottmann, K., & Südhof, T. C. (2003). α -Neurexins couple Ca^{2+} channels to synaptic vesicle exocytosis. *Nature*, *423*(6943). <https://doi.org/10.1038/nature01755>
- Monyer, H., Burnashev, N., Laurie, D. J., Sakmann, B., & Seeburg, P. H. (1994a). Developmental and Regional Expression in the Rat Brain and Functional Properties of Four NMDA Receptors. In *Neuron* (Vol. 12).
- Monyer, H., Burnashev, N., Laurie, D. J., Sakmann, B., & Seeburg, P. H. (1994b). Developmental and regional expression in the rat brain and functional properties of four NMDA receptors. *Neuron*, *12*(3). [https://doi.org/10.1016/0896-6273\(94\)90210-0](https://doi.org/10.1016/0896-6273(94)90210-0)

References

- Moretto, E., Murru, L., Martano, G., Sassone, J., & Passafaro, M. (2018a). Glutamatergic synapses in neurodevelopmental disorders. In *Progress in Neuro-Psychopharmacology and Biological Psychiatry* (Vol. 84, pp. 328–342). Elsevier Inc. <https://doi.org/10.1016/j.pnpbp.2017.09.014>
- Moretto, E., Murru, L., Martano, G., Sassone, J., & Passafaro, M. (2018b). Glutamatergic synapses in neurodevelopmental disorders. In *Progress in Neuro-Psychopharmacology and Biological Psychiatry* (Vol. 84, pp. 328–342). Elsevier Inc. <https://doi.org/10.1016/j.pnpbp.2017.09.014>
- Moutin, E., Raynaud, F., Roger, J., Pellegrino, E., Homburger, V., Bertaso, F., Ollendorff, V., Bockaert, J., Fagni, L., & Perroy, J. (2012). Dynamic remodeling of scaffold interactions in dendritic spines controls synaptic excitability. *Journal of Cell Biology*, 198(2). <https://doi.org/10.1083/jcb.201110101>
- Mukherjee, K., Sharma, M., Urlaub, H., Bourenkov, G. P., Jahn, R., Südhof, T. C., & Wahl, M. C. (2008). CASK Functions as a Mg²⁺-Independent Neurexin Kinase. *Cell*, 133(2), 328–339. <https://doi.org/10.1016/j.cell.2008.02.036>
- Mulatinho, M. V., de Carvalho Serao, C. L., Scalco, F., Hardekopf, D., Pekova, S., Mrasek, K., Liehr, T., Weise, A., Rao, N., & Llerena, J. C. (2012). Severe intellectual disability, omphalocele, hypospadias and high blood pressure associated to a deletion at 2q22.1q22.3: Case report. *Molecular Cytogenetics*, 5(1). <https://doi.org/10.1186/1755-8166-5-30>
- Murthy, A. S. N., Mains, R. E., & Eipper, B. A. (1986). *THE JOURNAL OF BIOLOGICAL CHEMISTRY Purification and Characterization of Peptidylglycine α -Amidating Monooxygenase from Bovine Neurointermediate Pituitary** (Vol. 261, Issue 4).
- Nakao, K., Jeevakumar, V., Jiang, S. Z., Fujita, Y., Diaz, N. B., Pretell Annan, C. A., Eskow Jaunarajs, K. L., Hashimoto, K., Belforte, J. E., & Nakazawa, K. (2019). Schizophrenia-Like Dopamine Release Abnormalities in a Mouse Model of NMDA Receptor Hypofunction. *Schizophrenia Bulletin*, 45(1). <https://doi.org/10.1093/schbul/sby003>

References

- Nakazawa, K., & Sapkota, K. (2020). The origin of NMDA receptor hypofunction in schizophrenia. In *Pharmacology and Therapeutics* (Vol. 205). Elsevier Inc. <https://doi.org/10.1016/j.pharmthera.2019.107426>
- Neupert, C., Schneider, R., Klatt, O., Reissner, C., Repetto, D., Biermann, B., Niesmann, K., Missler, M., & Heine, M. (2015). Regulated Dynamic Trafficking of Neurexins Inside and Outside of Synaptic Terminals. *The Journal of Neuroscience*, 35(40). <https://doi.org/10.1523/JNEUROSCI.4041-14.2015>
- Nishimura, K., Murayama, S., & Takahashi, J. (2015). Identification of Neurexophilin 3 as a Novel Supportive Factor for Survival of Induced Pluripotent Stem Cell-Derived Dopaminergic Progenitors. *STEM CELLS Translational Medicine*, 4(8), 932–944. <https://doi.org/10.5966/sctm.2014-0197>
- Nusser, Z. (2018). Creating diverse synapses from the same molecules. In *Current Opinion in Neurobiology* (Vol. 51, pp. 8–15). Elsevier Ltd. <https://doi.org/10.1016/j.conb.2018.01.001>
- O'Connor, V. M., Shamotienko, O., Grishin, E., & Betz, H. (1993). On the structure of the 'synaptosecretosome' Evidence for a neurexin/synaptotagmin/syntaxin/Ca²⁺ channel complex. *FEBS Letters*, 326(1–3). [https://doi.org/10.1016/0014-5793\(93\)81802-7](https://doi.org/10.1016/0014-5793(93)81802-7)
- Oelsner, K. T., Guo, Y., To, S. B. C., Non, A. L., & Barkin, S. L. (2017). Maternal BMI as a predictor of methylation of obesity-related genes in saliva samples from preschool-age Hispanic children at-risk for obesity. *BMC Genomics*, 18(1). <https://doi.org/10.1186/s12864-016-3473-9>
- Okabe, M., Motojima, M., Miyazaki, Y., Pastan, I., Yokoo, T., & Matsusaka, T. (2018). *Downloaded from www.physiology.org/journal/ajprenal by \$individualUser. www.physiology.org/journal/ajprenal*
- O'Rourke, N. A., Weiler, N. C., Micheva, K. D., & Smith, S. J. (2012). Deep molecular diversity of mammalian synapses: Why it matters and how to measure it. In *Nature Reviews Neuroscience* (Vol. 13, Issue 6, pp. 365–379). <https://doi.org/10.1038/nrn3170>

References

- Ovsepian, S. v. (2017a). The birth of the synapse. In *Brain Structure and Function* (Vol. 222, Issue 8, pp. 3369–3374). Springer Verlag. <https://doi.org/10.1007/s00429-017-1459-2>
- Ovsepian, S. v. (2017b). The birth of the synapse. In *Brain Structure and Function* (Vol. 222, Issue 8, pp. 3369–3374). Springer Verlag. <https://doi.org/10.1007/s00429-017-1459-2>
- Owen, M. J., Williams, H. J., & O'Donovan, M. C. (2009). Schizophrenia genetics: advancing on two fronts. *Current Opinion in Genetics & Development*, 19(3). <https://doi.org/10.1016/j.gde.2009.02.008>
- Paul, A., Crow, M., Raudales, R., He, M., Gillis, J., & Huang, Z. J. (2017). Transcriptional Architecture of Synaptic Communication Delineates GABAergic Neuron Identity. *Cell*, 171(3), 522-539.e20. <https://doi.org/10.1016/j.cell.2017.08.032>
- Pereda, A., Bell, T., & Faber, D. (1995). Retrograde synaptic communication via gap junctions coupling auditory afferents to the Mauthner cell. *The Journal of Neuroscience*, 15(9). <https://doi.org/10.1523/JNEUROSCI.15-09-05943.1995>
- Pereda, A. E. (2014). Electrical synapses and their functional interactions with chemical synapses. In *Nature Reviews Neuroscience* (Vol. 15, Issue 4, pp. 250–263). Nature Publishing Group. <https://doi.org/10.1038/nrn3708>
- Pereda, A. E., Curti, S., Hoge, G., Cachope, R., Flores, C. E., & Rash, J. E. (2013). Gap junction-mediated electrical transmission: Regulatory mechanisms and plasticity. *Biochimica et Biophysica Acta - Biomembranes*, 1828(1), 134–146. <https://doi.org/10.1016/j.bbamem.2012.05.026>
- Perroud, N., Uher, R., Ng, M. Y. M., Guipponi, M., Hauser, J., Henigsberg, N., Maier, W., Mors, O., Gennarelli, M., Rietschel, M., Souery, D., Dernovsek, M. Z., Stamp, A. S., Lathrop, M., Farmer, A., Breen, G., Aitchison, K. J., Lewis, C. M., Craig, I. W., & McGuffin, P. (2012). Genome-wide association study of increasing suicidal ideation during antidepressant treatment in the GENDEP project. *Pharmacogenomics Journal*, 12(1), 68–77. <https://doi.org/10.1038/tpj.2010.70>

References

- Perroy, J., Raynaud, F., Homburger, V., Rousset, M.-C., Telley, L., Bockaert, J., & Fagni, L. (2008). Direct Interaction Enables Cross-talk between Ionotropic and Group I Metabotropic Glutamate Receptors. *Journal of Biological Chemistry*, 283(11). <https://doi.org/10.1074/jbc.M705661200>
- Petrenko, A. G., Ullrich, B., Missler, M., Krasnoperov, V., Rosahl, T. W., & Südhof, T. C. (1996). Structure and Evolution of Neurexophilin. *The Journal of Neuroscience*, 16(14). <https://doi.org/10.1523/JNEUROSCI.16-14-04360.1996>
- Pettem, K. L., Yokomaku, D., Luo, L., Linhoff, M. W., Prasad, T., Connor, S. A., Siddiqui, T. J., Kawabe, H., Chen, F., Zhang, L., Rudenko, G., Wang, Y. T., Brose, N., & Craig, A. M. (2013). The Specific α -Neurexin Interactor Calsyntenin-3 Promotes Excitatory and Inhibitory Synapse Development. *Neuron*, 80(1). <https://doi.org/10.1016/j.neuron.2013.07.016>
- Puchkov, D., Leshchyn'ska, I., Nikonenko, A. G., Schachner, M., & Sytnyk, V. (2011). NCAM/Spectrin Complex Disassembly Results in PSD Perforation and Postsynaptic Endocytic Zone Formation. *Cerebral Cortex*, 21(10). <https://doi.org/10.1093/cercor/bhq283>
- Reiner, A., & Levitz, J. (2018). Glutamatergic Signaling in the Central Nervous System: Ionotropic and Metabotropic Receptors in Concert. *Neuron*, 98(6). <https://doi.org/10.1016/j.neuron.2018.05.018>
- Reisinger, V., & Eichacker, L. A. (2006). Analysis of membrane protein complexes by blue native PAGE. *Proteomics*, 1(1-2 SUPPL.), 6–15. <https://doi.org/10.1002/pmic.200600553>
- Reissner, C., Klose, M., Fairless, R., & Missler, M. (2008). Mutational analysis of the neurexin/neurologin complex reveals essential and regulatory components. *Proceedings of the National Academy of Sciences*, 105(39). <https://doi.org/10.1073/pnas.0801639105>
- Reissner, C., Runkel, F., & Missler, M. (2013). Neurexins. *Genome Biology*, 14(9). <https://doi.org/10.1186/gb-2013-14-9-213>
- Reissner, C., Stahn, J., Breuer, D., Klose, M., Pohlentz, G., Mormann, M., & Missler, M. (2014). Dystroglycan Binding to α -Neurexin Competes with Neurexophilin-1 and Neurologin

References

in the Brain. *Journal of Biological Chemistry*, 289(40).
<https://doi.org/10.1074/jbc.M114.595413>

Rissone, A., Monopoli, M., Beltrame, M., Bussolino, F., Cotelli, F., & Arese, M. (2007). Comparative Genome Analysis of the Neurexin Gene Family in *Danio rerio*: Insights into Their Functions and Evolution. *Molecular Biology and Evolution*, 24(1).
<https://doi.org/10.1093/molbev/msl147>

Rollenhagen, A., & Lübke, J. H. R. (2006). The morphology of excitatory central synapses: from structure to function. *Cell and Tissue Research*, 326(2), 221–237.
<https://doi.org/10.1007/s00441-006-0288-z>

Roper, S. D., & Chaudhari, N. (2017). Taste buds: Cells, signals and synapses. In *Nature Reviews Neuroscience* (Vol. 18, Issue 8, pp. 485–497). Nature Publishing Group.
<https://doi.org/10.1038/nrn.2017.68>

Rowen, L., Young, J., Birditt, B., Kaur, A., Madan, A., Philipps, D. L., Qin, S., Minx, P., Wilson, R. K., Hood, L., & Graveley, B. R. (2002). Analysis of the Human Neurexin Genes: Alternative Splicing and the Generation of Protein Diversity. *Genomics*, 79(4).
<https://doi.org/10.1006/geno.2002.6734>

Rudenko, G. (2019). Neurexins — versatile molecular platforms in the synaptic cleft. In *Current Opinion in Structural Biology* (Vol. 54, pp. 112–121). Elsevier Ltd.
<https://doi.org/10.1016/j.sbi.2019.01.009>

Rudkowska, I., Guénard, F., Julien, P., Couture, P., Lemieux, S., Barbier, O., Calder, P. C., Minihane, A. M., & Vohl, M. C. (2014). Genome-wide association study of the plasma triglyceride response to an n-3 polyunsaturated fatty acid supplementation. *Journal of Lipid Research*, 55(7), 1245–1253. <https://doi.org/10.1194/jlr.M045898>

Salyakina, D., Cukier, H. N., Lee, J. M., Sacharow, S., Nations, L. D., Ma, D., Jaworski, J. M., Konidari, I., Whitehead, P. L., Wright, H. H., Abramson, R. K., Williams, S. M., Menon, R., Haines, J. L., Gilbert, J. R., Cuccaro, M. L., & Pericak-Vance, M. A. (2011). Copy

References

number variants in extended autism spectrum disorder families reveal candidates potentially involved in autism risk. *PLoS ONE*, 6(10). <https://doi.org/10.1371/journal.pone.0026049>

Sans, N., Petralia, R. S., Wang, Y.-X., Ii, J. B., Hell, J. W., & Wenthold, R. J. (1996). for review, see Sheng. In *The Journal of Neuroscience* (Vol. 20, Issue 3).

Sanz-Clemente, A., Nicoll, R. A., & Roche, K. W. (2013). Diversity in NMDA Receptor Composition. *The Neuroscientist*, 19(1). <https://doi.org/10.1177/1073858411435129>

Savas, J. N., Ribeiro, L. F., Wierda, K. D., Wright, R., DeNardo-Wilke, L. A., Rice, H. C., Chamma, I., Wang, Y.-Z., Zemla, R., Lavallée-Adam, M., Vennekens, K. M., O'Sullivan, M. L., Antonios, J. K., Hall, E. A., Thoumine, O., Attie, A. D., Yates, J. R., Ghosh, A., & de Wit, J. (2015). The Sorting Receptor SorCS1 Regulates Trafficking of Neurexin and AMPA Receptors. *Neuron*, 87(4). <https://doi.org/10.1016/j.neuron.2015.08.007>

Schachner, M. (1997). Neural recognition molecules and synaptic plasticity. *Current Opinion in Cell Biology*, 9(5). [https://doi.org/10.1016/S0955-0674\(97\)80115-9](https://doi.org/10.1016/S0955-0674(97)80115-9)

Schekman, R., & Südhof, T. (2014). An interview with Randy Schekman and Thomas Südhof. *Trends in Cell Biology*, 24(1), 6–8. <https://doi.org/10.1016/j.tcb.2013.11.006>

Seielstad, M., Page, G. P., Gaddis, N., Lanteri, M., Lee, T. H., Kakaiya, R., Barcellos, L. F., Criswell, L. A., Triulzi, D., Norris, P. J., & Busch, M. P. (2018). Genomewide association study of HLA alloimmunization in previously pregnant blood donors. *Transfusion*, 58(2), 402–412. <https://doi.org/10.1111/trf.14402>

Shagin, D. A., Barsova, E. v., Yanushevich, Y. G., Fradkov, A. F., Lukyanov, K. A., Labas, Y. A., Semenova, T. N., Ugalde, J. A., Meyers, A., Nunez, J. M., Widder, E. A., Lukyanov, S. A., & Matz, M. v. (2004). GFP-like Proteins as Ubiquitous Metazoan Superfamily: Evolution of Functional Features and Structural Complexity. *Molecular Biology and Evolution*, 21(5). <https://doi.org/10.1093/molbev/msh079>

Shen, L., Kim, S., Risacher, S. L., Nho, K., Swaminathan, S., West, J. D., Foroud, T., Pankratz, N., Moore, J. H., Sloan, C. D., Huentelman, M. J., Craig, D. W., DeChairo, B. M.,

References

- Potkin, S. G., Jack, C. R., Weiner, M. W., & Saykin, A. J. (2010). Whole genome association study of brain-wide imaging phenotypes for identifying quantitative trait loci in MCI and AD: A study of the ADNI cohort. *NeuroImage*, *53*(3), 1051–1063. <https://doi.org/10.1016/j.neuroimage.2010.01.042>
- Sheng, M., & Kim, E. (2011). The Postsynaptic Organization of Synapses. *Cold Spring Harbor Perspectives in Biology*, *3*(12). <https://doi.org/10.1101/cshperspect.a005678>
- Shetty, A., Sytnyk, V., Leshchyns'ka, I., Puchkov, D., Haucke, V., & Schachner, M. (2013). The Neural Cell Adhesion Molecule Promotes Maturation of the Presynaptic Endocytotic Machinery by Switching Synaptic Vesicle Recycling from Adaptor Protein 3 (AP-3)- to AP-2-Dependent Mechanisms. *Journal of Neuroscience*, *33*(42). <https://doi.org/10.1523/JNEUROSCI.2192-13.2013>
- Siddiqui, T. J., Pancaroglu, R., Kang, Y., Rooyakkers, A., & Craig, A. M. (2010a). LRRTMs and Neuroligins Bind Neurexins with a Differential Code to Cooperate in Glutamate Synapse Development. *Journal of Neuroscience*, *30*(22). <https://doi.org/10.1523/JNEUROSCI.0470-10.2010>
- Siddiqui, T. J., Pancaroglu, R., Kang, Y., Rooyakkers, A., & Craig, A. M. (2010b). LRRTMs and Neuroligins Bind Neurexins with a Differential Code to Cooperate in Glutamate Synapse Development. *Journal of Neuroscience*, *30*(22). <https://doi.org/10.1523/JNEUROSCI.0470-10.2010>
- Singh, S. K., Stogsdill, J. A., Pulimood, N. S., Dingsdale, H., Kim, Y. H., Pilaz, L. J., Kim, I. H., Manhaes, A. C., Rodrigues, W. S., Pamukcu, A., Enustun, E., Ertuz, Z., Scheiffele, P., Soderling, S. H., Silver, D. L., Ji, R. R., Medina, A. E., & Eroglu, C. (2016). Astrocytes Assemble Thalamocortical Synapses by Bridging NRX1 α and NL1 via Hevin. *Cell*, *164*(1–2), 183–196. <https://doi.org/10.1016/j.cell.2015.11.034>
- Song, H., Ramus, S. J., Kjaer, S. K., DiCioccio, R. A., Chenevix-Trench, G., Pearce, C. L., Hogdall, E., Whittemore, A. S., McGuire, V., Hogdall, C., Blaakaer, J., Wu, A. H., van den Berg, D. J., Stram, D. O., Menon, U., Gentry-Maharaj, A., Jacobs, I. J., Webb, P. M., Beesley, J., ... Pharoah, P. D. P. (2009). Association between invasive ovarian cancer susceptibility

References

and 11 best candidate SNPs from breast cancer genome-wide association study. *Human Molecular Genetics*, 18(12), 2297–2304. <https://doi.org/10.1093/hmg/ddp138>

Song, J.-Y., Ichtchenko, K., Südhof, T. C., & Brose, N. (1999). Neuroligin 1 is a postsynaptic cell-adhesion molecule of excitatory synapses. *Proceedings of the National Academy of Sciences*, 96(3). <https://doi.org/10.1073/pnas.96.3.1100>

Sterky, F. H., Trotter, J. H., Lee, S.-J., Recktenwald, C. v., Du, X., Zhou, B., Zhou, P., Schwenk, J., Fakler, B., & Südhof, T. C. (2017). Carbonic anhydrase-related protein CA10 is an evolutionarily conserved pan-neurexin ligand. *Proceedings of the National Academy of Sciences*, 114(7). <https://doi.org/10.1073/pnas.1621321114>

Strehlow, V., Heyne, H. O., Vlaskamp, D. R. M., Marwick, K. F. M., Rudolf, G., de Bellecize, J., Biskup, S., Brilstra, E. H., Brouwer, O. F., Callenbach, P. M. C., Hentschel, J., Hirsch, E., Kind, P. C., Mignot, C., Platzner, K., Rump, P., Skehel, P. A., Wyllie, D. J. A., Hardingham, G. E., ... Willemsen, M. H. (2019). *GRIN2A* -related disorders: genotype and functional consequence predict phenotype. *Brain*, 142(1). <https://doi.org/10.1093/brain/awy304>

Südhof, T. C. (2018). Towards an Understanding of Synapse Formation. In *Neuron* (Vol. 100, Issue 2, pp. 276–293). Cell Press. <https://doi.org/10.1016/j.neuron.2018.09.040>

Südhof, T. C. (2021). The cell biology of synapse formation. *Journal of Cell Biology*, 220(7). <https://doi.org/10.1083/jcb.202103052>

Sugita, S., Saito, F., Tang, J., Satz, J., Campbell, K., & Südhof, T. C. (2001). A stoichiometric complex of neurexins and dystroglycan in brain. *Journal of Cell Biology*, 154(2). <https://doi.org/10.1083/jcb.200105003>

Sytnyk, V., Leshchyns'ka, I., Delling, M., Dityateva, G., Dityatev, A., & Schachner, M. (2002). Neural cell adhesion molecule promotes accumulation of TGN organelles at sites of neuron-to-neuron contacts. *Journal of Cell Biology*, 159(4). <https://doi.org/10.1083/jcb.200205098>

References

- Sytnyk, V., Leshchyns'ka, I., Nikonenko, A. G., & Schachner, M. (2006). NCAM promotes assembly and activity-dependent remodeling of the postsynaptic signaling complex. *Journal of Cell Biology*, *174*(7). <https://doi.org/10.1083/jcb.200604145>
- Tabuchi, K., & Südhof, T. C. (2002). Structure and Evolution of Neurexin Genes: Insight into the Mechanism of Alternative Splicing. *Genomics*, *79*(6). <https://doi.org/10.1006/geno.2002.6780>
- Tan, C. L., Cooke, E. K., Leib, D. E., Lin, Y.-C., Daly, G. E., Zimmerman, C. A., & Knight, Z. A. (2016). Warm-Sensitive Neurons that Control Body Temperature. *Cell*, *167*(1). <https://doi.org/10.1016/j.cell.2016.08.028>
- Tanabe, Y., Naito, Y., Vasuta, C., Lee, A. K., Soumounou, Y., Linhoff, M. W., & Takahashi, H. (2017). IgSF21 promotes differentiation of inhibitory synapses via binding to neurexin2 α . *Nature Communications*, *8*(1). <https://doi.org/10.1038/s41467-017-00333-w>
- Tanaka, H., Nogi, T., Yasui, N., Iwasaki, K., & Takagi, J. (2011). Structural Basis for Variant-Specific Neuroligin-Binding by α -Neurexin. *PLoS ONE*, *6*(4). <https://doi.org/10.1371/journal.pone.0019411>
- Terunuma, M. (2018). Diversity of structure and function of GABAB receptors: A complexity of GABAB-mediated signaling. In *Proceedings of the Japan Academy Series B: Physical and Biological Sciences* (Vol. 94, Issue 10, pp. 390–411). Japan Academy. <https://doi.org/10.2183/pjab.94.026>
- Thomas, P., & Smart, T. G. (2005). HEK293 cell line: A vehicle for the expression of recombinant proteins. *Journal of Pharmacological and Toxicological Methods*, *51*(3). <https://doi.org/10.1016/j.vascn.2004.08.014>
- Thomas-Jinu, S., & Houart, C. (2013). Dynamic expression of neurexophilin1 during zebrafish embryonic development. *Gene Expression Patterns*, *13*(8), 395–401. <https://doi.org/10.1016/j.gep.2013.07.006>

References

- Tong, X. J., López-Soto, E. J., Li, L., Liu, H., Nedelcu, D., Lipscombe, D., Hu, Z., & Kaplan, J. M. (2017). Retrograde Synaptic Inhibition Is Mediated by α -Neurexin Binding to the $\alpha 2\delta$ Subunits of N-Type Calcium Channels. *Neuron*, *95*(2), 326-340.e5. <https://doi.org/10.1016/j.neuron.2017.06.018>
- Tu, J. C., Xiao, B., Naisbitt, S., Yuan, J. P., Petralia, R. S., Brakeman, P., Doan, A., Aakalu, V. K., Lanahan, A. A., Sheng, M., & Worley, P. F. (1999). Coupling of mGluR/Homer and PSD-95 Complexes by the Shank Family of Postsynaptic Density Proteins. *Neuron*, *23*(3). [https://doi.org/10.1016/S0896-6273\(00\)80810-7](https://doi.org/10.1016/S0896-6273(00)80810-7)
- Tuskan, R. G., Tsang, S., Sun, Z., Baer, J., Rozenblum, E., Wu, X., Munroe, D. J., & Reilly, K. M. (n.d.). *Real-time PCR analysis of candidate imprinted genes on mouse chromosome 11 shows balanced expression from the maternal and paternal chromosomes and strain-specific variation in expression levels.* <http://phenome.jax.org/pub-cgi/phenome/mpdcgi?rtn=snp/door>
- Uemura, T., Lee, S.-J., Yasumura, M., Takeuchi, T., Yoshida, T., Ra, M., Taguchi, R., Sakimura, K., & Mishina, M. (2010a). Trans-Synaptic Interaction of GluR δ 2 and Neurexin through Cbln1 Mediates Synapse Formation in the Cerebellum. *Cell*, *141*(6). <https://doi.org/10.1016/j.cell.2010.04.035>
- Uemura, T., Lee, S.-J., Yasumura, M., Takeuchi, T., Yoshida, T., Ra, M., Taguchi, R., Sakimura, K., & Mishina, M. (2010b). Trans-Synaptic Interaction of GluR δ 2 and Neurexin through Cbln1 Mediates Synapse Formation in the Cerebellum. *Cell*, *141*(6). <https://doi.org/10.1016/j.cell.2010.04.035>
- Ullrich, B., Ushkaryov, Y. A., & Südhof, T. C. (1995). Cartography of neurexins: More than 1000 isoforms generated by alternative splicing and expressed in distinct subsets of neurons. *Neuron*, *14*(3). [https://doi.org/10.1016/0896-6273\(95\)90306-2](https://doi.org/10.1016/0896-6273(95)90306-2)
- Um, J. W., Choi, T.-Y., Kang, H., Cho, Y. S., Choi, G., Uvarov, P., Park, D., Jeong, D., Jeon, S., Lee, D., Kim, H., Lee, S.-H., Bae, Y.-C., Choi, S.-Y., Airaksinen, M. S., & Ko, J. (2016). LRRTM3 Regulates Excitatory Synapse Development through Alternative Splicing and Neurexin Binding. *Cell Reports*, *14*(4). <https://doi.org/10.1016/j.celrep.2015.12.081>

References

Ushkaryov, Y. A., Petrenko, A. G., Geppert, M., & Südhof, T. C. (1992). Neurexins: Synaptic cell surface proteins related to the α -latrotoxin receptor and laminin. *Science*, *257*(5066). <https://doi.org/10.1126/science.1621094>

Ushkaryov, Y. A., & Südhof, T. C. (1993). Neurexin III α : Extensive alternative splicing generates membrane-bound and soluble forms. *Proceedings of the National Academy of Sciences of the United States of America*, *90*(14). <https://doi.org/10.1073/pnas.90.14.6410>

Ushkaryov, Y., Petrenko, A., Geppert, M., & Südhof, T. (1992). Neurexins: synaptic cell surface proteins related to the alpha-latrotoxin receptor and laminin. *Science*, *257*(5066). <https://doi.org/10.1126/science.1621094>

Ushkaryov, Y. A., Hataso, Y., Ichtchenko, K., Moomaw, C., Afendiss, S., Slaughter, C. A., & Südhof, T. C. (1994). *THE JOURNAL OF BIOLOGICAL CHEMISTRY* Conserved Domain Structure of P-Neurexins UNUSUAL CLEAVED SIGNAL SEQUENCES IN RECEPTOR-LIKE NEURONAL CELL-SURFACE PROTEINS* (Vol. 269, Issue 16).

Vallée Marcotte, B., Cormier, H., Guénard, F., Rudkowska, I., Lemieux, S., Couture, P., & Vohl, M. C. (2016). Novel Genetic Loci Associated with the Plasma Triglyceride Response to an Omega-3 Fatty Acid Supplementation. *Journal of Nutrigenetics and Nutrigenomics*, *9*(1), 1–11. <https://doi.org/10.1159/000446024>

Varoqueaux, F., Jamain, S., & Brose, N. (2004). Neuroligin 2 is exclusively localized to inhibitory synapses. *European Journal of Cell Biology*, *83*(9). <https://doi.org/10.1078/0171-9335-00410>

Vieira, M., Yong, X. L. H., Roche, K. W., & Anggono, V. (2020). Regulation of NMDA glutamate receptor functions by the GluN2 subunits. In *Journal of Neurochemistry* (Vol. 154, Issue 2, pp. 121–143). Blackwell Publishing Ltd. <https://doi.org/10.1111/jnc.14970>

Williams, P. T. (2020). Gene-environment interactions due to quantile-specific heritability of triglyceride and VLDL concentrations. *Scientific Reports*, *10*(1). <https://doi.org/10.1038/s41598-020-60965-9>

References

- Wilson, S. C., White, K. I., Zhou, Q., Pfuetzner, R. A., Choi, U. B., Südhof, T. C., & Brunger, A. T. (2019). Structures of neurexophilin–neurexin complexes reveal a regulatory mechanism of alternative splicing. *The EMBO Journal*, *38*(22). <https://doi.org/10.15252/embj.2019101603>
- Wittig, I., Braun, H. P., & Schägger, H. (2006). Blue native PAGE. *Nature Protocols*, *1*(1), 418–428. <https://doi.org/10.1038/nprot.2006.62>
- Wouters, M. M., Lambrechts, D., Knapp, M., Cleynen, I., Whorwell, P., Agréus, L., Dlugosz, A., Schmidt, P. T., Halfvarson, J., Simrén, M., Ohlsson, B., Karling, P., van Wanrooy, S., Mondelaers, S., Vermeire, S., Lindberg, G., Spiller, R., Dukes, G., D’Amato, M., & Boeckxstaens, G. (2014). Genetic variants in CDC42 and NXP1 as susceptibility factors for constipation and diarrhoea predominant irritable bowel syndrome. *Gut*, *63*(7), 1103–1111. <https://doi.org/10.1136/gutjnl-2013-304570>
- Wu, X., Morishita, W. K., Riley, A. M., Hale, W. D., Südhof, T. C., & Malenka, R. C. (2019). Neuroligin-1 Signaling Controls LTP and NMDA Receptors by Distinct Molecular Pathways. *Neuron*, *102*(3), 621–635.e3. <https://doi.org/10.1016/j.neuron.2019.02.013>
- XiangWei, W., Jiang, Y., & Yuan, H. (2018). De novo mutations and rare variants occurring in NMDA receptors. *Current Opinion in Physiology*, *2*. <https://doi.org/10.1016/j.cophys.2017.12.013>
- Xin, G., Chen, R., & Zhang, X. (2018). Identification of key microRNAs, transcription factors and genes associated with congenital obstructive nephropathy in a mouse model of megabladder. *Gene*, *650*, 77–85. <https://doi.org/10.1016/j.gene.2018.01.063>
- Yashiro, K., & Philpot, B. D. (2008). Regulation of NMDA receptor subunit expression and its implications for LTD, LTP, and metaplasticity. In *Neuropharmacology* (Vol. 55, Issue 7, pp. 1081–1094). <https://doi.org/10.1016/j.neuropharm.2008.07.046>
- Zeisel, A., Hochgerner, H., Lönnerberg, P., Johnsson, A., Memic, F., van der Zwan, J., Häring, M., Braun, E., Borm, L. E., la Manno, G., Codeluppi, S., Furlan, A., Lee, K., Skene,

References

- N., Harris, K. D., Hjerling-Leffler, J., Arenas, E., Ernfors, P., Marklund, U., & Linnarsson, S. (2018). Molecular Architecture of the Mouse Nervous System. *Cell*, 174(4). <https://doi.org/10.1016/j.cell.2018.06.021>
- Zeng, X., Sun, M., Liu, L., Chen, F., Wei, L., & Xie, W. (2007). Neurexin-1 is required for synapse formation and larvae associative learning in *Drosophila*. *FEBS Letters*, 581(13). <https://doi.org/10.1016/j.febslet.2007.04.068>
- Zhang, C., Atasoy, D., Araç, D., Yang, X., Fucillo, M. v., Robison, A. J., Ko, J., Brunger, A. T., & Südhof, T. C. (2010a). Neurexins Physically and Functionally Interact with GABAA Receptors. *Neuron*, 66(3). <https://doi.org/10.1016/j.neuron.2010.04.008>
- Zhang, C., Atasoy, D., Araç, D., Yang, X., Fucillo, M. v., Robison, A. J., Ko, J., Brunger, A. T., & Südhof, T. C. (2010b). Neurexins physically and functionally interact with GABAA receptors. *Neuron*, 66(3), 403–416. <https://doi.org/10.1016/j.neuron.2010.04.008>
- Zhang, P., Lu, H., Peixoto, R. T., Pines, M. K., Ge, Y., Oku, S., Siddiqui, T. J., Xie, Y., Wu, W., Archer-Hartmann, S., Yoshida, K., Tanaka, K. F., Aricescu, A. R., Azadi, P., Gordon, M. D., Sabatini, B. L., Wong, R. O. L., & Craig, A. M. (2018). Heparan Sulfate Organizes Neuronal Synapses through Neurexin Partnerships. *Cell*, 174(6). <https://doi.org/10.1016/j.cell.2018.07.002>
- Zhang, Q., Wang, J., Li, A., Liu, H., Zhang, W., Cui, X., & Wang, K. (2013a). Expression of neurexin and neuroligin in the enteric nervous system and their down-regulated expression levels in Hirschsprung disease. *Molecular Biology Reports*, 40(4). <https://doi.org/10.1007/s11033-012-2368-3>
- Zhang, Q., Wang, J., Li, A., Liu, H., Zhang, W., Cui, X., & Wang, K. (2013b). Expression of neurexin and neuroligin in the enteric nervous system and their down-regulated expression levels in Hirschsprung disease. *Molecular Biology Reports*, 40(4). <https://doi.org/10.1007/s11033-012-2368-3>

References

Zhong, C., Shen, J., Zhang, H., Li, G., Shen, S., Wang, F., Hu, K., Cao, L., He, Y., & Ding, J. (2017). Cbln1 and Cbln4 Are Structurally Similar but Differ in GluD2 Binding Interactions. *Cell Reports*, 20(10), 2328–2340. <https://doi.org/10.1016/j.celrep.2017.08.031>

Zhou, H., Xu, Y., Yang, Y., Huang, A., Wu, J., & Shi, Y. (2005). Solution Structure of AF-6 PDZ Domain and Its Interaction with the C-terminal Peptides from Neurexin and Bcr. *Journal of Biological Chemistry*, 280(14). <https://doi.org/10.1074/jbc.M411065200>

Zhou, J. J., Li, D. P., Chen, S. R., Luo, Y., & Pan, H. L. (2018). The 2-1-NMDA receptor coupling is essential for corticostriatal long-term potentiation and is involved in learning and memory. *Journal of Biological Chemistry*, 293(50), 19354–19364. <https://doi.org/10.1074/jbc.RA118.003977>

Summary

Neurexins are synaptic cell adhesion molecules that play an essential role in synaptic transmission. They are widely expressed in the whole CNS and are primarily located on the neuronal presynaptic sites. Three genes encode neurexins, and each gives rise to two isoforms: long α -neurexins composed of six LNS6 domains separated by three EGF domains and short β -neurexins that possess only a single LNS domain, an equivalent of α -neurexins LNS6 domain. LNS domains are involved in forming complexes with postsynaptic partners, and most of them bind to LNS6/ β LNS domains, i.e., neuroligins, dystroglycan or LRRTMs. However, some exceptions like, i.e., neurexophilins combine with α -neurexins and form a tight complex with α -neurexins LNS2 domain. Although neurexophilins has been studied for the last thirty years, their functions remain unsolved. Here, I confirmed that although neurexophilins are expressed in distinct brain parts, they behave similarly by binding to the same epitope on the $Nrxn1\alpha$ LNS2 domain. The only neurexophilin that stands out from other family members is $Nxph4$ which seems to act slightly differently, which a difference in sequence can probably explain.

To further investigate functions of neurexophilins, I performed pulldown screening from transgenic mice brains, which overexpress $Nxph1$ -GFP and $Nxph3$ -GFP. In my work, I discovered that $Nrxn$ - $Nxph$ complexes bind to NMDAR, GABABR, $mGluR3$ and $mGluR5$ in an age-specific manner. I also validated in a recombinant experiment that the $GluN1$ subunit of NMDAR binds directly to the LNS6/ β LNS domain of neurexins.

|

Abbreviations

AMPA	α -amino-hydroxy-5-methyl-4-isoxazole propionic acid
BSA	Bovine serum albumin
CaV	Voltage-gated calcium channel
Cbln1	Cerebellin precursor protein 1
cKO	Conditional knockout
CMV	cytomegalovirus
CNS	Central nervous system
CTD	C-terminal domain
DMEM	Dulbecco's Modified Eagle's Medium
DMSO	Dimethyl sulfoxide
EDTA	ethylenediaminetetraacetic acid
EGF	Epidermal growth factor-like
eGFP	Enhanced green fluorescent protein
EPSC	Excitatory postsynaptic current
EtOH	Ethanol denatured
FCS	Fetal calf serum
GABA	γ -aminobutyric acid
GluR	Glutamate receptor
GPI	Glycosyl-phosphatidylinositol
HA	Hemagglutinin
HEK	Human embryonic kidney
HEPES	4-(2-hydroxyethyl)-1-piperazineethanesulfonic acid
iGluR	Ionotropic glutamate receptor
IPSC	Inhibitory postsynaptic current
kb	Kilobase
KO	Knockout
LNS	Laminin-neurexin-sex hormone binding globulin
LRRTM	Leucine rich repeat transmembrane
mGluR	Metabotropic glutamate receptor
NGS	Normal goat serum

References

NMDA	N-methyl-D-aspartic-acid
PBS	Phosphate buffered saline
PCR	Polymerase chain reaction
PDZ	Post-synaptic density 95, Drosophila Discs-large, and Zonula occludens-1
RE	Restriction enzyme
rpm	Revolutions per minute
SS	Splicing sites
TKO	Triple knockout

List of figures

Figure 1.1. Domain organisation of neurexins and neurexophilins.	11
Figure 1.2. Domain structure of neurexophilins.....	16
Figure 1.2. Domain structure of neurexophilins.....	16
Figure 1.3. Primary structure of rat neurexophilins.	17
Figure 3.1. Immunoblot alignment of Nxph1, Nxph2, Nxph3 and Nxph4 variants used in this project.....	52
Figure 3.2. Mapping Nrnx1 α binding epitope to neurexophilins.....	56
Figure 3.3. Binding of Nxph4-Myc to Nrnx1 α LNS2 is weak at high salt concentration	58
Figure 3.4. Diagram of recombinant proteins used for binding assays.....	60
Figure 3.5. Screening for potential new binding partners of neurexins in transgenic Nxph3-GFP ^{tg/-} mice brains.....	62
Figure 3.6. α -Nrnx/Nxph-GFP pulled down NMDAR from adult mice brains..	66
Figure 3.7. Neurexins pulled GABABR from P7 mice brains.....	67
Figure 3.8. Searching for new potential binding partners of Nxph3 in adult Nxph3-GFP ^{tg/-} mice.....	72
Figure 3.9. The Nxph3-GFP/ α -Nrnx complex binds to GABA _B R, LRRTM2, mGluR3 and mGluR5 but not to NMDAR in P7 Nxph3-GFP ^{tg/-} brain.....	75
Figure 3.10. GluN1-GFP binds to Neurexins.....	73
Figure 4.1. Model explaining age-dependent interactions between neurexins and their binding partners in excitatory synapses of Nxph3-GFP ^{tg/-} brain..	86

List of tables

Table 1. Interaction partners of neurexins.	13
Table 2. Observed and calculated molecular weight of neurexophilins.	55
Table 3. Synaptic receptors successfully co-sedimented by the GFP-trap from adult and P7 Nxph3-GFP ^{tg/-} brain lysates (Fig. 3.9 and 3.10).	74

References

|

References

|Acknowledgment

I would like to thank Prof. Dr. Markus Missler for the opportunity to join the lab and work on the project. I appreciate all the discussions we have and the valuable suggestions I received during my time in Münster.

Thank Prof. Dr. Bruno Moersbacher and Prof. Dr. Andreas Püschel as my doctoral committee.

Thank Dr. Carsten Reißner for technical supervision and guidance of my thesis. His precious suggestions and deep insights into research inspire and encourage me to continue working in a field of neuroscience.

Thank Ilka Wolff and Kai Kerkhoff for their generous technical support, and thanks to Enno Löffler for administration work.

Thank my amazing colleagues Dr. Astrid Rohlmann, Dr. Johannes Brockhaus, Dr. Daniele Repetto, Dr. Bianca Brüggem, Dr. Oliver Klatt, Dr. Miao Sun, Keertana Srimat Kandadai, Celeste Nilges, Malin Lammers, Vivien Rieping, Dr. Anna Schober, and Dr. Anja Blanqué. I appreciate all the scientific help and advice from all of them.

Thank my family for their unconditional support, their acceptance and encouragement. Especially thank Adrian for his cheerful spirit, kindness, and love.